NASA CR-111803

A STUDY OF AIR CUSHION LANDING SYSTEMS

FOR

SPACE SHUTTLE VEHICLES

By John M. Ryken

Prepared under Contract No. NAS1-9992 by
BELL AEROSPACE COMPANY DIVISION OF TEXTRON INC.
Buffalo, N. Y.

for

NATIONAL AERONAUTICS AND SPACE ADMINISTRATION

December 1970

NASA CR-111803

A STUDY OF AIR CUSHION LANDING SYSTEMS

FOR

SPACE SHUTTLE VEHICLES

By John M. Ryken

Prepared under Contract No. NAS1-9992 by
BELL AEROSPACE COMPANY DIVISION OF TEXTRON INC.
Buffalo, N. Y.

for

NATIONAL AERONAUTICS AND SPACE ADMINISTRATION

December 1970

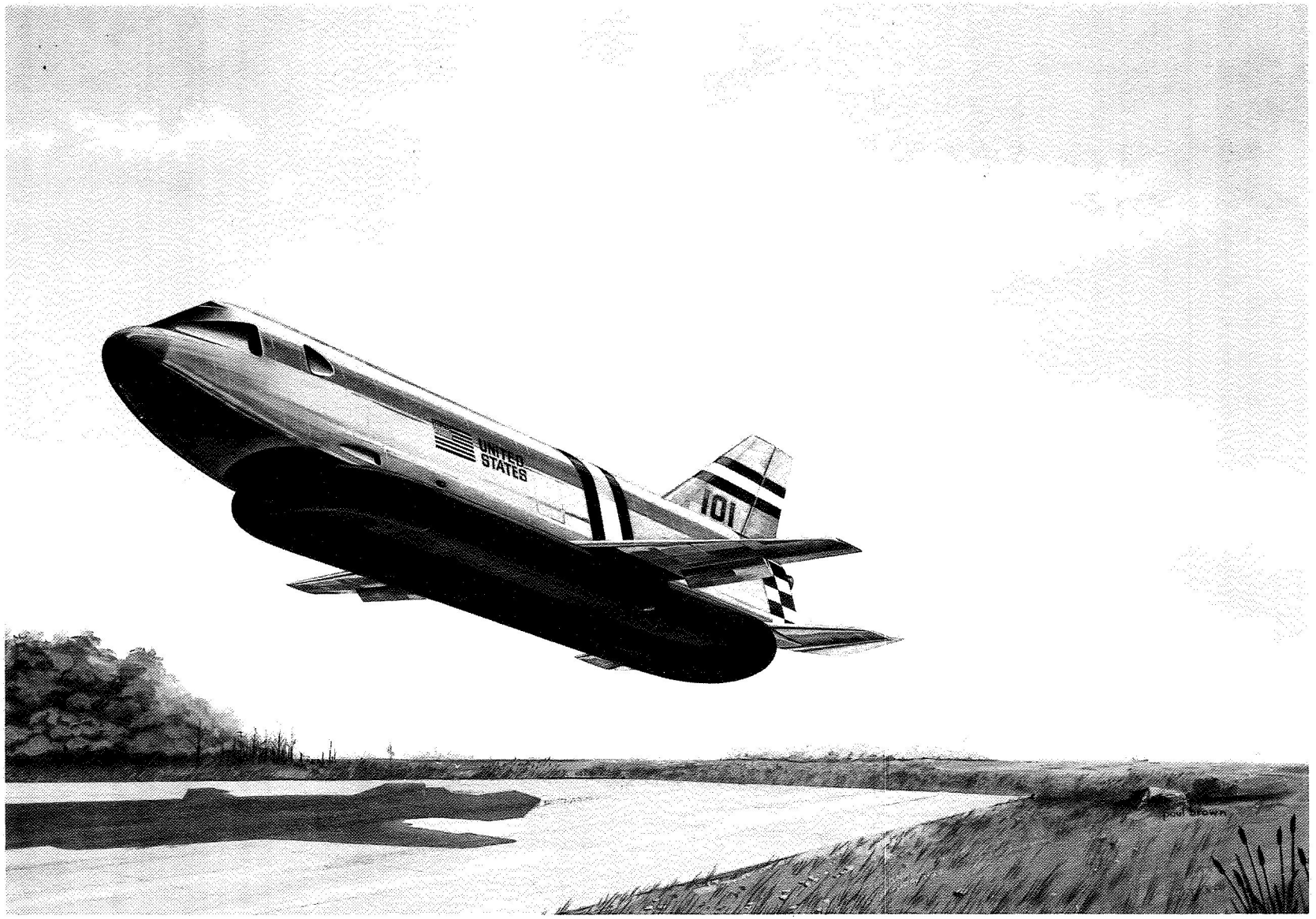
UNITED
STATES
101

CONTENTS

CONTENTS (CONT)

A STUDY OF AIR CUSHION

LANDING SYSTEMS

FOR SPACE SHUTTLE VEHICLES

By John M. Ryken

SUMMARY

A study was made to determine the feasibility of using an air cushion landing system (ACLS) instead of conventional landing gear, on space shuttle boosters and orbiters. Results indicate that such a system is feasible and that its weight will be less than the weight of conventional gear. Volume requirements and aerodynamic effects will be comparable to those of conventional gear. If air cushion landing system parameters are properly selected, a small structural weight saving may be possible. Materials are available for externally stowed trunks on boosters, but orbiter trunks must be stowed internally or otherwise protected.

INTRODUCTION

An Air Cushion Landing System (ACLS) replaces a conventional landing gear with a peripheral jet air cushion similar to that employed by an Air Cushion Vehicle (ACV) or Hovercraft.

The feasibility of the ACLS has been demonstrated by flight testing an ACLS installed on a Lake LA-4 amphibian. Testing included landings on runways, unprepared surfaces, and water. Braking and taxi tests have demonstrated ground performance and braking equal to or better than conventional gear.

The ACLS feasibility demonstrations with the LA-4 and design studies of ACLS application to other aircraft have indicated that the following advantages could be expected if the ACLS were used on Space Shuttle Vehicles:

(1) Reduced weight of ACLS relative to the weight of conventional gear
(2) Reduced vehicle structural weight due to reduced landing load factors and distributed rather than concentrated loads
(3) Land, water, and rough field capability with resulting reductions in runway requirements and/or increased probability of safe recovery from launch aborts or emergency landings

(4) Ability to land in cross winds without decrabbing at touchdown
(5) Increased ground mobility: towing or taxiing over unprepared sites; lateral ground handling in confined spaces
(6) High speed landing capability, with possible reduction in landing attitude or reduced subsonic aerodynamic requirements

Because of these potential advantages, Bell Aerospace Company under contract to the NASA Langley Research Center, has made a study of the application of the Air Cushion Landing System to Space Shuttle boosters and orbiters. The objectives of this study were to:

(1) Confirm the feasibility of ACLS installation on space shuttle booster and orbiter vehicles
(2) Make preliminary estimates of loads imposed on the vehicles by an ACLS and the effects of these loads on vehicle structure
(3) Estimate effects of an ACLS on vehicle L/D and pitching moments
(4) Establish requirements for trunk and brake materials and investigate availability of suitable materials
(5) Indicate advantages and disadvantages of possible alternate means of providing air flow required for an ACLS
(6) Estimate ACLS weight and vehicle structural weight savings and penalties due to an ACLS for comparison with conventional landing gear
(7) Indicate sensitivity of above items to perturbations in vehicle and ACLS design parameters

Although a straight wing booster and a delta wing/body orbiter were used for these studies, results are generally applicable to other shuttle vehicle configurations shown in refs. 1 through 6. Results of the study indicate that it is feasible to use an ACLS on either shuttle booster or orbiter vehicles and that the previously listed advantages of an ACLS can be expected to result from its use.

Recommendations are made for additional design efforts, analyses, and tests to confirm these conclusions and to refine the quantitative results presented in this report.

SYMBOLS

A_b	area of brake tread, ft^2
A_c	area of cushion, ft^2
A_{TM}	area of trunk material in unstretched condition, ft^2
AR_c	cushion aspect ratio; equals cushion length divided by cushion width (dimensionless)
C_d	discharge coefficient of the gap between the trunk and the ground (dimensionless)
C_D	drag coefficient (dimensionless)
C_L	aerodynamic lift coefficient, (dimensionless)
C_M	aerodynamic moment coefficient, 1/deg
C_{M_δ}	change in aerodynamic moment coefficient per deg of control deflection, 1/deg
C_p	specific heat $\frac{\text{Btu}}{\text{lb - °F}}$
C_{y_β}	coefficient of side force due to sideslip, 1/deg
D	aerodynamic drag, lb
D_M	momentum drag, lb
E	efficiency of fan and gearbox (dimensionless)
F_V	vertical force acting on a one foot length of trunk, lb/ft
H_o	in flight depth of trunk, ft
h	height of center of gravity above the ground, ft
h_g	height of gap between trunk and the ground, in.
$\dot{h}$	sink speed, ft/sec
hp	horsepower
k	thermal conductivity, $\frac{\text{Btu}}{\text{ft}^2\ \text{hr}\ (°\text{F/in.})}$

SYMBOLS (continued)

L_s	length of side trunk, ft
l	length of trunk material in a stretched condition, ft
l_u	length of trunk material in its unstretched condition, ft
P_b	brake pillow pressure, lb/ft^2
P_c	Cushion pressure, lb/ft^2
P_F	fan discharge pressure, lb/ft^2
P_p	parking bladder pressure, lb/ft^2
P_T	trunk pressure, lb/ft^2
P_{T_o}	trunk pressure, prior to touchdown and with zero cushion pressure, lb/ft^2
p	perimeter of trunk; measured at centerline of retracted trunk for booster; measured at centerline of uninflated trunk with doors fully open, for the orbiter, ft
p_t	perimeter of trunk measured at ground tangent, ft
Q	air flow, ft^3 /sec
$\dot{q}$	heating rate, Btu/ft^2 , sec
q_{REF}	reference heating rate at stagnation point, Btu/ft^2 , sec
q	dynamic pressure, lb/ft^2
R_N	radius of nose used for stagnation point heating, ft
R_o	radius of trunk cross section, prior to touchdown and with zero cushion pressure, ft
S	aerodynamic reference area, ft^2
T	tension in trunk cross section, lb/ft
T_o	tension in trunk cross section, prior to touchdown and with zero cushion pressure, lb/ft
t	thickness of material, in.
V	velocity, ft/sec

SYMBOLS (continued)

W_A	width or distance between inner and outer trunk attachments, ft
W_0	width or distance between the two outer trunk attachments, ft
W_v	weight of vehicle, lb
X_1	distance from vehicle centerline to inner trunk attachment, ft
X_2	distance from inner trunk attachment to inner point of trunk tangency with ground, ft
X_3	width of trunk flattened area, ft

α	angle of attack, deg
β	side slip angle, deg
ΔP	pressure loss from fan discharge to trunk, lb/ft^2
δ	vertical deflection of trunk measured from its pretouchdown depth, ft
θ	pitch angle, deg
$\dot{\theta}$	pitch rate, deg/sec
μ	friction coefficient
ρ	density of air, $slugs/ft^3$
ρ_M	density of trunk material, $lb/in.^3$
ψ	yaw angle, deg
ϕ	roll angle, deg

SYSTEM DESCRIPTION AND DEVELOPMENT STATUS

System Description

An ACLS replaces conventional aircraft alighting gear with a peripheral jet air cushion arrangement, the same principle employed by the Air Cushion Vehicle (ACV) or Hovercraft (figs. 1 through 3).

The ACV operates continuously on its cushion, whereas an ACLS is only used for takeoff and landing. Significant differences in design and operation result.

Like an ACV, an ACLS (fig. 4) embodies a large flexible understructure, a pneumatic "boot" or "bag" or "trunk" as it is variously referred to. During operation of the system, continuous airflow from an onboard power source maintains this trunk inflated while producing a peripheral jet flow through a large number of jet holes. These are arranged in a regular pattern at its base, close to the ground tangent.

The trunk is attached to the bottom of the fuselage. When inflated, it forms itself into an elongated doughnut shape, making a cavity beneath the fuselage. The escaping air creates a pressure within this cavity whenever the aircraft is close to the takeoff or landing surface (fig. 5). It is this pressure which supports the aircraft friction-free on the surface. Air clearance beneath the trunk is minimal to conserve power, because large surface irregularities can be tolerated by the resilience of the flexible trunk itself. The trunk inflation pressure is very low (on the order of 2-4 $lb/in.^2$. Footprint pressure is 1-2 $lb/in.^2$. The material proposed for the trunk is a special highly elastic composite developed by Bell for air cushion landing gear. Capable of 300% elongation and of very high ultimate strength, its use permits external or internal retraction. The external retraction scheme used by Bell for the LA-4 aircraft, which has been used to demonstrate ACLS feasibility and advantages, is similar to the retraction of pneumatic deicing boots on a wing leading edge. There are no moving parts. When pressure is released, the sheet simply contracts to hug the aircraft contour.

Unlike ACV, the ACLS incorporates a braking subsystem, illustrated in figs. 6 and 7. It is a skid brake system wherein a number of tread elements (six on the LA-4) are attached to the bottom of the trunk locally. These are pushed into ground contact by the operation of an internal pneumatic pillow. The inflation of the pillows also distorts the trunk to vent cushion pressure and thereby transfers load from the cushion to the brake treads. Differential operation of the right and left hand sets provides an excellent means of controlling aircraft heading and turns when the aircraft is cushionborne. This has been demonstrated by the LA-4.

An ACLS also incorporates the parking and mooring subsystem shown in fig. 6. This consists of a lightweight bladder, normally furled inside the trunk. The bladder acts to seal the jets, much as an automobile inner tube. For parking, it is inflated to normal trunk pressure so that the trunk inflation is maintained without jet flow. The aircraft then rests on the trunk for parking on the ground or floats on it in the water. When resting on the ground, the friction locks the aircraft in place. When overwater, the inflated trunk is automatically a perfect fender but the aircraft must be moored. This inner bladder can also be used to kneel, if required, since partial deflation will lower the aircraft until the fuselage bottom is at ground level.

Development Status

After Bell's conceptual studies and preliminary tests in 1964, the USAF supported a feasibility study and model test program. This is reported in ref. 7. Because of the success of these programs Bell installed an ACLS on a light aircraft for reduction to practice. A Lake LA-4 light amphibian (2500 lb gross weight) was selected. The system was installed and the first air cushion takeoff and landing was made on August 4, 1967, (fig. 8). These were performed without brakes. Meanwhile, Bell conducted small-scale brake system experiments on an LA-4 model, fig. 9, and was awarded a further contract, for brake development and wear testing on a large model, fig. 10. The results of these latter tests (which also included model scale overwater evaluations) are reported in ref. 8.

After the initial air cushion reduction to practice, the aircraft was equipped with the cushion braking system and the complete system reduced to practice on September 12, 1968 performing a takeoff, landing and a series of taxi, turning and stopping maneuvers.

On October 1, 1968, an LA-4 overland evaluation program was started under contract to the USAF. This program has been completed. It included operation over various surfaces including obstacles, etc. The purpose of the program was to demonstrate the validity of the concept and to provide data for the extrapolation of performance to larger aircraft. This program was also successful. Takeoffs and landings were made from hard runway, thick grass, and deep snow. Taxi tests were conducted over simulated tree stumps, ditches, an 8-in. step (at speed), long stubble and clover, ploughed ground and sand. Takeoffs and landings from these latter surfaces were shown to be practical though the surfaces were not available where actual takeoffs and landings could be performed. Takeoff, landing, and close quarters maneuvers were also performed in strong cross winds with complete success demonstrating the cross wind gear feature. The results of the program are reported in ref. 9. Bell also completed an overwater and maximum braking evaluation program for the USAF. The first overwater takeoffs and landings were made on September 11, 1969 in moderate wind (20 knots) and choppy water. Results of these tests are summarized in ref. 10.

It is clear that in the ACV, air cushion technology has reached a well developed stage. In addressing the exploratory development, several technology requirements of ACLS were considered as possible problem areas. The following were particularly examined:

Cushion retractability
Aircraft rotation and flare
Vertical energy absorption
Braking
Control in confined quarters and crosswind
Total system weight

The simplest retraction method, the use of elastic material as described above, was used on Bell's LA-4; the material being deflated to the outside of the aircraft hull. An alternative method was also determined whereby the sheet may be stowed inside metal doors, (fig. 11). This may be preferred for very high speed aircraft. A small working model was made and tests to verify the feasibility were conducted. Methods of fabricating the elastic trunk have also been developed by Bell. Fig. 12 shows an LA-4 trunk before trimming. This is a single composite sheet of stretch nylon/rubber. In the slack condition shown, it measures 8 x 20 ft. It will stretch to 20 x 20 ft easily, after which the embedded nylon fibers carry considerable load. Ultimate strength is about 100 lb/in. Laboratory samples of suitable material for larger aircraft have also been made.

The ACLS aircraft makes a normal rotation on takeoff and a normal flare on landing. An important phenomenon is brought into play in these maneuvers. This is illustrated in fig. 13. At touchdown the rear of the bag is flattened in ground contact. However, this does not cause significant drag or wear even though cushion cavity pressure may not have developed, because of air lubrication effect. Adequate nozzle area (porosity) is provided in this region so that the trunk pressure is transmitted to the air between the trunk and the ground. Low friction results.

Early experiments on a USAF C-119 flying boxcar model were conducted at the NASA Langley Research Center. Model takeoffs and landings from a moving ground were made in a wind tunnel by remotely controlling the elevator from outside the tunnel, (fig. 14). These confirmed early Bell experiments of the air lubrication effect. Subsequently 12 takeoff and landings of the LA-4 using a concrete/blacktop runway have produced only negligible wear of the 0.020-in. thick soft neoprene outer layer of the trunk in this "contact" region.

The third problem area is vertical energy absorption. Drop tests were conducted on a large model (fig. 15). It was found that the static heave stiffness was greatly increased by transient pressure rise of both trunk and cushion pressures. Damping was very good. Variable sink rate landings were also made on the LA-4 to confirm energy absorption capacity. Heave stiffness (static and dynamic) is a parameter largely under the designer's control, since the trunk pressure can be varied over a wide range.

It has not been found necessary to incorporate braking into conventional air cushion vehicles. The amphibious capability of the ACV has been used rather as a transition capability (water/land/water) and the overland use has been secondary to overwater. Indeed, overland control has been deficient in most instances; on the other hand, with ACLS, braking is considered mandatory and an integral part of the system. Additionally, in the aircraft application, aerodynamic controls are more effective because of the larger control surface and thrust moment arms about the c.g. The system employed in ACLS is not radical in that skid brake systems have been used in the past and found effective and also shown to have reasonable life. Braking wear tests of the large model on the whirling arm (fig. 16) were conducted. A large number of start/stop cycles were completed on one unit from which it was predicted that between 40 and 50 normal braked landings of a C-119 could be made with the particular neoprene tread used, without replacing the skids/treads.

Using differential brake and rudder, standing turns can be made on the LA-4 with a turn radius of 3 ft and precise taxi-to-park maneuvers, amongst traffic, have been demonstrated in wind up to about 18 knots, a strong wind for a light aircraft with a wing loading of only 14 lb/ft^2.

For the takeoff and landing maneuvers, the cushion is markedly superior as to stability and controllability; this is because it is an ideal crosswind gear and can takeoff and land yawed to the track as easily as headed along it. On the LA-4, takeoff and landing has been accomplished in a crosswind of 23 knots at 60° to the track. In this and all other runway takeoffs and landings made, all of which include some crosswind component, the pilot has controlled the aircraft so that there has been no noticeable deviation from the painted centerline of the runway. This applies throughout acceleration and deceleration. Takeoffs from rough surfaces and snow have included a side gradient of a few degrees as well as crosswind. This is countered by yaw as in the crosswind case. There is no sideforce reaction at the ground as there is with wheels so that if the aircraft is not yawed to maintain track in these circumstances it will not tend to roll-over as it will on wheels, but will drift sideways. This behavior is illustrated in the comparative sketches in fig. 17.

There is an exception to this. At extreme roll angles it is possible to ventilate the air cushion and by making substantial ground contact on the trunk outside the jet area, induce friction. On the LA-4 excess roll is prevented by the use of whisker skids mounted from the wing floats. These are fully castering fiberglass springs: they have worked very well, add very little drag, and are compatible with overwater operation. The initial LA-4 flight was made without them and the need depends on cushion roll stiffness compared with applied torque which varies widely in particular cases. Retractable versions would not seem to present much problem.

Catastrophic ground loop also is prevented by the inability of the air cushion to provide side force. Here, ACV experience is the guide. ACV operators easily develop the ability to 'pirouette' these machines, in effect a series of ground loops, intentionally, and under control. While not a recommended maneuver, it will be appreciated that because roll-over does not occur should loss of control somehow result in ground looping, it will not likely have serious consequences.

The final item for which the ACV provides no applicable information is weight. ACLS weight has been estimated for some military aircraft and LA-4 experience is available. Table I states the comparative figures of interest. In the case of civil aircraft reduced weight fractions are expected to result from less stringent terrain requirements. In the case of the light aircraft where piston engines may be mandatory the system is heavier, but will show weight benefit for amphibious aircraft.

Bell is continuing ACLS laboratory research and development and the incorporation and trial of system improvements. The planning of the U.S. Air Force and Canadian Armed Forces includes installation and testing of an ACLS on a 41,000-lb deHavilland DHC-5, C-8 light logistics aircraft. An ACLS on an aircraft of this size will provide valuable data and operational experience on an aircraft much larger than the 2,500-lb LA-4.

BOOSTER CONFIGURATION STUDIED

Figs. 18, 19 and 20 are drawings of a straight wing space shuttle booster with low,medium, and high pressure air cushion landing systems. Fig. 21 shows a shematic of the ACLS with representative values of ACLS parameters shown for the low pressure system of fig. 18. Table II, summarizes the characteristics of these three air cushion landing systems. Even the high pressure system of fig. 20, with a cushion pressure of 270 lb/ft^2 (1.9 lb/in^2) and a trunk pressure of 540 lb/ft^2 (3.8 lb/in^2) has very low pressures compared to pressures normally used in aircraft tires (50 to 250 lb/in^2).

The air cushion systems of figs. 18, 19 and 20 were drawn with geometrically similar cushion planforms. As the design pressures were increased, the trunk depth was decreased to give all three systems approximately equal energy absorption capability.

Although only a straight wing booster was studied, results are generally applicable to other booster configurations shown in refs. 1 through 6.

Summary of Results for Booster

Table II shows that all three ACLS systems have estimated weights between 13,000 and 14,000 lb or 3.03 to 3.22% of the landing weight of 433,800 lb. These weights include the ACLS and its attachment to the booster. Other than weight for ACLS attachment, they do not include any vehicle structure weight savings or penalties which may result from the ACLS. Because of limited vehicle structural data available for this study, it was not possible to accurately assess the effects of the ACLS on vehicle structure. However, studies which were made indicate that reduced landing loads resulting from the ACLS, and their distributed rather than concentrated nature, may result in a small structural weight saving if the low pressure ACLS is used. The high pressure ACLS may result in structural penalties up to 5300 lb if, as indicated in ref. 1, the lower surface of the booster is designed for 3 lb/in^2 ultimate. However, if the booster lower surface is designed for a pressure of 5.6 lb/in^2 ultimate or more, the effect of even the high pressure ACLS on vehicle structure should be very small.

Table III presents a summary weight statement for a conventional landing gear for a booster having a configuration that is geometrically similar to the vehicle used for the ACLS studies of this report. The conventional landing gear weight shown in table III, equal to 4.86% of the landing weight, is typical of weight estimates from other Phase A Shuttle Booster studies (4.0 to 5.6% of booster landing weight). These conventional gear weight estimates probably do not account for items such as wheel wells and landing gear doors which should also be charged to the conventional gear. Therefore, this preliminary study indicates that the ACLS has a potential for a weight saving of at least 1.5 to 2.0% of the booster landing weight.

The study has also indicated that despite the thermal environment, materials that make it feasible to stow the ACLS trunk externally are available. External stowage is possible because of the relatively low level and short duration of the peak heat flux. This permits an outer layer of trunk material to be used as an insulator and a heat sink to protect the load carrying inner plys. External stowage of the trunk results in a very simple and lightweight system. The trunk will be extended and retracted by initiating and terminating airflow into the stretchable trunk.

Estimated lift, drag, and pitching moment increments due to the ACLS are comparable to those due to a conventional gear. This result was also found in previous wind tunnel tests of an ACLS on a model of the C-119 airplane (ref. 7), tests of an ACLS on an HL-10 lifting body model (unpublished), and flight tests of an ACLS on a LA-4 airplane (ref. 9).

Both turboshaft engines with fans and the vehicle landing engines were considered as means of supplying the air flow for the ACLS. Weights shown in table II, are for a system employing dual turboshaft engines and fans. There are several ways in which the landing engines might be used to provide the air flow for the ACLS; however, most of the Phase A studies showed landing engines in locations remote from the ACLS trunk. Because of practical installations problems resulting from these locations and complications that could result from the need to provide relatively constant ACLS pressures and flow at landing engine throttle settings from near idle to maximum power, the use of separate engine/fan combinations for the ACLS is recommended.

One objective of this preliminary study was to determine the sensitivity of the ACLS to changes in vehicle and ACLS design parameters. It has confirmed previous studies which showed that the ACLS weight, as a percentage of landing weight, tends to decrease as vehicle weight increases (fig. 22). However, this percentage will decrease only from approximately 3.5 to 3.2% as the design landing weight is increased from 250,000 to 500,000 lb.

The tendency of ACLS weight, as a percentage of vehicle landing weight, to decrease as the vehicle is made larger is due primarily to two factors. The first of these is the fact that as the cushion is made larger the ratio of cushion perimeter to cushion area decreases inversely with a characteristic dimension of the cushion. As a result, if cushion pressure is held constant the ACLS power requirement and engine fan system weight tend to increase in proportion to the square root of vehicle weight, rather than the first power of vehicle weight. The second factor is due to the tendency of peak vertical acceleration to decrease as the stroke is increased. If the vehicles are designed for the same sink rate and the same peak vertical acceleration at landing, the trunk weight becomes a lower percentage of vehicle weight as vehicle size is increased.

As in previous studies the ACLS system without thermal protection for the trunk was found to be lightest when low cushion pressures were used. Table II shows that the weight of the ACLS system without thermal protection increased from 11,187 to 13,278 lb when the ACLS was designed with a static cushion pressure of 270 lb/ft^2 instead of 90 lb/ft^2.

When an outer layer was added to the trunk to protect the load carrying plys from the thermal environment, the minimum weight point was shifted toward the medium pressure configuration. The larger thermal protection weight for the low pressure configuration is due both to the larger area of trunk material and to the lower trunk thickness, and hence lower heat capacity, of the basic trunk.

Unless further studies or tests indicate that the weight penalty for thermal protection is greater than present estimates, or booster lower surfaces are designed so high ACLS pressures can be tolerated without penalty, it appears desirable to make the booster ACLS cushion near the maximum size permitted by vehicle geometry. Resulting low ACLS pressures not only result in low system weight, but they result in lower landing load factors, improved damping, and reduced sensitivity to weight increase in the event that additional ACLS airflow is found to be desirable.

If subsequent studies show that the minimum weight point for a booster ACLS occurs with a cushion smaller than the largest size permitted by vehicle geometry, the decrease in size should be made by decreasing cushion length rather than cushion width. This should result in acceptable pitch and roll stiffnesses, whereas if the cushion planform shape is held constant, as in figs. 18 through 20, the roll stability becomes marginal or unacceptable as the cushion size is decreased.

If the booster trunk is stored externally, the ACLS volume requirement is determined by the air supply engine, fan, and ducting. It has been estimated that approximately 700 ft^3 will be required for this purpose. The final value will depend on factors such as the relative locations of the air supply and the trunk and the acceptable pressure drop from the fan to the trunk. However the above figure is probably accurate to within ± 30%.

For comparison the volumes required by conventional landing gear were estimated by scaling gear and wheel well dimensions from drawings in Phase A vehicle study reports. Volumes ranging from 400 to 2600 ft^3 were obtained in this manner. The lower figure was for a system employing two main gear; the large volume was for a system employing four main gear.

These figures leave a considerable uncertainty as to relative volume requirements of an ACLS and conventional landing gear; however, in most previous studies of air cushion landing systems it was found that the ACLS required less volume than the aircrafts conventional gear. A similar situation is anticipated for shuttle vehicles.

In conclusion, it should be noted that at this time there are uncertainties in the weight estimates for both the ACLS and for the conventional gear. However, the ACLS weight estimates of table II could increase by approximately 50% before they are equal to the estimated percentage of landing weight for conventional gear, as given in table III. A subsequent section recommends additional studies and tests that should significantly improve on the accuracy of present ACLS weight estimates. These additional studies and tests should also significantly increase confidence in other aspects of the ACLS, such as the ability of trunk materials to withstand repeated missions while stowed externally.

ORBITER CONFIGURATION STUDIED

Fig. 23 is a drawing of a highly swept lifting body orbiter with an ACLS. The cushion pressure for this ACLS is 180 lb/ft^2, the same as that of the medium pressure booster ACLS of fig. 19. A triangular cushion planform was used to conform to vehicle geometry, reduce aerodynamic drag, and provide additional trunk length at the rear of the cushion for energy absorption at high landing attitudes.

Fig. 23 shows trunk thermal protection doors that are integral with the trunk. After unlatching of the doors, trunk extension can be accomplished by initiating airflow into the trunk. Partial retraction can be accomplished by shutting off the air supply, but small actuators or a suction pressure in the trunk will be required for final closure. Further discussions of this and alternate concepts of orbiter trunk protection are presented in the section on Trunks.

Although only a lifting body orbiter was studied, results are generally applicable to other orbiter configruations shown in refs. 1 through 6.

Summary of Results for Orbiter

Table IV summarizes characteristics of this ACLS. The weight of the ACLS without doors to protect the trunk from the thermal environment is 2.44% of the 260,000-lb landing weight of this orbiter. This figure compares to 2.78% for the medium pressure booster ACLS without a thermal protective layer on its trunk.

Materials such as graphite fibers or fabrics, with suitable oxidation protection, show a potential for being used for trunks that could be stowed externally on orbiters; however, the present status of these materials relative to requirements of such trunks is such that their use can be considered only after further development. Therefore, for the present study it was assumed that doors or other thermal protection must be provided for the orbiter trunk.

When a weight increment is added to account for the weight of orbiter trunk protection doors being greater than the weight of conventional landing gear doors, the percentage of the 260,000 lb landing weight is 3.53. This compares to 5.6% estimated for conventional landing gear weight (Vol I, page 3-33 of ref. 2).

Estimates of vehicle structural weight savings or penalties due to the ACLS were not made for the orbiter; however, based on studies of the booster, it is believed that the effect could range from a small saving to a maximum penalty of 1% of the landing weight. Actual effects will depend primarily on relative design pressures for the orbiter lower surface and the ACLS.

Estimates of ACLS aerodynamic effects were not made for the orbiter; however, based on analyses for the booster and tests of a simulated ACLS trunk on a model of an HL-10 lifting body, it is expected that the total drag of the orbiter with an ACLS will not be significantly different than with conventional gear.

Except for trunk thermal protection, the effect of changes in ACLS and orbiter parameters on ACLS weight and performance will be similar to those discussed for the booster; additional details are presented in succeeding sections.

The volume required for the orbiter ACLS engine, fan, and ducts was estimated to be approximately 400 ft^3. This compares to an estimate of 370 ft^3 for conventional landing gear that was obtained by scaling gear dimensions from drawings SK 100769 and SK 100869 of ref. 2.

The volume required by trunk protection doors was computed as 360 ft^3 based on a door area of 728 ft^2 and a door depth of six in. However, it is believed that these requirements can be reduced by techniques such as allowing temperatures on these doors to become higher than temperatures on primary structure, and incorporating insulation inside the doors to maintain presently estimated primary structure temperatures.

Presently there are uncertainties in weight estimates for both the orbiter ACLS and conventional gear. However, the ACLS weight estimate of table IV could increase by approximately 54% before it would equal the estimated weight of a conventional gear.

PRESSURE AND AIRFLOW REQUIREMENTS

Fig. 24 shows the relationship between cushion area and static cushion pressure for vehicles having landing weights from 200,000 to 500,000 lb. This figure is a plot of the equation

$$P_c A_c = W_v$$

It is independent of cushion planform geometry, height of the gap between the trunk and the ground, trunk depth and trunk pressure. The notations, 005, 006A, and 007A refer to the ACLS configurations of figs. 18 through 20. The 008A notation refers to the orbiter ACLS shown in fig. 23.

Fig. 25 illustrates how the length, width, and perimeter of the booster cushion vary vs static cushion pressure. These dimensions are measured at the ground tangent line of the trunk with the vehicle weight supported by the cushion. Because this figure is for the geometrically similar cushions of figs. 18 through 20, with cushion lengths four times the cushion widths, the lengths vary in proportion to the square roots of the areas shown in fig. 24 and inversely with the square root of cushion pressure.

The corresponding dimensions for the triangular planform orbiter cushion of fig. 23 are shown for comparison. For geometrically similar cushion planforms these dimensions would, as for the booster, vary inversely with the square root of cushion pressure.

Fig. 26 shows how the static trunk pressure, P_T, varies with static cushion pressure, P_c, if the ratio of trunk pressure to cushion pressure is kept constant as the design static cushion pressure is changed. Based on previous experience, a ratio of 2 was selected as a nominal value for these studies and variations of ±25% were considered.

The trunk pressure is a primary factor in determining the amount of energy absorbed by the ACLS and the vertical loads during landing; it is also a primary factor in pitch and roll stiffness or stability. For a given trunk cross section shape, trunk depth, and cushion planform, the vertical force per foot of trunk compression is proportional to trunk pressure. The air supply horsepower also increases as trunk pressure is increased. It is desirable to use the lowest possible trunk pressure consistent with energy and stability requirements to keep landing load factors and engine/fan weights low. There is no direct dependency of trunk pressure on cushion planform geometry, height of the gap between the trunk and the ground, or trunk depth; however, energy absorbed by the trunk depends on $P_T \times H_o^2$. Therefore if the trunk depth, H_o, is decreased it may be necessary to increase P_T to provide sufficient energy absorption. Similarly roll stiffness (ft-lb/deg) depends primarily on the square of the cushion width (W_c), the length of the side trunk (L_s), and the trunk pressure. Therefore, if the cushion planform geometry is changed, P_T must also be changed to maintain $(W_c)^2 \ (L_s) \ (P_T)$ constant, if a constant roll stiffness is desired. A similar relationship exists for pitch stiffness.

Fig. 27 presents ACLS airflow requirements vs cushion pressure. This flow was computed as

$$Q = \frac{(C_d h_g)}{12} \quad (p_t) \quad \sqrt{\frac{2 P_c}{\rho}}$$

where p_t is the perimeter of the trunk measured at the static ground tangent.

A nominal value of $C_d h_g = 0.6$ in. was used and variations of ±50% were studied. A value of $C_d h_g = 0.6$ represents a 2 in. gap between the trunk and the ground if the effective orifice coefficient of the gap is 0.3. Similarly it could represent a 1-in. gap with a coefficient of 0.6. It is desirable to design the trunk and the orifices or nozzles in the lower portion of the trunk so that a low value of this coefficient is achieved. For a given cushion pressure and airflow this results in a high clearance between the trunk and the ground with resulting low friction and trunk wear. With a single annular jet near the trunk/ground tangent line, a coefficient of approximately 0.3 can be achieved. With the distributed trunk orifices which have been used on past ACLS designs to provide air lubrication between the trunk and the ground, it may not be possible to achieve this low a value; however, it is believed that a coefficient of 0.6 or less can be achieved and this value, together with the airflow provided for the nominal designs of this study, will result in adequate ground clearance.

For a given value of $C_d h_g$, the airflow of fig. 27 is independent of cushion pressure because the ground tangent perimeter, p_t, varies inversely with the square root of cushion pressure (see fig. 25). Therefore, the product $p_t \sqrt{P_c}$ is a constant. The airflow required for the orbiter is less than for the booster primarily because of the lower orbiter weight and corresponding lower cushion area and perimeter.

Fig. 28 shows the effect of vehicle landing weight and cushion length to width ratio or cushion aspect ratio, AR_c, on airflow requirements if $C_d h_g$ is maintained at 0.6 in. The curves are presented for rectangular cushion planforms with rounded ends. The $AR_c = 4$ curve applies to the cushions of figs. 18 through 20. $AR_c = 1$ represents a circular cushion planform. Because it has the lowest possible ratio of perimeter to cushion area, it requires the lowest airflow to maintain a specified clearance between the trunk and the ground.

The triangular orbiter cushion planform lies just above the curve for $AR_c = 2$ rectangular cushions. Therefore for a given vehicle weight, this shape requires less airflow than the $AR_c = 4$ rectangular shape shown for the booster ACLS in figs. 18 through 20. For a given cushion aspect ratio and $C_d h_g$, the airflow requirement increases in proportion to the square root of the design landing weight. The airflow requirement is independent of cushion pressure, trunk depth and trunk pressure.

AIR SUPPLY SYSTEMS

Self Contained Systems

Tables V and VI summarize air supply system characteristics for the booster and the orbiter. The horsepower that must be delivered by the engine driving the fan that supplies the ACLS air flow can be computed as

$$hp = \frac{(P_T + \Delta P)\ (Q)}{550 \times E} \quad , \qquad (1)$$

where ΔP is the pressure loss from the fan to the trunk, and E is an efficiency which accounts for the fan efficiency and engine/gearbox losses. For this study ΔP and E were assumed to be constant at 60 lb/ft^2 and 0.85 respectively.

Fig. 29 shows how, for a constant value of $C_d h_g$, horsepower and engine/fan system weight increase as cushion pressure is increased. It also illustrates the strong dependency on $C_d h_g$, the product of the effective discharge coefficient of the gap between the trunk and the ground and the actual clearance between the trunk and the ground. To keep the horsepower requirement and the engine/fan system weight low, it is essential to design the trunk and its orifices to give a low value of C_d and to provide the minimum acceptable gap. For landings on concrete or macadam runways, a gap of 1 in. is expected to be acceptable and a coefficient of 0.6 or less is believed to be attainable. Therefore, $C_d h_g = 0.6$ in. has been used as the nominal value for this study. Because of the sensitivity of system weight to this parameter, additional analyses supported by tests should be performed to establish more firmly the required gap and the value of C_d that can be achieved. This is essential if it is necessary, for other reasons, to use a cushion pressure greater than 90 lb/ft^2.

If, it could be established that for a given vehicle weight the value of $C_d h_g$ can be allowed to decrease inversely with P_c, the horsepower requirement would become independent of P_c. Then instead of the air supply system for the high pressure ACLS of fig. 20 being more than 2400 lb heavier than that for the low pressure ACLS, the weights would be equal. The total weight of the high pressure ACLS would then be close to the weight of the low pressure ACLS. Although presently there is insufficient data to justify such a variation of $C_d h_g$ with P_c, it does seem reasonable to expect better air lubrication between the trunk and the ground at the higher cushion pressures. This should permit use of smaller gaps at the higher pressures.

The engine/fan system weights shown in fig. 29 and subsequent figs. were obtained from fig. 31. Fig. 31 was obtained by making weight estimates for the engine/fan systems for the booster air cushion landing systems of figs. 18, 19, and 20 and plotting the resulting weight vs horsepower. This weight vs horsepower curve was then used to estimate all engine/fan system weights for both the booster and the orbiter. Basic dry engine weights of approximately 0.2 lb/hp were used. Fuel was provided for 10 min at rated power at a fuel flow of 0.5 lb/hp - hr and 30 min at idle with a flow 10% of that at rated power. Weight estimates for the fans and for items such as oil, instruments, controls, inlets, firewalls, mounts, etc., were made on the basis of previous design studies and experience with similar systems.

Fig. 30 presents horsepower and subsystem weight vs vehicle weight for $C_d h_g = 0.6$. Curves are presented for cushion pressures of 90 and 180 lb/ft^2 and for rectangular cushions (with semicircular

ends) having aspect ratios of 2 to 4. Points representing low and medium pressure booster ACLS configurations 005 and 006A are shown, together with a point for medium pressure orbiter ACLS configuration 008A. Although the orbiter ACLS uses the same cushion pressure as the 006A booster ACLS, its horsepower requirement is much less because of the smaller vehicle weight and also because its triangular cushion planform is more efficient than the $AR_c = 4$ cushions used on the booster.

Fig. 32 compares the shuttle booster and orbiter ACLS horsepower requirements with the lift horsepower requirements of current state-of-the-art air cushion vehicles and with the horsepower of the LA-4 ACLS. The lift horsepowers of the air cushion vehicles generally are close to the curve $hp = 0.117 \times W^{5}/^{6}$. The variation of hp as the 5/6 power of vehicle weight results if vehicle weight is assumed to vary as L^3. Then for geometrically similar cushions, P_c varies as $W^{1}/^{3}$. However, if P_c is maintained constant, a variation of hp as $W^{1}/^{2}$ results as shown in fig. 30.

Although the ACV lift horsepower data gives a general indication of ACLS power requirements, it is not directly applicable because the ACV is designed for water and/or very rough field operation whereas the shuttle vehicle will normally land on a prepared runway. Also ACV trunk configurations are significantly different from those for an ACLS.

Although an extrapolation over a large weight range is involved, it is believed that experience with the LA-4 airplane fitted with an ACLS is more applicable. This aircraft with its ACLS weighs approximately 2500 lb, uses an ACLS engine rated at 92.5 hp, has a cushion pressure of 60 lb/ft^2 and a trunk pressure of 180 lb/ft^2.

The LA-4 ACLS horsepower was scaled to the orbiter and booster air cushion landing systems by using the formula

$$hp = \frac{\sqrt{2/\rho}}{550E} (C_d h_g) (P_c) \frac{(P_T + \Delta P)}{P_c} (W)^{1/2} \left\{ \frac{[\pi + 2 (AR_c - 1)]}{\sqrt{\pi/4 + (AR_c - 1)}} \right\} \qquad (2)$$

Differences in cushion pressure, weight, and cushion aspect ratio were accounted for. It was assumed that $C_d h_g$ and $(P_T + \Delta P)/P_c$ (the ratio of fan discharge pressure to cushion pressure) were the same for the LA-4 and the shuttle vehicles. Results of this scaling are plotted on fig. 32. These results are very close to the previously presented shuttle horsepower requirements based on $C_d h_g = 0.6$ in. The LA-4 has demonstrated an ability to operate on plowed fields, snow, and water as well as on prepared runways; this is believed to assure that computed shuttle horsepower requirements are adequate and probably conservative. However, additional analyses and tests are recommended to determine the effects of vehicle size and thus to further validate these calculations.

Fig. 33 shows the effect of trunk pressure on the horsepower and engine/fan system weight for the low pressure booster ACLS (005 configuration). Similar trends would exist for the orbiter and for the other booster air cushion configurations. Equation 2, can be used to estimate the effects of P_T and ΔP (fan to trunk losses).

Fig. 34 shows typical ACLS pressure vs flow curves. The fan flow curves shown here were used for the landing simulations discussed in the section on energy absorption.

Alternative Air Supply Systems

Weight estimates presented in figs. 29 through 33 were based on the assumption that the air flow for the ACLS would be provided by dual turboshaft engines driving one or two stage fans. Many alternate methods of supplying this airflow could be considered. These include auxiliary power units that use residual hydrogen or hydrogen and oxygen, and the landing/ferry jet or turbofan engines. Shuttle vehicle auxiliary power units provided for other systems or elements of rocket propulsion systems might be incorporated into the ACLS air supply system. However, the present study included only a cursory examination of alternates.

Therefore an investigation of alternates was limited to a brief study to establish feasibility and possible benefits of using landing/ferry engines to provide the ACLS air flow and pressures. The following methods were considered:

(1) Mechanically driven fans operated from the engine accessory drive pads
(2) Diversion of part of the bypass air to ACLS; throttling the air to the required pressure when necessary
(3) Diversion of part of the hot gas before entry to the power turbine and expanding it in a separate turbine to drive a fan supplying air to the ACLS
(4) Compressor bleed:

    (a) to supply the ACLS directly by throttling
    (b) to drive an air turbine-fan combination
    (c) to provide the primary air for an air supply ejector
    (d) to supply a separate combustion chamber and turbine-fan

The study was limited to the booster low pressure ACLS. Four turbo fan engines of bypass ratio 5 in the 40,000 thrust class were assumed to have the following characteristics:

(1)	Bypass fan pressure ratio	1.5
(2)	Bypass fan air flow	2000 lb/sec
(3)	Core engine air flow	400 lb/sec
(4)	Available specific gas power	120 Btu/lb
(5)	Normal maximum permissible compressor air bleed	3%
(6)	Engine inlet conditions	S.L.S.

It was concluded that:

(1) Each of these methods is theoretically feasible with the exception of 4 (a), which is definitely not possible because the air flow required by the ACLS is considerably more than the allowable bleed. Method (1) is the most economical in terms of engine thrust degradation. At rated engine power the reduction of thrust would be about 1.5%, increasing at lower engine power settings.

(2) Method (2) is more costly at full engine power as the bypass air is at a higher pressure than required by the ACLS. The thrust loss would be about 5% increasing at lighter loads.
(3) Method (3) is comparable to method (1) but would inevitably have higher losses due to the ducting of hot gas to a small and possibly less efficient turbine.
(4) Method (4) is the least desirable unless the engine is specially designed for a high percentage customer bleed. Even so, method 4 (a) is not at all feasible and the thrust degradation with methods 4 (b), 4 (c) and 4 (d) is likely to be higher than for methods (1), (2) and (3).

Although there are several ways in which landing/ferry engines might be used to provide ACLS air flow, the potential weight savings are relatively small, at least for low pressure air cushion systems. Because the landing engines will probably be located a considerable distance from the ACLS trunk, installation of ducting etc., could be complex with attendant high losses and weight penalties. The requirement for relatively constant ACLS pressure and flow during wide ranges of landing engine power settings could result in undesirable complexity.

It is tentatively recommended that separate turbo-shaft engines be employed to drive the fans for the ACLS as this would ensure adequate cushion flow under all conditions regardless of the landing engine power settings and the use of thrust reversal, etc.

These conclusions are very preliminary and should be reviewed before proceeding with design of an ACLS for shuttle vehicles. In addition it would be desirable to investigate other possible means of providing the air flow.

TRUNKS, ATTACHMENTS AND THERMAL PROTECTION

Summary of Booster and Orbiter Trunk Characteristics

Table VII summarizes characteristics of the trunks for the booster air cushion landing systems shown in figs. 18 through 20. Weights of the basic trunks required because of static and dynamic loads, weights of an outer protective layer to protect the load carrying plys, and weights of attachments on the vehicle are shown separately. Also shown are the insulation weights that would be provided on the area now covered by the trunk (ref. 1). Because the temperatures at the inner surface of the trunk are predicted to be comparable to those on the inside of the insulation, it has been assumed that this insulation can be removed. The last line of table VII presents the net weight of the trunk, including its protective layer and its attachments, minus the weight of vehicle insulation removed.

Table VIII presents a similar summary for the trunk of the orbiter shown in fig. 23. Instead of a protective layer on the trunk, doors are provided so the trunk can be stowed internally.

The trunk cross sections used for the booster are shown in figs. 18 through 20. These shapes corresponding to section 2 of fig. 35 with $W_A/H_O = 1$. This shape was selected after a study of the effect of the cross section on tensions in the cross section, trunk weight, and energy absorption by the trunk.

The trunk cross section for the orbiter, as shown in fig. 23, has a section with $W_A/H_O = 0.5$. The smaller W_A/H_O was selected to minimize door width.

Fig. 35 shows how the tension in the cross section varies as the shape of the cross section is changed, with the trunk depth and trunk pressure held constant and with zero cushion pressure. The curve has been nondimensionalized so it can be applied to trunks of any depth with any pressure.

The cushion pressure equal to zero case represents a situation prior to touchdown. During touchdown, the rear trunk is compressed, the radius decreases, and if trunk pressure remained constant the tension in the rear trunk would decrease. Computer simulations have shown that, even though trunk pressure does increase during the landing, the decrease in radius more than compensates for this and during the initial phase of the landing the tension in the rear trunk is generally less than prior to touchdown. The simulation results also show that as the rear trunk compression decreases, the tension again increases, but generally it does not exceed 150% of the pretouchdown tension.

If the vehicle lands at a significant angle of attack, the compression of the rear trunk may result in an increase in trunk pressure before the front trunk touches the ground. This causes the tension in the front trunk to increase. Computer simulations of booster and orbiter landings have shown the maximum tension to be of the order of 150% of the pretouchdown tension.

Fig. 36 shows static vertical force vs deflection curves for a 1-ft trunk section of the booster low pressure ACLS. This trunk is 13 ft deep prior to touchdown. These curves also apply to the

medium and high pressure air cushion systems of figs. 19 and 20 if the nondimensional scales are used. For a given pressure and initial trunk depth, the trunk cross section shape selected for the orbiter produces somewhat lower vertical forces.

The curves of fig. 36 are plotted for various constant values of trunk pressure and cushion pressure. The vertical force includes the contributions of cushion pressure acting on an area (1 ft x X_2) and trunk pressure acting on an area (1 ft x X_3) as shown in fig. 38. The variations of X_2 and X_3 with trunk compression and with trunk and cushion pressure are accounted for in fig. 36.

The circles at the left ends of the curves of fig. 36 represent cases with no flattening of the trunks ($X_3 = O$). The solid circle on the $P_C = 90$; $P_T = 180$ curve represents the situation with the vehicle static on the ground with the cushion supporting the weight of the vehicle.

Curve A of fig. 37 is a nondimensional form of the trunk material tension vs elongation characteristic used to generate fig. 36. It was based on tests of an early material developed for a C-119 ACLS. Vertical force vs deflection curves computed for a trunk having the material characteristic of Curve B of fig. 37 were very similar to those shown in fig. 36.

Trunk Materials

The trunk for the LA-4 ACLS was fabricated with two plys of a one-way stretch nylon fabric, natural rubber and an outer layer of neoprene for abrasion resistance. Subsequent trunk material development at Bell has resulted in one and two-way stretchable materials employing nylon cords wrapped around a core instead of the nylon fabric. Materials for the ranges of tensions required for the shuttle have been made with varying degrees of stretch in two perpendicular directions. Elongations from 100 to over 300% at ultimate load have been demonstrated. These trunk materials are suitable only for the temperature ranges encountered by subsonic aircraft; however, thermal analyses and a survey of potential high temperature trunk materials have indicated the feasibility of similar stretchable trunks for external stowage on a booster or internal stowage on an orbiter.

Thermal analyses of booster trunks, discussed in a subsequent section, indicate that temperatures of the load carrying plys can be kept below 350°F by adding a protective outer elastomeric layer weighing 0.7 to 1.2 lb/ft^2. Temperatures at the outer surface of this layer are predicted to be in the 400 to 600°F range. Materials suitable for fabrication of trunks for these temperatures are available. Considerably higher temperatures can probably be tolerated for short periods of time without significant degradation. Therefore, external stowage of trunks on the booster and reuse for up to 100 flights appears feasible. Further study of possible extreme thermal environments, fabrication of samples of trunk material, and testing with simulated booster thermal environments are recommended to substantiate this conclusion.

Thermal analyses of trunks for orbiters indicate that fabrication of trunks for external stowage is not feasible with materials presently available. Temperatures on the outer surface of an external trunk would approach the 1800 to 2200°F vehicle lower surface temperatures presented in Vol. I of ref. 2. Graphite fabrics might be used to provide the required strength at weights competitive with present low temperature trunks; however, oxidation of these materials is severe at elevated temperatures, and to date stretchable fabrics or cords have not been fabricated. Even multiple plys of such fabric are expected to have unacceptable leakage. Because of the weight advantage and

simplicity of an externally stowed trunk, further investigations of graphite and other advanced materials for possible future application to orbiters or other high speed aircraft is recommended. However, for the present study it has been assumed that trunk materials used for the booster would also be used for the orbiter but these must be stowed internally or otherwise protected from the thermal environment.

Fig. 39 presents room temperature strengths of natural rubber and of several high temperature elastomers, after exposure to temperatures up to 600°F. Because the elastomers are used primarily to contain the low pressure air in the trunk and strength of the trunk material is due primarily to cords rather than the elastomers, the strength capability of EPDM (ethylene propylene diene), silicone and Viton B (when properly compounded with heat stabilizers) should be more than adequate even after long exposure to temperatures up to 600°F.

It is believed that the strength degradation shown for the Viton B and EPDM is due primarily to oxidation rather than to an instability due to the heating. The anticipated exposure of the booster trunk to temperatures in excess of 350°F is a few minutes per flight rather than hours and these temperatures will be experienced only in outer portions of the material.

Proprietary data from other contractors has shown that elastomeric compounds can be developed for short time exposure to temperatures over 1000°F with very little surface degradation. Also thin samples of silicon rubber compounds have been tested at Bell with very high heat flux rates for short periods. One sample tested at 30 Btu/ft^2 sec for 2.25 sec (15 times the booster lower surface peak heating rate of fig. 45) experienced an average thickness loss of only 0.002 in.

The applicable data on elastomers for ACLS trunks designed for high temperatures is rather limited and the data is for test conditions that may not be directly applicable to shuttle vehicles; however, it is concluded that basic elastomeric materials suitable for booster trunks are available. If these basic materials are properly compounded it is expected that they can withstand temperatures considerably higher than presently predicted trunk temperatures and can be used for many missions before replacement or refurbishment. These conclusions should be confirmed by tests at conditions representative of and more severe than anticipated booster trunk thermal, pressure, and flow environments.

Figs. 40, 41, and 42 present strength and elasticity characteristics of Nomex during and after exposure to elevated temperatures. Nomex is a temperature resistant nylon that is considered to be a prime candidate for cords to provide the strength of shuttle vehicle trunks.

For this study, trunks have been designed with protective outer layers to maintain the load carrying cords at temperatures below 350°F. During exposure to these temperatures, loads on the retracted trunk will be low compared to the design loads experienced during landing. By the time of peak loads, temperatures of the cords should be well below 350°F. Fig. 42 shows that even after exposure to 500°F for 100 hr the after exposure strength is almost equal to the original strength. It is concluded that Nomex is a suitable candidate material for cords in externally stowed booster trunks or protected orbiter trunks.

Basic Trunk Weights

Fig. 43 presents the trunk material unit weights (lb/ft^2) used to estimate the weights of the trunks without thermal protection. Also shown are the ultimate tensions required for the low, medium and high pressure trunks for the booster and the medium pressure trunk for the orbiter. These ultimate tensions are five times the pretouchdown tensions in the trunks.

Also shown are computed strengths of 2, 4, and 6 ply trunk materials with 16, 22, and 28 Nomex cords per in. The double circle represents the estimated weight and strength of a trunk material for the DHC-5, C-8 airplane. These estimates were based on an assumed use of multiple plys of a material developed and tested for the LA-4 ACLS.

It may appear that the use of an ultimate tension five times the pretouchdown tension plus the additional safety factor due to using a weight vs ultimate line well above the computed points is unnecessarily conservative if maximum dynamic tensions are not expected to exceed 150% of the pretouchdown tensions. This conservatism should provide for local reinforcement at trunk to fuselage attachments, brake attachments, etc. It should also provide for reinforcement that may be required because of stress concentrations that may occur in the trunk near the inner radii of the end trunks. Subsequent paragraphs will also show that if the basic trunk were made lighter any saving would be offset by the need for additional thickness of an outer layer for thermal protection if the trunk is to be stowed externally on the booster.

Booster Trunk Thermal Protection and Total Trunk Weights

After a review of Phase A vehicle study reports (refs. 1 to 6), fig. 44 - was selected as a representative stagnation point heat flux curve. On the basis of data in ref. 5 a heat flux 12% of this stagnation point heating was used to compute temperatures, at the forward portion of the booster low pressure ACLS trunk (fig. 45).

Temperature-time histories at several points through trunks having thicknesses 0.1 to 1.0 in. were computed for trunk materials having the following properties:

	Density $lb/in.^3$	Thermal Conductivity $(Btu/ft^2\ hr)\ (°F/in.)$	Specific Heat $Btu/lb°F$
a.	.064	1.32	.33
b.	.0436	1.44	.35

Although thermal properties of candidate trunk materials are not well known at this time, the above values and ±50% variations of conductivity that were studied should bracket actual characteristics. The basic trunk material composites of fig. 43 have densities of 0.053 lb/in^3, midway between the above densities.

Fig. 46 and 47 present computed temperatures in 0.3 in. thick trunks made of materials having the above properties. It will be noted that the peak temperatures are 510 and 560°F, well below the booster maximum lower surface temperatures shown in fig. 48. Also, maximum midplane

temperatures are 240 and 300°F. The trunk outer surface temperatures are well below those of fig. 48 primarily because the trunk acts as a heat sink. Midplane temperatures are even lower because outer layers insulate them.

Fig. 49 shows the computed temperature gradients thru the 0.3-in. thick trunks at three selected times. Figs. 50 and 51 show the effect of trunk thickness on the temperature gradients at the time of maximum outer surface temperature. As trunk thickness is decreased, the outer surface temperatures approach those of fig. 48.

Fig. 52 shows the effects of ±50% changes in thermal conductivity on the temperature gradients at the time of maximum outer surface temperature. Figs. 53 and 54 present the maximum temperatures experienced at any time as a result of the heat flux profile of fig. 45. It will be noted that for trunks 0.3 in. thick or thicker the inner 50% of the trunk never exceeds 300°F with either material.

The preceding data was replotted and interpolated to determine the thickness of a protective layer needed to keep the outer surface of the basic load carrying plys of the trunk below 350°F. This total thickness was plotted on fig. 55. This thickness of the protective layer from fig. 55 was corrected for the assumed 25% prestretch of the retracted trunk and used to determine the unit weight of the protective layer plotted in fig. 56. The unit weight of the basic trunk from fig. 43 was added to obtain the unit weight of the protected trunk in its unstretched condition. The weight estimates of fig. 56 are based on an outer protective layer having properties of material (a) with a density of 0.064 in^3. If material (b) were used, a thicker protective layer would be required but trunk weight would increase less than 5%. Also shown in fig. 56 are unit weights for two low temperature trunk materials based on test data.

Fig. 57 shows the variation of booster trunk unit weight (lb/ft^2) vs cushion pressure and fig. 58 shows the area of unstretched trunk material and total trunk material weight vs cushion pressure. Also shown in figs. 57 and 58 are data for the orbiter. The orbiter trunk weight is 0.53% of the landing weight. The booster trunk without thermal protection is 0.68% of the landing weight. Figs. 59 and 60 show the booster weight increments due to the booster trunks, if existing vehicle external insulation in the trunk area is removed.

Booster Trunk Attachment, Extension and Retraction

Fig. 61 illustrates a concept for attachment of a trunk designed for external stowage. This concept employs a piano type hinge similar to those which have been used on some air cushion vehicles. The fitting on the vehicle side of the hinge transmits the trunk tension loads past the lower surface honeycomb panels and into existing beams that extend across the bottom of the fuselage to support the panels.

The estimated 0.2 to 0.3-in. thickness of the trunks with an outer layer for thermal protection is comparable to the thickness of booster outer surface insulation. Therefore by removing the vehicle insulation in the trunk area a flush installation can be made.

The trunk attachment fittings would be made of high temperature material (titanium was assumed for weight estimates). By extending the outer layer of the trunk over the fittings their temperature can be kept in the 400 to 500°F range.

An externally stowed trunk made of stretchable material acts much like a deicer boot. It is extended by pressurizing the trunk and retracted by cutting off the air supply. Fig. 62 illustrates a typical sequence of events during approach and landing.

Orbiter Trunk Attachment,Extension and Retraction

The orbiter trunk shown in fig.23 is attached to fittings on vehicle primary structure along its inner edge and to the edges of the doors along its outer edge. An exception exists at the front of the trunk where both inner and outer attachments are to the fuselage. ViewC-C of fig. 23 shows that there is a smooth transition from the door attachment to the fuselage attachment at the front ends of the doors.

A stretchable trunk material would be used for the trunk to minimize folding required when the trunk is retracted. When the trunk is retracted, a double thickness would exist over approximately half of the area between the door hinge and the outer attachment.

After unlatching the doors the trunk could be extended, as for the booster, by pressurizing the trunk. Partially retraction could be accomplished by cutting off the air flow. The stretchable material would then pull the doors to a nearly closed position. Free stream dynamic pressure may be sufficient for final closure of the side doors. If not, an assist can be provided by a small negative pressure inside the trunk or by small actuators. This negative pressure could be supplied by a reversible pitch air supply fan, by diverting the air supply through a venturi, or by venting the trunk to a low pressure area on the vehicle after the air supply is shut off.

Because dynamic pressure will oppose rather than assist closure of the rear door, pressure or actuator assistance must be provided there. On the side doors it may be necessary to provide friction devices or dampers to prevent dynamic pressure from closing the doors before the trunk material is clear. The previously mentioned negative pressure, or bungees/springs attached near the mid points of the trunk cross section may be required to assist in producing the single fold required for trunk stowage.

Orbiter Trunk Protection Doors

It was not possible to make detailed designs or perform detailed analyses and weight estimates for trunk protection doors; however, fig. 63 shows the effect of static cushion pressure on the size of ACLS doors. Also shown are ACLS and conventional landing gear door weights based on assumed unit weights of 5 and 10 lb/ft^2. Preliminary estimates indicate that ACLS doors could be made for approximately 5 lb/ft^2 if a depth of the order of 6 in. can be used. ACLS door weight estimates, and the incremental weight due to ACLS door weight minus conventional door weight, presented in the orbiter ACLS weight summaries were estimated with the assumption that both doors weighed 5 lb/ft^2.

The orbiter ACLS was designed with what is considered to be a near minimum door width in order to minimize door weight. Also because of the large increase of door weight with a decrease in cushion pressure (increase in cushion perimeter) was anticipated, the orbiter ACLS was designed with a medium (180 lb/ft^2) cushion pressure rather than a lower value. Further study might show a

somewhat higher or lower pressure may be optimum. Fig. 63 shows that trunk protection weight will be a strong factor in selecting such an optimum, unless very light doors or other means of protection can be developed.

The ACLS doors as presently conceived would not disrupt basic vehicle structure. The trunk would be stored between the basic structure and the ACLS doors. The insulation and/or outer surface panels employed for the basic vehicle would be mounted on the external surface of the doors. Because the weight of this thermal protection is required with or without the ACLS, it has not been considered to be part of the ACLS door weight. It was assumed that a portion of the maximum pressure load on the closed doors could be transmitted to the basic structure via compression of the retracted trunk and/or via spacers in the area not occupied by the trunk. Thus structural loads on the closed doors should be sufficiently low to permit somewhat higher temperatures than are allowed on basic structure. This would permit placing some of the vehicle insulation inside the door rather than on the external surface and could result in a depth increase less than the depth of the doors.

Because the design of such doors is intimately involved with details of the vehicle structure and its thermal protection system, the preliminary concept presented here should be examined in much greater depth along with alternate trunk protection concepts.

Alternate Concepts for Orbiter Trunk Thermal Protection

A variation of the door concept presented in the preceding section would be doors that are not integral with the trunk. Such doors could possibly be opened by the trunk pressure, at least as a backup mode, but actuators would be required if they are to be closed for ferry flights. Preliminary analyses have indicated such doors could be made for approximately 5 lb/ft^2.

Another concept that could be investigated further employs a trunk that is made from a flat sheet, as for the LA-4 ACLS, and is rolled or folded in a compartment that extends across the vehicle at the front or rear of the trunk. Side and center attachments would consist of fittings in which small trunk edge fittings would slide or roll. This is similar to a drapery rod or the concept used for the sail/mast interface on some sailboats. Ratchets or teeth could be incorporated to take drag loads.

Extension could be by cables or lead screws. Retraction for ferrying would not be required because the unrolled trunk would be similar to an externally stowed trunk.When the air supply was cut off,the trunk would fit snugly against the fuselage. The doors, or disposable covers, over the attachment fittings and over the exit to the stowage area would be only a few inches wide and could be left open or off for ferrying.

External protected trunks could also be employed on the orbiter. Such trunks would be designed to fit snugly against the fuselage when retracted; however, instead of being on the outside they would be beneath a thermal protective cover. If the external insulation and/or protective panels used elsewhere on the vehicle lower surface were employed, weight penalties should be small; but unless such thermal protection is mounted on a door, it would be necessary to jettison it prior to landing. This would be acceptable only if a low cost protection system is developed and jettisoning can be accomplished over an uninhabited area.

A variation of this might employ a flexible, but inelastic, cover made of alternate layers of metallic or graphite fabric and insulation. Suitable oxidation protection would have to be developed for the fabrics; however, the development of such a multi-layer inelastic cover should be much easier than the development of the high temperature stretchable material that would be required if the trunk itself were exposed to the orbiter thermal environment.

If such a flexible blanket could be developed, it could be rolled out of the way prior to trunk extension, in a manner similar to the previously discussed method of unrolling an internally stowed trunk.

Drawings or weight estimates were not made for these alternate trunk protection concepts. However, it is believed that several orbiter trunk protection concepts could be developed for weights comparable to or less than the estimated weight of trunk protection doors. Because present ACLS weight estimates are significantly below weights estimates for conventional landing gear, emphasis should probably be placed on simplicity and reliability, with weight an important but secondary consideration.

If expendable heat shields are excluded, a door concept similar to the one shown in fig. 23 is believed to have the desired simplicity and reliability because of its self-extending feature. However, additional study of alternate concepts and their integration with the vehicle design is recommended.

Trunk Flutter

Trunk flutter investigations were not included in this study. Flutter of the trunk is not anticipated to be a problem but it should be investigated analytically and experimentally to ensure that a problem will not exist. Hysterisis inherent in trunk materials and the large mass, relative to the mass of aircraft panels, may be beneficial in supression of trunk flutter. The LA-4 has flown at velocities in excess of 80 knots without any indication of trunk flutter or vibration. Air cushion vehicles have operated at comparable velocities with much larger trunks with no known cases of trunk flutter; however, there is no known data available that is directly applicable to a study of flutter of large ACLS trunks at higher speeds.

When the trunk is retracted, the curvature of the fuselage bottom and trunk pretension are factors to be considered. Steel Velcro beneath the trunk has been suggested as a means of providing additional support for the retracted trunk. It could also be beneficial for flutter prevention.

When the trunk is inflated, trunk geometry and pressure are probably among the significant flutter parameters. Small tubes of trunk material could be fastened to the inside of the trunk and pressurized to several times trunk pressure (i.e., from the braking pressure source) to stiffen the trunk and to effectively divide it into small panels.

In summary, trunk flutter is not likely to be a factor that would make ACLS trunks unfeasible on shuttle vehicles, but neither should it be ignored. If further analyses or tests indicate a possibility of flutter it is believed methods of preventing it can be found as they have been for other aircraft components.

PARKING SYSTEM

The parking system illustrated in fig. 6 consists of a bladder inside the trunk and a control valve to divert flow from the ACLS fan to the inside of the bladder and to seal the pressure inside the bladder for parking. When inflated, the bladder acts much like the inner tube of an automobile tire. The bladder can also provide flotation prior to takeoff or after landing on water. The bladder material can be much lighter weight than the trunk material. Use of a stretchable material simplifies stowage problems. Weight of this system is a small percentage of the total ACLS weight; see tables II and IV.

BRAKING SYSTEMS

Brake Effectiveness and Tread Temperatures

Figs. 6 and 7 illustrate an ACLS braking concept that has been successfully demonstrated with the LA-4 aircraft. Fig. 21 shows a schematic of a brake system. The brake pillows are pressurized by the pilot depressing his brake pedals. Yaw control is obtained by differential pressurization of the pillows on the left and right sides of the aircraft.

The pillows have two functions: first, to depress the brake pads through the small air gap below the trunk and into contact with the ground; second, to deflect the trunk upward to increase the gap beneath the trunk. This reduces cushion pressure so the weight of the aircraft is supported by the brake pads rather than by the cushion.

Tests of a C-119 ACLS braking model and braking and maneuvering tests with the LA-4 have demonstrated proportional braking, braking forces of the order of 1/4 g, and excellent yaw control. The LA-4 uses braking pressures up to 6 lb/in.^{2} (865 lb/ft^2); the C-119 model used brake pressures up to 9.2 lb/in.^{2} (1330 lb/ft^2) which represented a full-scale pressure of 4000 lb/ft^2. These brake pressures bracket the pressures contemplated for shuttle ACLS brakes. Low speed friction coefficients were found to be 1.1 on an abrasive surface and 0.89 on painted plywood.

Because shuttle braking may occur at much higher velocities than those of the LA-4 and model tests, analyses were performed to determine if excessive brake pad temperatures can be expected. Gross estimates of tread wear were also made.

The calculations were made for the booster but can be interpreted for application to the orbiter. The tread material was assumed to be a 50/50 composite of an elastomer and aluminum wires. The aluminum wires were used to conduct the heat away from the surface and reduce surface temperatures. Assumed properties of the composite were:

ρ = .082 lb/in.^{3}

C_p = .28 Btu/lb°F

k = 626 Btu/(ft^2 Hr) (°F/in.)

Friction coefficients of 0.35 and 0.7 were studied. Only maximum braking was considered; i.e., the cushion pressure was assumed to be fully relieved so all the weight not supported by wing lift was on the brakes. It was assumed that landing flaps were deflected; this resulted in approximately 45% of the vehicle weight being on the brakes at a velocity of 200 ft/sec. Aerodynamic L/D was assumed to be 4.

Because of the assumption that the pilot had applied maximum pressure to the brake pillows, the tread area in contact was increased as the pillows flattened to support additional weight as aerodynamic lift decreased. This results in the tread area initially in contact receiving a maximum heat load and the area that comes in contact to support the final increment of weight receiving essentially zero. Temperatures presented here are for the tread area initially in contact.

On the basis of discussions with U.S. Air Force personnel who have conducted tests of ACLS type brake materials, 50% of the braking energy was assumed to contribute to heating of the brake tread. An exploratory test at Bell shows that this assumption may be conservative. Additional tests to determine relationships between brake tread heating, velocity, brake pressure, friction coefficient and wear are recommended so that future calculations will have a firmer base.

Maximum brake tread areas (A_b) of 200 to 2000 ft^2 were studied with maximum brake pressures selected for each case so that at zero velocity the maximum brake pressure times maximum brake area would support all of the vehicle weight.

Figs. 64 and 65 present time histories of several braking parameters for maximum braking started at a velocity of 200 ft/sec with friction coefficients of 0.7 and 0.35. Fig. 66 shows resulting heat flux rates to the areas initially in contact for the case with total brake area of 200 ft^2. The heat flux rate for cases with other maximum brake areas can be obtained from this figure by multiplying by $200 \div A_b$.

Figs. 67 and 68 show the effects of brake areas and tread thickness on tread temperature time histories. Temperatures shown are surface temperatures; however, with the assumed properties of the composite tread, it was found that although internal temperatures lagged the surface temperatures, soon after the end of the braking run they approached these peak surface temperatures.

Fig. 69 shows the effect of brake area on maximum tread temperatures. It will be noted that the friction coefficient had only a small effect on the maximum temperatures. Figs. 67 and 68 also indicate that maximum temperature rise (from initial 100°F) was dependent primarily on the total mass of the tread (i.e., fig. 67 shows comparable temperatures for $A_b = 200$; $t = 0.6$ and for $A_b = 400$; $t = 0.3$ in.).

Fig. 69 also shows the absolute maximum brake tread areas that could be provided on each of the booster air cushion systems of figs. 18 through 20. Because practically, it will be difficult to provide even half of these maximum areas, this indicates that the low pressure (005) ACLS has the advantage of room for more brake tread area with resulting lower tread temperatures.

Fig. 70 shows the effects of tread weight, velocity at the starting of braking, and friction coefficient on maximum brake temperatures. Also indicated is the weight of a brake tread having an area of 443 ft^2 and a thickness of 0.3 in. This area is required if all the vehicle weight is to be supported by the brakes with a brake pressure of 1000 lb/ft^2. Temperatures shown for this tread configuration are probably marginal if maximum braking is initiated at a velocity of 200 ft/sec. However, if instead of using a uniform tread thickness, the same tread weight was used but it was concentrated on the area that is in contact throughout the braking, the maximum temperatures could be reduced by 30 to 50%. In addition, it will probably not be practical to completely relieve cushion pressure as was assumed in the analyses.

If only 1/2 of the maximum available brake pressure is used, 1/2 of the weight not supported by aerodynamic lift will be supported by the cushion and 1/2 by the brakes. This would cut brake temperatures by approximately 50% at the expense of approximately doubling the braking distance.

Fig. 71 presents minimum booster stopping distance vs velocity at the start of maximum braking. This curve assumes that cushion pressure can be reduced to zero so all the weight not supported by aerodynamic lift is supported by the brake treads. If only 50% of this theoretical maximum braking is achievable (i.e., cushion supports half of weight not supported by aerodynamics), these distances would be doubled.

The preceding discussions assumed friction coefficients of 0.35 and 0.7. A coefficient of at least 0.7 should be attainable on dry runways at low speeds; however, ref. 13 and other NASA reports have shown the friction coefficients of skidding tires at 100 knots (169 ft/sec) can be as low as 1/3 of the low speed coefficient. The same report indicates a 50% increase of the very low speed friction coefficient as tire pressure is decreased from 300 lb/in.^{2} to the pressure range being considered for ACLS skid type brakes (1000 lb/ft^2 or 7 psi).

Ref. 13 also shows drastic reductions of tire friction coefficients on wet runways due to hydroplaning whereas ref. 14 shows relatively little effect of runway wetness on the friction coefficient of metal skids at a pressure of 3230 lb/ft^2 (22 lb/in.^{2}) at velocities up to 120 ft/sec. These metal skids had friction coefficients of 0.25 to 0.35 on the wet runways.

It is expected that ACLS type brakes will also be relatively unaffected by wet runways due to the forward skids wiping the runways for trailing skids. The ACLS air flow should also help to dry the runway; however, further investigations are needed to determine friction coefficients and temperatures of low pressure metallic and rubber skid type brakes at various velocities and runway conditions.

Although calculations in early paragraphs of this section were based on the booster, they were also used to estimate brake system weights for the orbiter. It was assumed that the orbiter would not be braked at velocities above 200 ft/sec although it has a higher landing speed than the booster. Also it was assumed that the orbiter braking system would be designed so brake pressures are comparable to those for the booster. Tables IX and X summarize estimated brake system weights for the booster and orbiter.

Brake Tread Wear

The LA-4 airplane ACLS and C-119 brake model used neoprene brake treads. Only qualitative wear data is available. Ref. 10 reports on 20 brake applications with the LA-4 at speeds from 10-45 mph to rest. Brake pads were still functional but wear was found to be uneven. It was concluded that braking effectiveness could be improved and wear reduced by redesign to give more even distribution of brake loads.

Ref. 8 reports on tests of a C-119 braking model. Tests were made at model velocities up to 31 ft/sec, which represented a full-scale velocity of 53 ft/sec. The neoprene tread showed satisfactory wear characteristics after 85 tests.

Because no other directly applicable data for wear of low pressure rubber skid brakes was found, an attempt to estimate wear of a rubber ACLS tread during a maximum braking was made by extrapolating results of a severe case of tire skidding presented in ref. 13. This tire had a vertical load of 10,000 lb on an area of 40 in.^{2} for a pressure of 250 lb/in.^{2} or 36,000 lb/ft^2. This is 36

times the maximum brake pressure proposed for the ACLS brakes. This tire skidded 60 ft on dry concrete at a speed of 100 knots (160 ft/sec). One inch of tread and carcass was melted and eroded away in 0.36 sec. During the skid the 40 in.^{2} of contact area was absorbing 460 hp or $\dot{q}$ = 1170 Btu/ft^2 sec. The corresponding heat input to a booster ACLS brake system having a brake area of 1000 ft^2, and a friction coefficient of 0.7 would be only 80 Btu/ft^2 sec even if all the heat generated at a velocity of 200 ft/sec went into the brake tread. However, the total heat load during the 0.36 sec tire skid was computed to be 420 Btu/ft^2. This is very comparable to the total energy per ft^2 in the area of maximum ACLS tread heating if maximum ACLS braking was used from 200 ft/sec to zero velocity with a maximum brake area of 1000 ft^2. This indicates that if the total energy is the primary factor in tread wear, and this maximum braking were attempted with the proposed ACLS brake system, approximately 1 in. of tread would be worn away; however, if the rate of energy absorption controls wear, the ACLS tread wear would be at least an order of magnitude less than that of this skidding tire.

The validity of the latter conclusion is supported by an exploratory test made at Bell with a rubber/aluminum composite having a vertical load of 2160 lb/ft^2. It was tested for 5.6 sec on concrete at a velocity of 85 ft/sec. Its friction coefficient was approximately 0.4 during the test. The total heat energy was computed to be 530 Btu/ft^2; this is more than the input to the skidding tire or the ACLS with maximum braking. However, wear on the 1-in. thick sample was almost imperceptible.

A possible explanation is that the excessive wear on the skidding tire was a result of the very high pressures and corresponding high rate of energy dissipation per ft^2 (1170 Btu/ft^2 sec) compared to that of the Bell test specimen (95 Btu/ft^2 sec) and that contemplated for the ACLS (less than 80 Btu/ft^2 sec).

Additional testing is required to explain differences in wear estimates based on data from these two sources; however, it is tentatively concluded that wear data from skidding high pressure tires is not applicable to ACLS low pressure brake treads. It is believed that ACLS skid brakes can be reused for a number of flights except possibly if emergency maximum braking is used at very high speeds.

If further testing shows that brake treads made from elastomers or elastor/metal composites are not satisfactory, metal facings could be added to the ACLS brake treads as indicated in fig. 61. Wear data presented in ref. 14 indicates metal skids can be expected to have a weight loss of 0.1 to 0.50 lb per million ft-lb of energy dissipated. A 433,800 lb-booster at a velocity of 200 ft/sec has a kinetic energy of 270 million ft-lb. If all of this were dissipated by the brakes, the wear should be from 27 to 135 lb with metal skids. This is 1.7 to 8.5% of the 1570-lb tread weight allowance in the booster ACLS weight estimates. This weight allowance would permit the use of steel treads with a thickness of 1/8 in. over the center third of the tread area and tapered to near zero at the edge of the tread area.

EFFECTS ON VEHICLE STRUCTURE

The study included an investigation of the effects of an ACLS on the structure of only one of the two vehicles. The booster was selected because at the beginning of the study, the feasibility of an ACLS on the orbiter was more open to question than an ACLS for the booster. Therefore, a study of effects on the orbiter structure would have been wasted effort, had the thermal environment made an ACLS impractical for the orbiter. Also the lack of information concerning effects on booster structure would have resulted in a gap concerning a system which appeared very attractive without consideration of structural effects.

The weights of attachments of the booster trunk to the vehicle structure have been included under Trunks, Attachments and Thermal Protection. An investigation was also made of the effects of trunk and cushion pressures on vehicle lower surface panels, and on the frames supporting the panels. The bending moments and shears due to the ACLS and conventional gear were also compared.

Ref. 1 indicates that the fiberglass honeycomb panels on the lower surface of the vehicle are designed for 3 $lb/in.^2$ ultimate (432 lb/ft^2). Page 8-239 of Vol. IV, ref. 1 presents a weight of 0.89 lb/ft^2 for these panels.

Table XI shows the trunk and cushion pressures for the booster low, medium and high pressure ACLS of figs. 18 through 20. The static pressures listed are the actual pressures present with the vehicle weight supported by the cushion. These pressures were multiplied by a factor of 1.5 to account for possible transient pressure rise during landing and an additional factor of 1.5 to give ultimate design pressures.

Table XI shows that the resulting ultimate pressures for the low pressure configuration are less than the 3 $lb/in.^2$ for which the panels and their supporting structure are designed. Hence, no weight penalty should result.

The ultimate ACLS trunk pressures shown for the medium and high pressure configurations exceeded the 3 $lb/in.^2$ figure. For these configurations, weight penalties for the panels were estimated by assuming that honeycomb face thicknesses would be increased to maintain a stress of 16,000 $lb/in.^2$ ultimate in the panels. Penalties of 1100 and 1650 lb resulted. These figures might be reduced if the honeycomb depth were increased.

Similar weight penalties were computed for the areas upon which the cushion pressure acts. These weight penalties are negligible for all three configurations.

Weight penalties were also computed for the frames extending across the fuselage to support the panels. Table XI again shows no penalty for the low pressure configuration but significant penalties for the medium and high pressure configurations.

It is believed that the weight penalties shown in table XI are very conservative. Computer simulations for both the booster and orbiter have shown that trunk pressure during 10-ft/sec landings may be 50% greater than pretouchdown pressures; however, they do not significantly exceed the pressures that exist with the vehicle static on the ground. Fig. 72 shows the estimated

weight penalties as presented in table XI and also the penalties if ultimate pressures are 1.5 times static pressures. Fig. 72 can also be interpreted to show the effect of a change in the static trunk pressure for a given cushion pressure.

Within the limits of this preliminary analysis, a change in cushion planform would not have a major effect on the penalties shown in fig. 72. This is because the penalties are associated with pressures acting on the area inboard of the outer trunk attachment. This area is approximately equal to the cushion area and will not change significantly as the shape of the cushion area is changed.

If the trunk depth is decreased with the distance between the inboard and outboard attachments held constant, there will be little effect on the vehicle structure weight increments shown in fig. 72. However, if the distance between inner and outer attachments is decreased in proportion to trunk depth, to maintain the same trunk cross section shape, the weight penalties of table XI that are associated with panels in the trunk area will decrease in proportion to the decrease in trunk depth.

Ref. 1 states that the lower surface is designed for 3 $lb/in.^2$ ultimate although lower surface limit pressures up to 788 lb/ft^2 (5.5 $lb/in.^2$) are shown in fig. 8.5-26 of Vol. IV of that report. Page 8-239 of ref. 1 states that it was assumed that the most severe pressure differential could be limited to 2 $lb/in.^2$ (3 $lb/in.^2$ ultimate) by proper control of the pressure between the heat shield support structure and the tank. If it is subsequently decided to design for an ultimate of 1.5 x 5.5 $lb/in.^2$ = 8.24 $lb/in.^2$ rather than to control the pressure differential there should be a negligible weight penalty even for the high pressure ACLS.

If the space between the heat shield support and the tanks is designed to limit the pressure differential, as stated in ref. 1, it may be possible to use a similar technique with the ACLS. By venting the trunk to this space, the pressure differential across the panels in the trunk area can be limited to near zero. The cushion area would then be subjected to an outward pressure of $P_T - P_C$; however, this area is much smaller than the area subjected to trunk pressure so penalties here should be small. The effect on the fuselage side panels subjected to an outward pressure of P_T would have to be compared to the effect of pressures due to the pressurization system mentioned in ref. 1. Further study would be required to determine whether structural penalties could be reduced by this venting technique.

Such a technique has the potential for another benefit. It would make the space between the tank and the outer panels effectively a part of the trunk volume. This additional volume should reduce peak trunk pressures during hard landings and consequently reduce landing loads. However, because peak trunk pressures and landing loads are already low, resulting benefits may be significant only if further studies or tests indicate significantly higher loads than those predicted at this time.

Results of computer simulated landings were used to estimate shear and bending moments due to 10-ft/sec landings with the low pressure ACLS. Because the initial load with this ACLS is well aft of the c.g., it was felt that this might produce higher bending moments than a conventional gear. However, it was found that loads on the structures were less than those indicated in ref. 1, for landings with conventional gear.

Fig. 8.5-3 of ref. 1 is a sketch indicating that a major portion of the bottom of the vehicle primary structure was designed by landing springback. This together with the lower loads predicted for the ACLS indicates that the ACLS's should result in some structure weight savings; however,

insufficient information was available to make a quantitative assessment of these potential savings. Ref. 1 shows that flight conditions produce body tension loading intensities much larger than the landing load compressive intensities; therefore, it is expected that landing loads are not contributing a large increment to vehicle primary structure weight. The comparative effects of conventional gear and ACLS should be reexamined when more detailed structure and loading data become available.

AERODYNAMIC EFFECTS

Fig. 73 summarizes the estimated out of ground effect drag coefficients for the booster with the high pressure (007A) ACLS, conventional gear, and the low pressure (005) ACLS. The tops of the ACLS bars are tapered to show the decrease in C_D due to ACLS engine/fan momentum drag as velocity is increased from 200 to 300 ft/sec. Because momentum drag is a function of velocity rather than velocity squared, its contribution to the drag coefficient decreases with velocity as shown in fig.74.

Figs. 75 and 76 show the estimated effect of changes in trunk depth on trunk and momentum drag increments for the low and high pressure configurations. Although these estimates indicate a somewhat higher drag for the low pressure ACLS than for conventional gear, the total drag of the aircraft with flaps down for landing is not much greater than with conventional gear.

Although the variations of drag with trunk depth shown in figs. 75 and 76 were estimated for geometrically similar trunk cross sections, they also indicate the potential drag reduction due to partial inflation of the trunk.

Because the trunk cross sections used for the ACLS of figs.18 through 20 are near circular, one might expect that a decrease in drag could be achieved by using a more nearly semicircular cross section of the same depth. However, unpublished results of exploratory tests made at NASA-Langley Research Center showed that adding a fairing to a simulated trunk on an HL-10 model to approximate such a section change had only a small effect.

A comparison of figs. 75 and 76 at points of equal trunk depth shows the estimated effect of a 3:1 change in cushion area or cushion pressure. The 007A high pressure configuration has significantly less drag than the 005 even when allowance is made for its narrower width. Although the smaller wetted area gives some drag reduction, the lower drag of the 007A configuration is largely due to the smaller frontal area and the smaller cushion cavity. If a trunk with the length of the 007A configuration were made as wide as the 005 configuration and with a comparable cushion cavity, drags would be comparable.

Fig. 77 compares estimated drag increments due to the trunk when the vehicle is out of ground effect and when it is on the ground. Although a significant percentage increase in the trunk drag in ground effect is indicated by this figure, a comparison with fig. 73 shows that as a percentage of total vehicle drag the effect is not large.

The out of ground effect ACLS drag coefficient increment of 0.038 predicted for the 005 configuration (fig. 75) is approximately 10% of the vehicle drag at $\alpha = 8°$ with flaps down or 20% of the flaps up drag. This compares with a ΔC_D of approximately 0.018 due to an ACLS on a model of a C-119 aircraft (ref. 7). Approximately the same ΔC_D was measured in free air and with the model on the ground. That increment was only 17% of the flaps up drag of that model at $\alpha = 8°$. The C-119 ACLS drag increment of 0.018 was very comparable to an increment of 0.0173 due to conventional gear. The use of techniques similar to those used for the estimates of shuttle ACLS drag resulted in roughly a 20% underestimation of C-119 ACLS drag out of ground effect and a 20% overestimation with the C-119 on the ground.

Unpublished results of NASA-Langley tests of an HL-10 model with a solid simulated trunk without cushion airflow resulted in an out of ground effect ΔC_D of 0.040. This was slightly greater than an increment of 0.0375 reported in ref. 15 for conventional gear. Using techniques similar to those used for estimates of shuttle ACLS drag, the ΔC_D of this trunk was computed to be 0.045 (12% greater than measured).

Estimates of shuttle booster ACLS pitching moment increments were made by assuming that the change in pitching moment is due primarily to the ACLS drag acting below the vehicle c.g. Based on a reference chord of 29.2 ft, this gives a ΔC_M of -0.024 for the 005 configuration out of ground effect. If C_{M_δ} is assumed to be 0.075 per deg, a control deflection of less than 1/3 deg would retrim the vehicle.

With the vehicle on the ground, the estimated aerodynamic pitch down moment increment due to ACLS drag acting below the c.g. is 80% greater than the inflight increment; however, results of wind tunnel tests of the C-119 model with an ACLS, reported in ref. 7 showed a 4° nose up trim change, with fixed elevator, as the ground was approached. This effect may be due to lift on the cushion with its c.p. ahead of the c.g. A similar effect should be experienced with the shuttle ACLS. It tends to give height stability and an automatic flare.

ACLS effects on shuttle lift are expected to be negligible when out of ground effect. In ground effect, increments may be quite significant, especially for the low pressure configuration with its large cushion area. Because of the complex flow field, analytical predictions were not attempted. Initial computer simulations of landings of the 005 configuration showed a negligible effect due to the cushion prior to touchdown; however, with an approximation of the effect of dynamic pressure at the front of the cushion included, maximum trunk compression during a 10-ft/sec landing was reduced by 12% indicating that the effect of q is quite significant for low pressure air cushion systems after the rear trunk is in close proximity to the ground.

Estimates of aerodynamic effects of the orbiter ACLS were not made; however, based on predictions for the booster, tests of the HL-10 and C-119 models, and an expectation that the triangular cushion planform should give somewhat lower drag than a rectangular cushion with rounded ends, it is believed that the orbiter ACLS will have aerodynamic effects comparable to conventional landing gear.

ENERGY ABSORPTION AND STABILITY

Booster Energy Absorption

Fig. 78 shows results of a computer simulation of a landing of the booster with the low pressure ACLS. The simulation was run without pilot inputs and the vehicle was flown into the ground at a 10-ft/sec sink rate with initial lift equal to vehicle weight.

The lift curve, with landing flaps, used for this simulation was such that over 65% of the vehicle weight would be supported by aerodynamic lift at $\alpha = 0$. Consequently, cushion pressure increased to only a small percent of the static value.

Vertical load factor due to the ACLS was only 0.7 g's for this 10-ft/sec landing. Although vehicle motions are reasonably well damped, drop tests of models of the LA-4 and flight tests of this aircraft indicate that greater damping may be expected from the actual shuttle ACLS.

Peak tension in the trunk was only 30% greater than the static value and peak trunk pressure was approximately equal to the static value. Initial trunk pressure is lower than the static value because of the reduced fan discharge pressure at the greater flow which is present when cushion pressure is zero.

Minimum trunk depth was 7 ft or 54% of the pretouchdown depth of 13 ft. Fig. 79 shows the trunk configuration at the time of maximum trunk deflection.

This simulation did not include the effect of dynamic pressure and inflow of air at the front of the cushion. When the effect of this inflow was included, cushion pressure was increased to 40 lb/ft^2 at the first peak. Corresponding load factor due to the ACLS was reduced by 0.1 g, trunk compression was 1 ft less than for the case shown here, and trunk tension was only 10% more than the static value.

Another simulation with an in flight trunk depth of 10 ft instead of 13 ft yielded very similar results except minimum trunk depth was 4 ft (40% of the initial depth) instead of 7 ft. If sufficient flap clearance were available at this condition, ACLS aerodynamic drag could be reduced by 16%. Because of the requirement for increased thermal protection as trunk thickness is decreased, the lower tension in the 10-ft deep trunk would have little effect on the unit weight (lb/ft^2) of the trunk material; however, the decrease in trunk material area would yield a weight saving over 600 lb. Together with an attachment weight saving of 150 lb, this would decrease the estimated weight of the 005 ACLS configuration by 5.4%.

A 15-ft/sec landing was also simulated with the 13-ft deep trunk. Initial conditions were the same as for the 10-ft/sec landing except that the initial pitch angle was reduced to again give an initial 8° angle of attack and lift equal to weight. Maximum load factor due to the ACLS only increased to 1.5 g's from the 0.7 g's obtained with 10-ft/sec landing. Minimum trunk depth was 6.5 ft compared to the previous 7 ft. This illustrates the tolerance of the ACLS for hard landings.

Fig. 80 shows the total load factor, at the c.g., versus sink rate. Curves of the total g's due to the ACLS plus aerodynamic lift and of the g's due to the ACLS only are shown. The latter curve shows the vertical load factor at the first peak of the time plots from the simulations. The load factor due to the ACLS will of course increase to 1 g as velocity decreases or the flaps are raised.

The peak total load factor at the rear of the fuselage is approximately a quarter of a g greater than that at the c.g. An ACLS with a shorter trunk length would be expected to produce a more even distribution of vertical load factor; however, a somewhat higher load factor at the c.g. would result.

Orbiter Energy Absorption

Fig. 81 presents results of a computer simulation of the orbiter with its medium pressure ACLS. Because of present limitations of the simulation it was necessary to approximate the triangular planform with an equivalent rectangular trunk; it is believed that this approximation did not significantly affect the results.

Aerodynamic lift was initially equal to 1.05 times vehicle weight, but because of the high initial attitude ($\theta = 12.5°$; $\alpha = 14.5°$), it was assumed that the pilot had moved his stick forward to command an angle of attack of 10° at the instant of touchdown.

The effect of dynamic pressure due to vehicle forward velocity was included by assuming that flow in or out of the front of the cushion was proportional to the square root of $q - P_C$.

Despite the greater initial pitch attitude and higher ACLS design pressures, relative to those of the low pressure booster ACLS, simulator results are quite similar to those shown for the booster. Maximum vertical load factor due to the ACLS was again 0.7 g's. Peak tension in the trunk was only 20% greater than the static value and peak trunk pressure was very near the static value. Cushion pressure was initially 40 lb/ft^2 rather than the zero shown initially in the booster simulation, because of the effect of dynamic pressure on the cushion. This cushion pressure together with aerodynamic lift produced an initial vertical load factor of 1.2 g's.

Minimum trunk depth was 50% of the pretouchdown depth. Fig. 82 shows the configuration of the simulated trunk at the time of maximum trunk compression. The shorter trunk, relative to that of the low pressure booster ACLS, resulted in less pitching motion than was shown for the booster. Also shown is the position that the front of the trunk would assume with the vehicle static on the ground. The more forward position is due to forward movement of the trunk as cushion pressure develops and due to the representation of the triangular trunk by a rectangular trunk.

At the end of the simulator run the orbiter was in near equilibrium but still at an attitude near 10°. In an actual landing the pilot would ease his stick forward to relieve aerodynamic lift and allow the vehicle weight to be supported by the cushion.

Booster Pitch/Roll Stiffness

Figs.83 and 84 present computed booster ACLS pitch and roll stiffnesses vs static or design cushion pressure. Pitch stiffnesses shown were computed with cushion pressures of zero. Thus the stiffnesses shown are due to the trunk and variations versus cushion pressure are due to cushion size and trunk pressure rather than cushion pressure. Stiffnesses with cushion pressures other than zero would be greater than those shown here.

Also shown are pitch angle and roll angle changes due to 0.35 g braking. The roll angle changes are shown for two values of $\psi + \beta$. Fig. 85 shows the values of $\psi + \beta$ required to maintain the vehicle on the runway without thrust. If C_D/C_{Y_β} is 10°, a $\psi + \beta$ of 30° or less is required down to a ground speed of 50 ft/sec in a 25-ft/sec crosswind. With 0.35 g braking maintained from a velocity of 50 ft/sec to zero, the vehicle would only travel an additional 65 ft. Therefore either braking and/or $\psi + \beta$ could be reduced for the final phase of rollout.

Although roll angles shown for 0.35 g braking may be tolerable, they are considered marginal for the narrow tread high pressure configurations 006A and 007A. Pitch angles due to braking are acceptable for all configurations but the pitch stiffness of the 005 configuration is probably higher than desirable for takeoff rotation unless C_{M_δ} is 0.075 per deg or more.

A more optimum configuration for pitch and roll stiffness would probably be a cushion with a pressure near 135 lb/ft^2, a width of approximately 42 ft and a length of about 80 ft.

Such an ACLS would have more roll stiffness and less pitch stiffness than the 005 configuration. Its weight would be comparable to the weights of the 005 and 006A configurations. Vertical accelerations at the c.g. would not be significantly greater than for the 005 configuration but pitching motion during landing would be reduced.

Orbiter Pitch/Roll Stiffness

The triangular cushion planform makes estimation of pitch/roll stiffness for the orbiter ACLS of fig. 23 rather complex. Based on ratios of trunk lengths and moment arms of this configuration and those of the medium pressure booster ACLS, it was concluded that stiffnesses of these two configurations differ approximately in proportion to their weights. Therefore, pitch and roll angles due to braking would be comparable for medium pressure booster and orbiter air cushion systems. Further analyses and tests to confirm this preliminary conclusion are recommended.

CONCLUSIONS

It is concluded that air cushion landing systems can be developed for space shuttle boosters and orbiters. The ACLS has a potential for saving 1.5 to 2.0% of the landing weight. Aerodynamic effects are expected to be comparable to those of conventional landing gear. Basic materials suitable for externally stowed trunks on boosters are available but internal stowage or other protection will be required for orbiter trunks.

RECOMMENDATIONS

It is recommended that:

(1) Thermal environments of the booster and orbiter be reviewed to ensure that the most critical environments are considered in ACLS design
(2) Tests be performed on candidate trunk materials to confirm temperature and strength estimates and on candidate brake materials to determine friction coefficients and wear
(3) A more detailed study be made of trunk protection concepts for the orbiter to more firmly establish feasibility and estimated weights
(4) Analyses and tests be performed to more firmly establish engine horsepower requirements; this should include a determination of the effective discharge coefficient of the gap between the trunk and the ground and the determination of gap size required on these large vehicles
(5) A more thorough study be made of the relative effects of an ACLS and a conventional gear on the vehicle structure; the limited information (from Phase A Vehicle Study Reports) on vehicle structure and the effect of conventional gear on this structure permitted only a gross assessment of the effects of the two types of landing gear on vehicle structure
(6) Wind tunnel tests be performed to determine the accuracy of predicted effects of an ACLS on aerodynamic characteristics; this should include investigations of the effect of dynamic pressure due to vehicle velocity on the cushion pressure during landing
(7) The computer simulation of an ACLS should be extended to make it more versatile, and parametric simulations of landings should be made to better determine effects of variations in vehicle and ACLS parameters, singly and in combination
(8) Tests should be performed with dynamic models to confirm accuracy of the computer simulation
(9) More detailed drawings and design analyses be made of an ACLS for a typical booster and for a typical orbiter to substantiate weight estimates and to ensure that ACLS/vehicle interface problems will not be encountered

REFERENCES

1. Anon: Study of Integral Launch and Reentry Vehicle System. NASA MSC 00192 and 00193;(also SD-69-573 vols. I thru V. Space Division, North American Rockwell, Dec. 1969).
2. Anon: Integral Launch and Reentry Vehicle Final Report. LMSC-A959837, vols. I thru III, Space Systems Division, Lockheed Missiles and Space Company, Dec. 1969.
3. Anon: Integral Launch and Reentry Vehicle Systems. NASA CR-66863, CR-66864, CR-66865, CR-66866. (Also - Report MDC E0049, vols. I thru IV McDonnell-Douglas Astronautics Company, Nov. 1969.)
4. Anon: A Two-Stage Fixed Wing Space Transportation System. MDC-0049 vols. I thru III, McDonnell–Douglas Astronautics Company, Dec. 1969.
5. Anon: A Two-Stage Fixed Wing Space Transportation System, Final Report. Report MDC E0056 vols. I thru III, McDonnell-Douglas Astronautics Company, Dec. 1969.
6. Anon: Space Shuttle Final Report. GDC-DCB69-046, vols. I thru X, General Dynamics Convair Division, Oct. 1969.
7. Earl, Desmond T.; Air Cushion Landing Gear Feasibility Study, AFFDL-TR-67-32, March 1967.
8. Earl, Desmond T.; and Cooper, Richard H.: Air Cushion Landing Gear for Aircraft, AFFDL-TR-68-124., Aug. 1968.
9. Stauffer, C.L.: Ground/Flight Test Report of Air Cushion Landing Gear (LA-4), AFFDL-TR-69-23, April 1969.
10. Stauffer, Charles L.: Water Operations and Overland Braking Test Report of Air Cushion Landing System (LA-4), AFFDL-TR-69-125, Dec. 1969.
11. Anon: High Temperature Resistant Aircraft Tires, WADC, MLTDR-64-226, July 1964.
12. Anon: Properties of Nomex High Temperature Resistant Nylon Fiber, New Product Technical Information Bulletin NP-33, E.I. DuPont DeNemours and Company, Oct. 1963.
13. Horne, Walter, B; Yager, Thomas J; and Taylor, Glenn R.: Review of Causes and Alleviation of Low Tire Traction on Wet Runways, NASA TN-D-4406, 1968.
14. Dreher, Robert C.; and Batterson, Sidney A.: Coefficients of Friction and Wear Characteristics for Skids Made of Various Metals on Concrete, Asphalt, and Lakebed Surfaces, NASA TN-D-999, 1962.
15. Gamse, Berl; and Mort, Kenneth L.: Full-Scale Wind Tunnel Investigation of the HL-10 Manned Lifting Body Flight Vehicle, NASA TM-X-1476, 1967.

TABLES

TABLE I

LANDING GEAR WEIGHT COMPARISON

	LA-4 (lb)	C-119 (lb)	C-130E (lb)	LIT (lb)
A/C Gross Weight	2500	60,000	130,000	80,000
Conventional Gear	190	4,569	5,375	-
Proposed High Flotation	-	-	8,217	6,000
ACLS	255	3,400	5,200	3,675

TABLE II

CHARACTERISTICS OF ACLS FOR 433,800 lb-BOOSTER

	Configuration		
	Low P_c	Med P_c	High P_c
Cushion Area, ft^2	4,820	2,410	1,607
Cushion Pressure, lb/ft^2	90	180	270
Trunk Pressure, lb/ft^2	180	360	540
Design Sink Speed, ft/sec	10	10	10
Trunk Depth (In Flight), ft	13	11.1	10.1
Trunk Ground Tangent Perimeter, ft	328	232	189
Trunk Static Tension, lb/ft	1,081	1,830	2,520
Weights			
Trunk and Attachment Wt	5,150 [a]	4,780	4,820
Brake System Wt	3,567	3,567	3,567
Parking System and Controls Wt	566	566	566
Engine/Fan System Wt	1,904	3,171	4,325
	Σ 11,187	12,084	13,278
Thermal Protection Wt, Increment	2,757	1,040	429
Total ACLS Weight	13,944	13,124	13,707
% of Landing Weight	3.22	3.03	3.16

[a] All weights in lb

TABLE III

WEIGHT OF CONVENTIONAL LANDING GEAR (STRAIGHT WING BOOSTER - LANDING WEIGHT 333,180 lb)

	Main Gear, lb	Nose Gear, lb
Struts and Beams	3,946	570
Attach Struc.	2,350	66
Rolling Assembly		
Wheels	840	113
Tires	1,120	150
Brakes	1,620	-
Air	80	10
Systems	1,205	230
	Σ 11,161[a]	Σ 1,139[a]
Structure Attachment	2,980[b]	839[b]
Gear & Attachment	14,141	1,978
Main Gear & Attachment	14,141	
Nose Gear & Attachment	1,978	
Total	16,119	
Gear Weight / Landing Weight	16,119 / 333,180 =	4.86%

[a] see fig. 19 Vol. III of ref. 5

[b] see fig. 4 of Vol. III of ref. 5

TABLE IV

CHARACTERISTICS OF ACLS FOR 260,000-lb ORBITER

	Configuration		
		Med P_c	
Cushion Area, ft^2		1,445	
Cushion Pressure, lb/ft^2		180	
Trunk Pressure, lb/ft^2		360	
Design Sink Speed, ft/sec		10	
Trunk Depth, (In Flight), ft		10.8	
Trunk Ground Tangent Perimeter, ft.		151	
Trunk Static Tension, lb/ft		1,550	
Weights			
Trunk and Attachment Weight		2,004[b]	
Brake System Weight		1,600	
Parking System and ACLS Controls Weight		400	
Engine/Fan System Weight		2,340	
ACLS System Weight		Σ6,344	
Doors Weight Increment [a]		2,830	
Total Weight lb		9,174	
% of Landing Weight		3.53	

[a] ACLS Doors - Conventional Gear Doors

[b] All Weights in lb

TABLE V

BOOSTER ACLS AIR SUPPLY SYSTEM CHARACTERISTICS

	Configuration			
	Low P_c	Med P_c	High P_c	
Trunk Pressure, P_T, lb/ft^2	180	360	540	
Air Flow, Q, ft^3/sec	4,520	4,520	4,520	Nominal 2 in.Gap, Q Proportional to p x P_c
Horsepower, hp	2,313	4,050	5,780	hp = Q x (P_T + 60) ÷ Efficiency
Dry Engine, Gear Box, Fan Wt, lb	1,294	2,092	2,973	Dry Engine Wt: approx. 0.2 lb/hp
Mounts, Ducts, Controls, Oil, etc. lb	417	640	869	
Fuel: 10 min Full Power; 30 min Idle	251	439	625	
Σ Engine/Fan System Wt. lb	1,962	3,171	4,467	

TABLE VI

ORBITER ACLS AIR SUPPLY SYSTEM CHARACTERISTICS

	Configuration			
	Low P_c	Med P_c	High P_c	
Trunk Pressure, P_T, lb/ft^2		360		
Air Flow, Q, ft^3 sec		3,240		
Horsepower		2,910		
Σ Engine/Fan System Wt, lb		2,340		

TABLE VII

ACLS TRUNK CHARACTERISTICS (BOOSTER WITH 433,800-lb LANDING WEIGHT)

	Configuration			
	Low P_c	Med P_c	High P_c	Notes
Cushion Area, ft^2	4,820	2,410	1,607	
Cushion Pressure, lb/ft^2	90	180	270	
Trunk Pressure, lb/ft^2	180	360	540	
Trunk Depth, ft	13	11.1	10.1	
Trunk Perimeter, ft	293	207	170	At Centerline of Retracted Trunk
Trunk Material Area, ft^2	3,090	1,860	1,390	Unstretched Condition
Tension in Cross Section, lb/ft	1,081	1,830	2,520	Static Condition
Basic Trunk Material Wt, lb/ft^2	1.0[a]	1.7	2.3	
Trunk Material Wt, lb	3,090	3,160	3,200	
Trunk Attachment Wt, lb	2,060	1,620	1,620	
Σ Basic Trunk and Attachment Wt	5,150	4,780	4,820	
Trunk Thermal Protection Unit Wt, lb/ft^2	1.26	.93	.68	
Trunk Thermal Protection Wt, lb	3,900	1,730	945	
Vehicle Insulation Removed, lb	1,143	690	516	
Thermal Protection Wt, Increment lb	2,757	1,040	429	
Basic Trunk and Attachment Plus Thermal Protection Increment, lb	7,907	5,820	5,249	

TABLE VIII

ORBITER ACLS TRUNK CHARACTERISTICS

	Configuration			Notes
		Med P_c		
Cushion Area, ft^2		1,380		
Cushion Pressure, lb/ft^2		180		
Trunk Pressure, lb/ft^2		360		
Trunk Depth, ft		10.8		
Trunk Perimeter, ft		125		(℄ of Uninflated Trunk with Doors fully Open)
Trunk Material Area, ft^2		952		Unstretched Condition
Tension in Cross Section, lb/ft		1,580		Static Condition
Basic Trunk Unit Wt. lb/ft^2		1.42		
Basic Trunk Wt. lb		1,350		
Trunk Attachment Wt. lb		654		
Σ Basic Trunk and Attachment Wt. lb		2,004		
Trunk Protection Door, Unit Wt. lb/ft^2		5.0		
Trunk Protection Door Wt. lb		3,640		728 ft^2 at 5 lb/ft^2
Conventional Door Wt. Removed		810		162 ft^2 at 5 lb/ft^2
Door Wt. Increment lb		2,830		
Basic Trunk and Attachments Plus Door Wt. Increment		4,834		

TABLE IX

BOOSTER ACLS BRAKE SYSTEM CHARACTERISTICS

	Configuration			
	Low P_c	Med P_c	High P_c	
Brake Tread Area, ft^2 (Max. P_c = 750)	443	443	443	Est Deceleration > 0.25 G;
Brake Tread Wt, lb	1,570	1,570	1,570	Est 5 to 10 Max. Braking Landings
Brake Pillows and Attachments, lb	1,250	1,250	1,250	or > 25 Normal Landings Before
Brake Controls Wt, lb	304	304	304	Refurbishment
Brake System Wt, lb	3,567	3,567	3,567	

TABLE X

ORBITER ACLS BRAKE SYSTEM CHARACTERISTICS

	Configuration		
		Med P_c	
Brake Tread Area, ft^2 (Max.P_b = 750 lb/ft^2)		260	
Brake Tread Wt. lb		900	
Brake Pillows and Attachments, lb		396	
Brake Controls, W. lb		304	
Brake System Wt, lb		1,600	

TABLE XI

EFFECT OF ACLS ON BOOSTER STRUCTURE

	ACLS Configuration		
	Low Pressure	Med Pressure	High Pressure
Trunk Static Pressure, lb/ft^2	180	360	540
Trunk Static Pressure, lb/in.^{2} Limit	1.25	2.50	3.75
Trunk Static Pressure, lb/in.^{2} Design Ultimate = 1.5 x 1.5[a] (Limit Value)	2.82	5.64	8.45
Weight of Honeycomb Panels = .89 lb/ft^2 for 3 lb/in.^{2} Ultimate (ref. 1, p. 8-239 of Vol. IV)			
Weight of Honeycomb Panels, lb/ft^2	.89	1.38	1.96
Weight Penalty lb/ft^2	0	.49	1.07
Area for the Panels, ft^2	3,820	2,240	1,640
Weight Penalty for Honeycomb Panels, lb (Trunk Region)	(0)	(1,100)	(1,650)
Moment for Frame Extension (ref. 1, p. 8-239 of Vol. IV)	39,200	73,700	110,000
Surface Area for Frames, ft^2	-	3,420	2,880
Weight Penalty, lb/ft^2	0	.754	1.244
Weight Penalty Framework, lb	(0)	(2,580)	(3,600)
Cushion Static Pressure, lb/ft^2	90	180	270
Cushion Static Pressure lb/in.^{2} Limit	.625	1.25	1.875
Cushion Static Pressure lb/in.^{2}, Design Ult. = 1.5 x 1.5[a] (Limit Valve)	1.41	2.82	4.225
Weight of Honeycomb Panels, lb/ft^2	.89	.89	1.175
Weight Penalty, lb/ft^2	0	0	.285
Cushion Area at Fuselage Surface, ft^2	1,332	373	116.6
Weight Penalty for Honeycomb Panels, lb (Cushion Region at Fuselage Surface)	(0)	(0)	(33)
ΔW, lb Σ =	0 lb	3,680	5,283

[a] This factor is intended to account for dynamic magnification effects. Preliminary studies show that this factor may ultimately prove to be too conservative.

ILLUSTRATIONS

Fig. 1. Bell SK-5, 10-Ton ACV

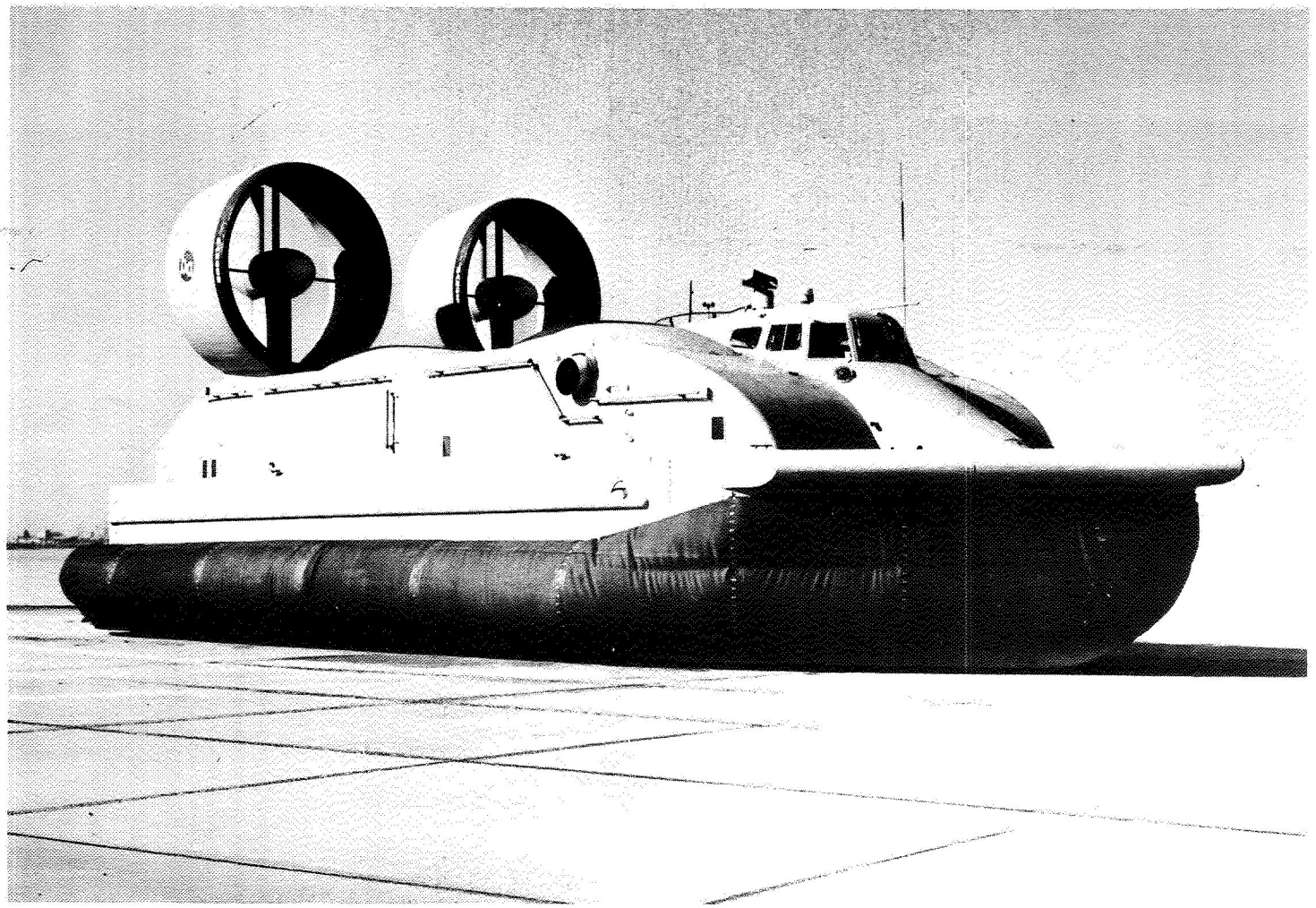

Fig. 2. Bell SK-1, 30-Ton Hydroskimmer

Fig. 3. BHC SRN-4, 170 Ton Hovercraft

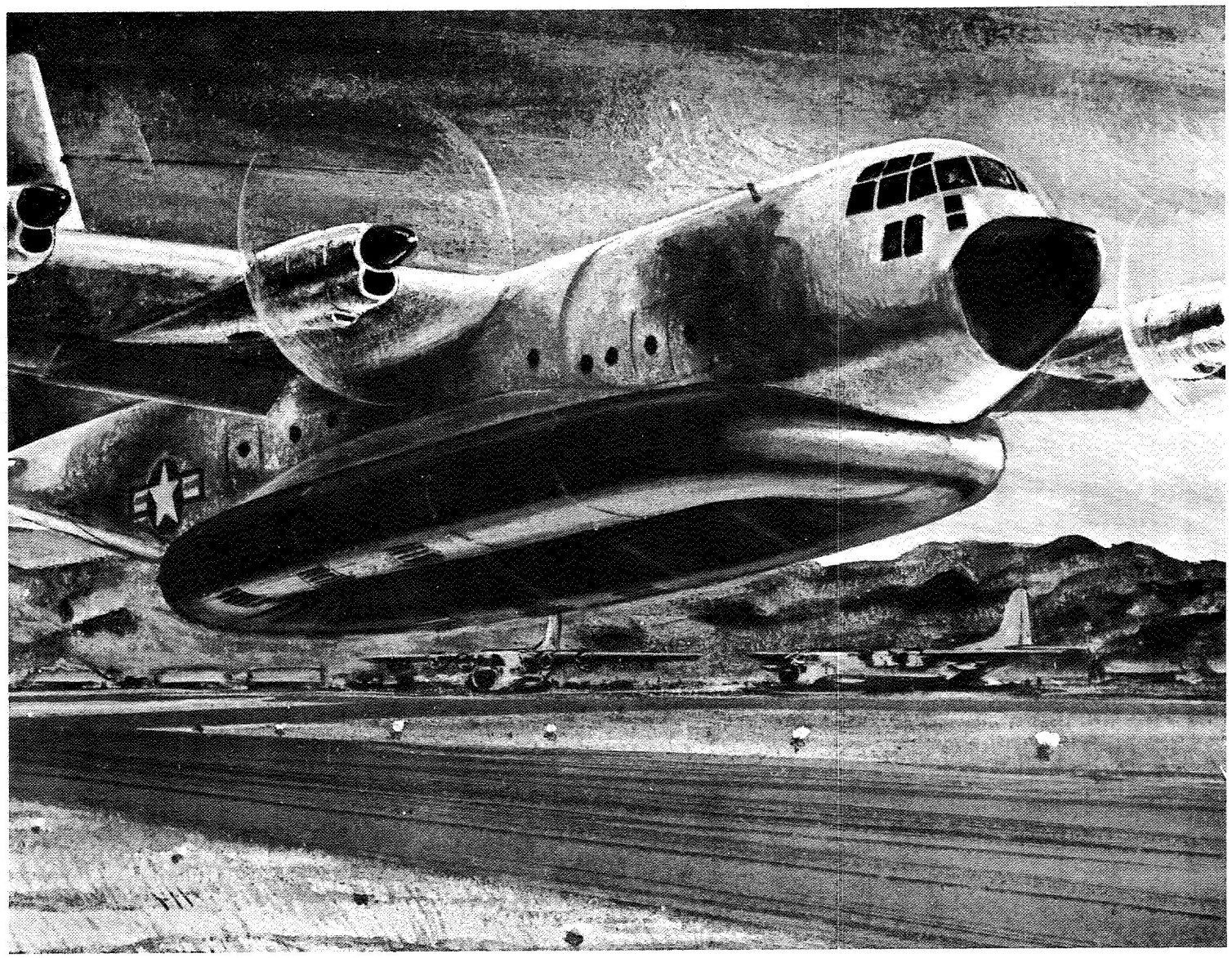

Fig. 4. Artist's Concept of Aircraft with Trunk Inflated

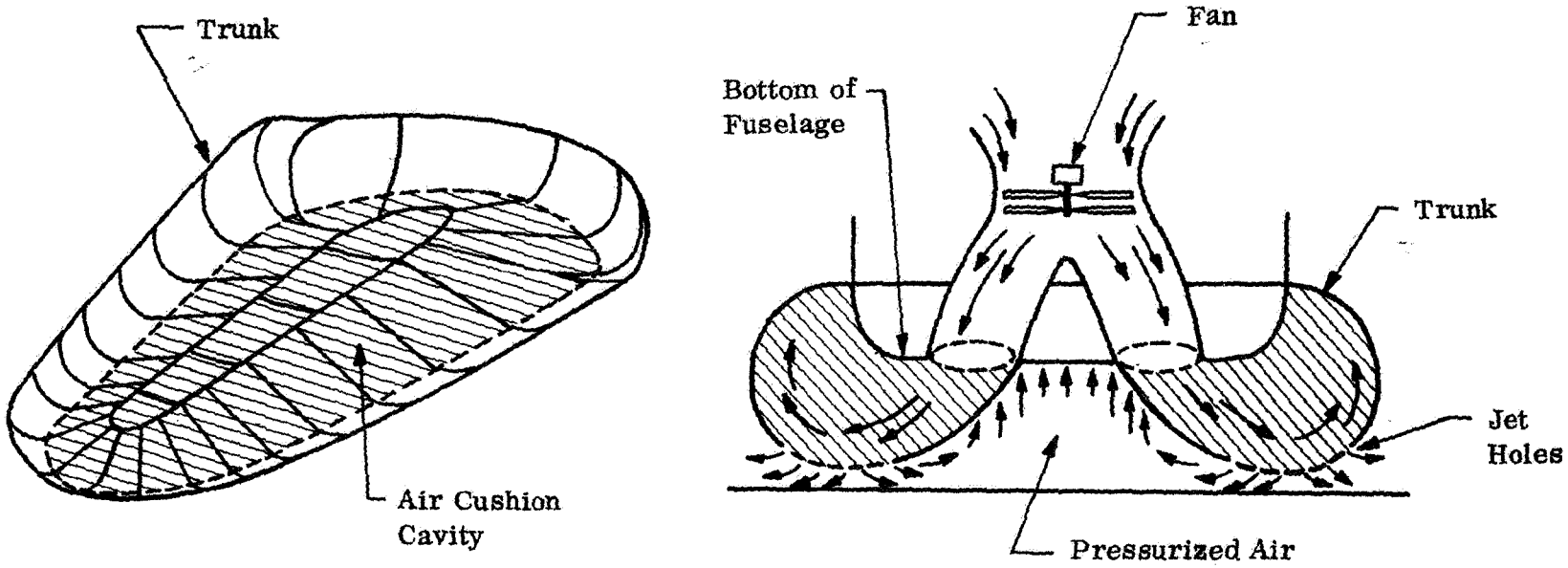

- Function of inflated trunk is to contain the pressurized air in the air cushion cavity. This cushion of air supports the weight of the aircraft.

- Air continually forced through the jet holes pressurizes the air cushion cavity. It also provides air bearing lubrication between the trunk and landing surface.

- When not in use the trunk deflates and hugs the fuselage similar to deicing boots.

Fig. 5. Air Cushion Landing System Principle

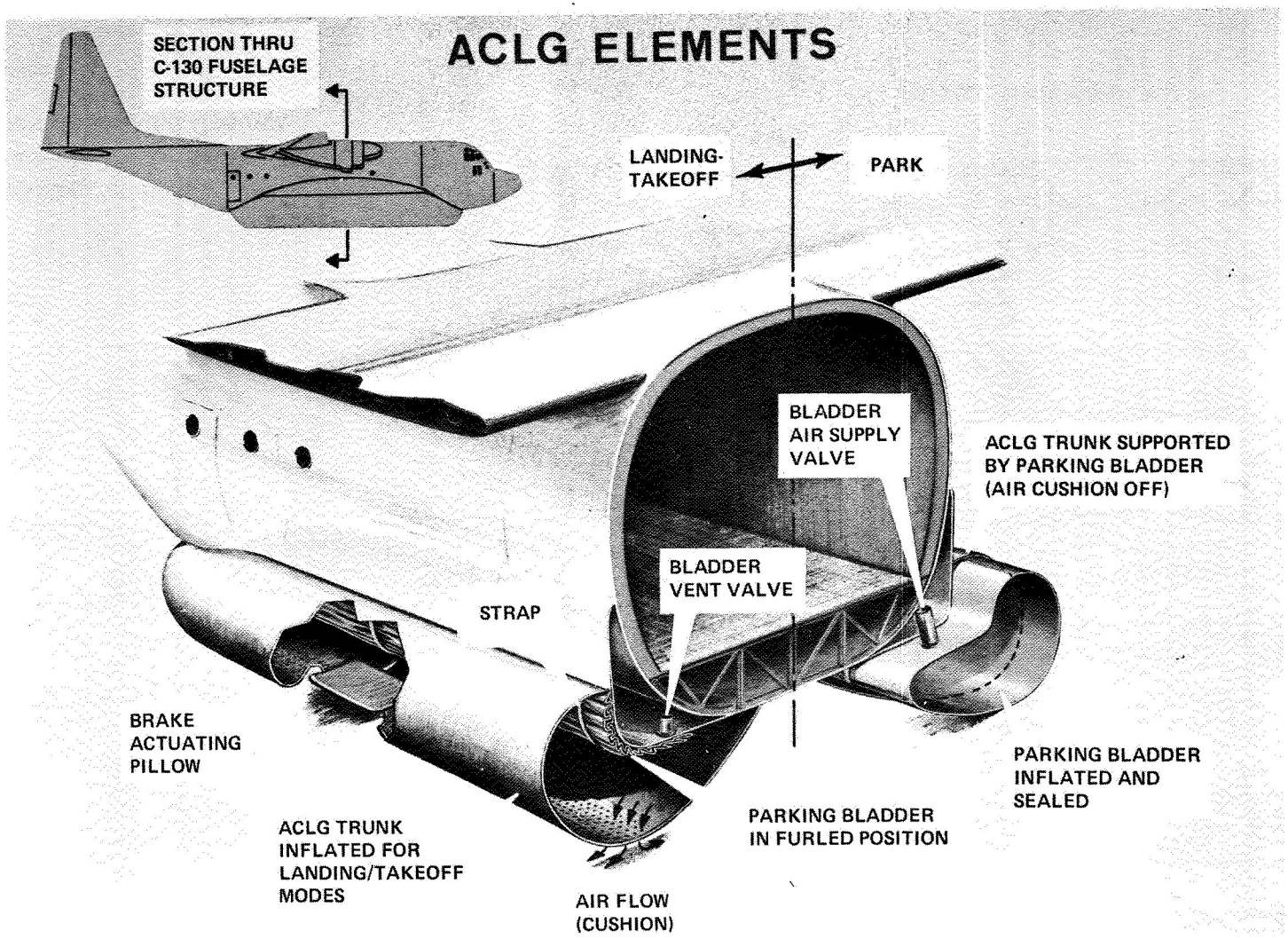

Fig. 6. ACLS Features

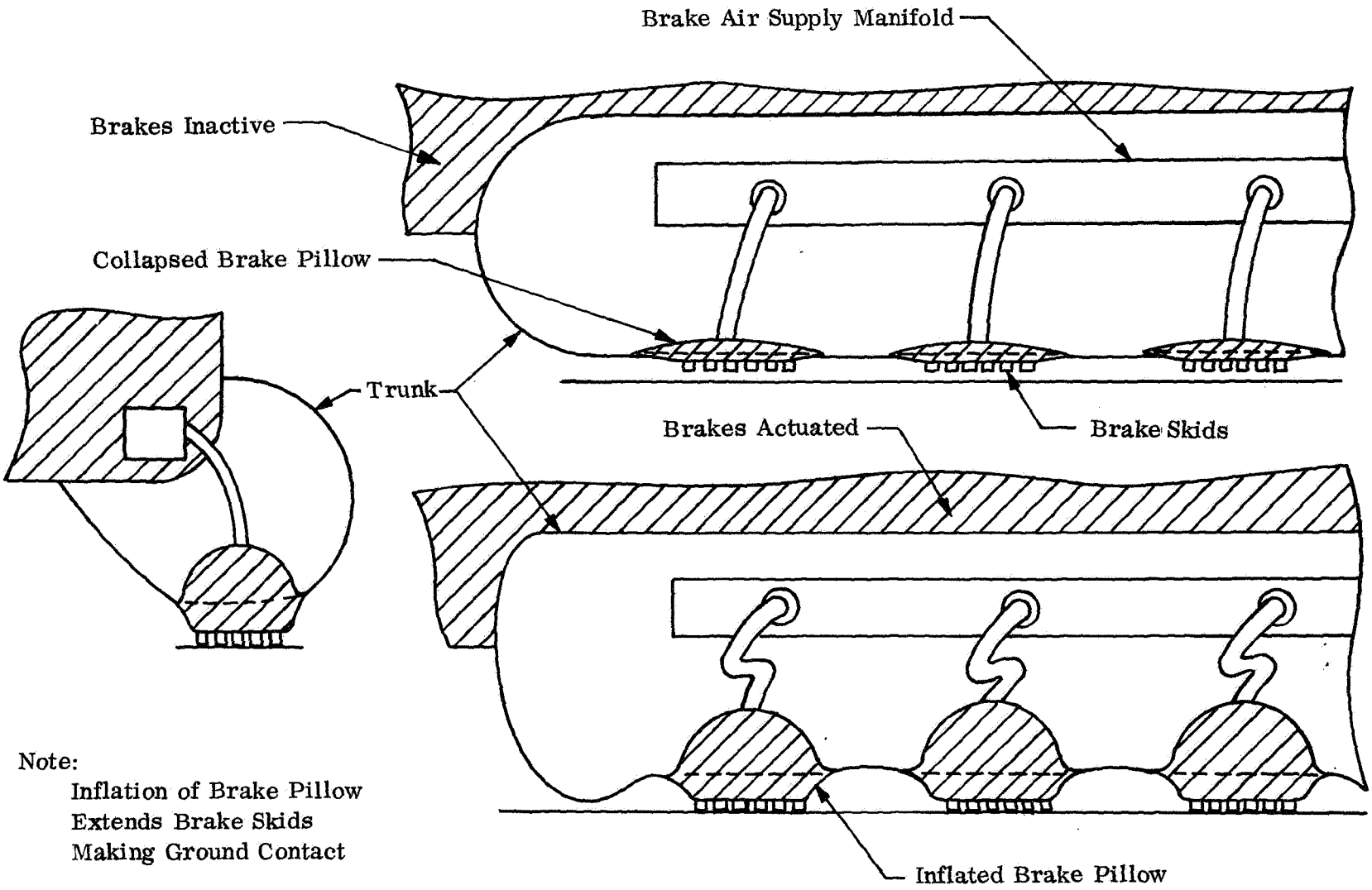

Fig. 7. ACLS Brake System

Fig. 8. LA-4 Taking Off August 4, 1967

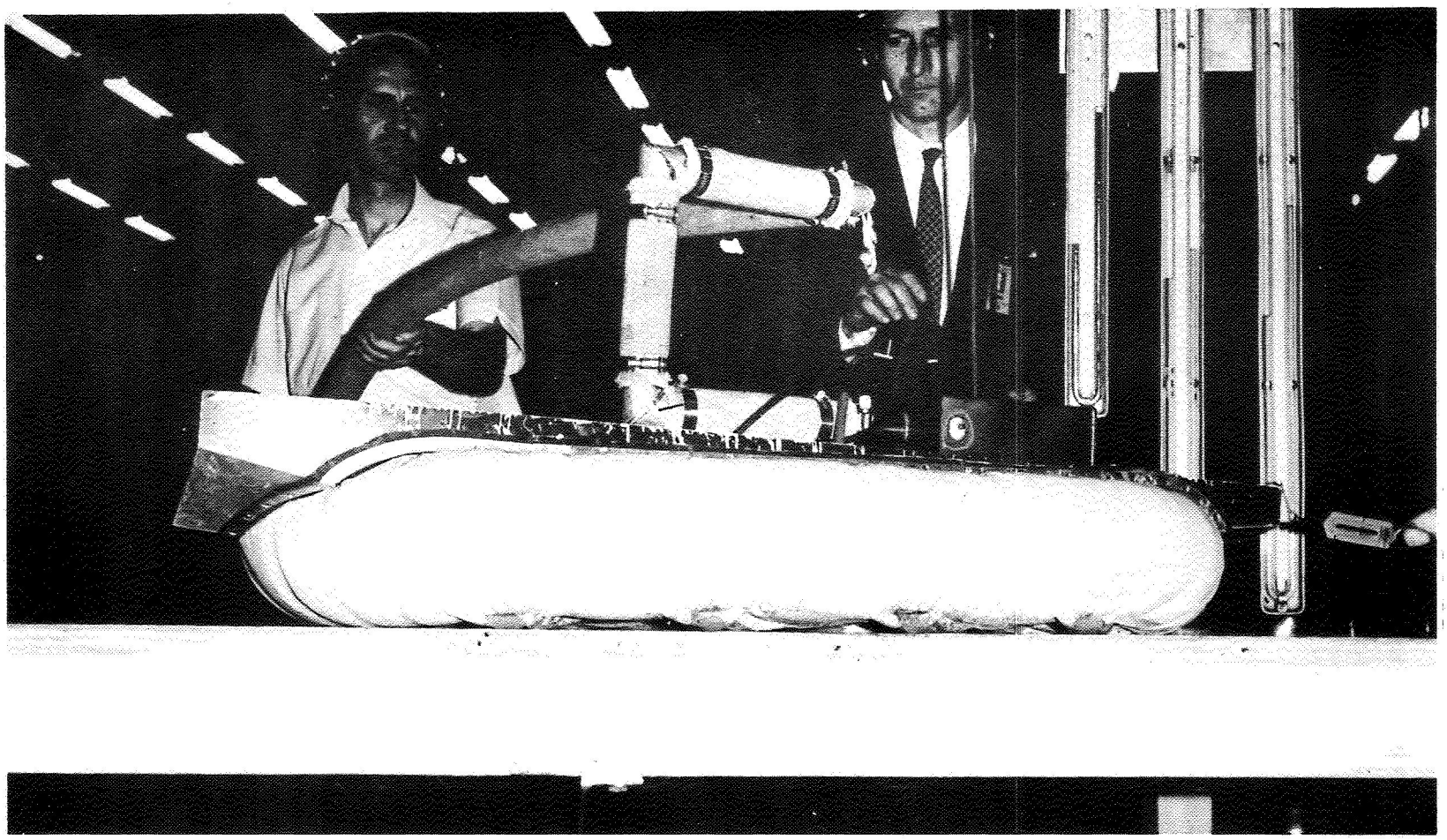

Fig. 9. 1/4-Scale LA-4 Model with Braking

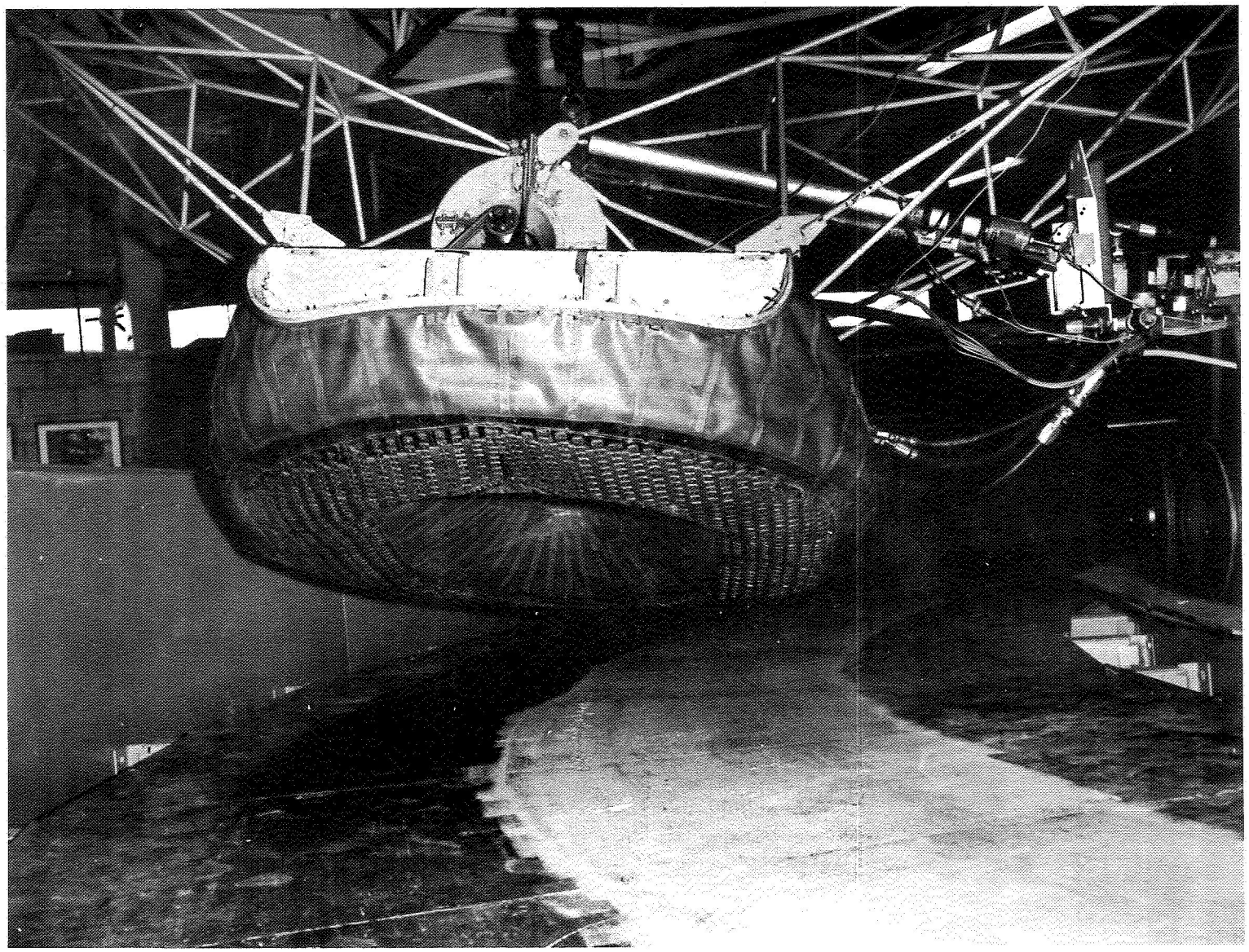

Fig. 10. Whirling Arm Model for Braking Tests

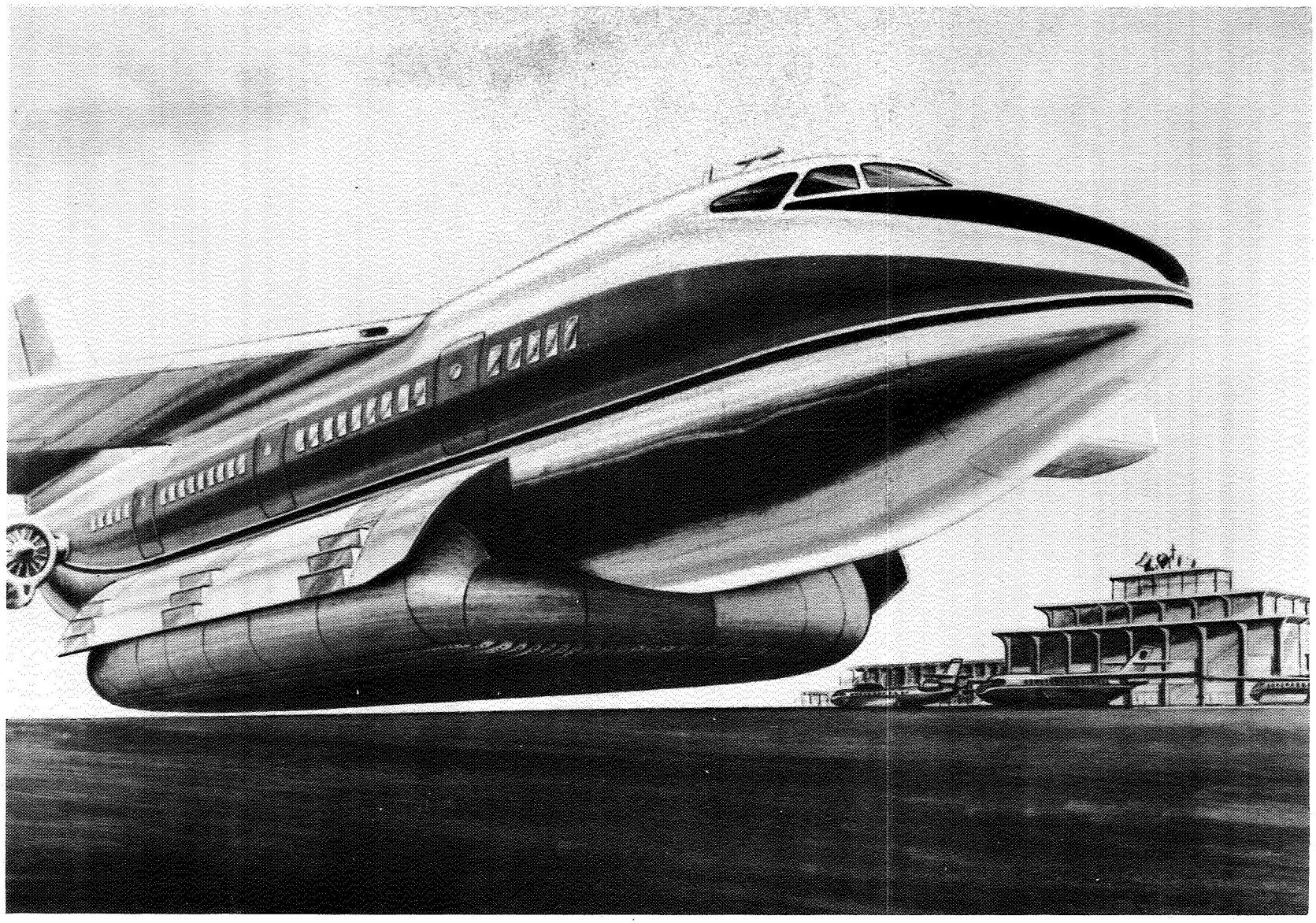

Fig. 11. Civil Aircraft with Internally Stowed Trunk

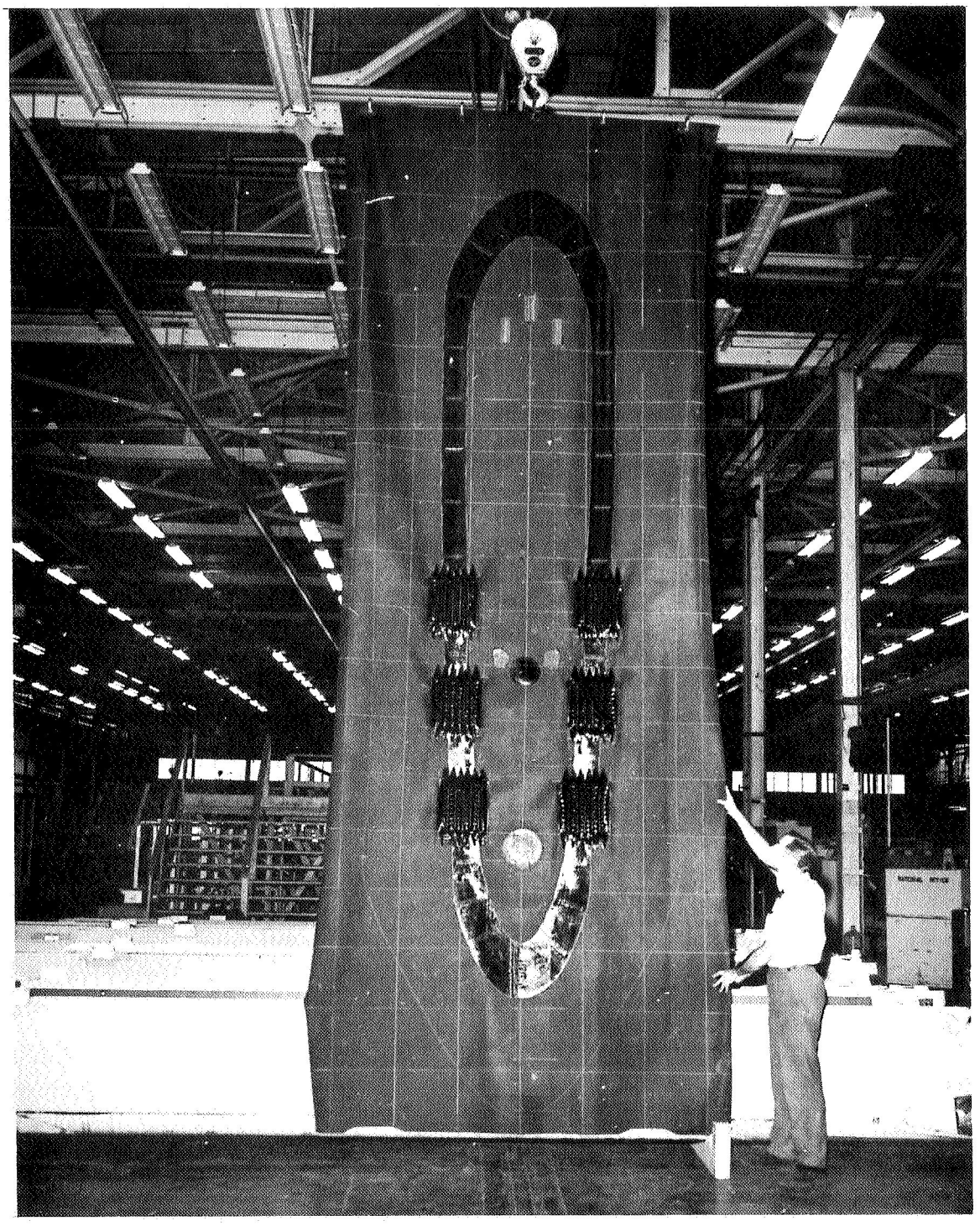

Fig. 12. Completed LA-4 Trunk Sheet

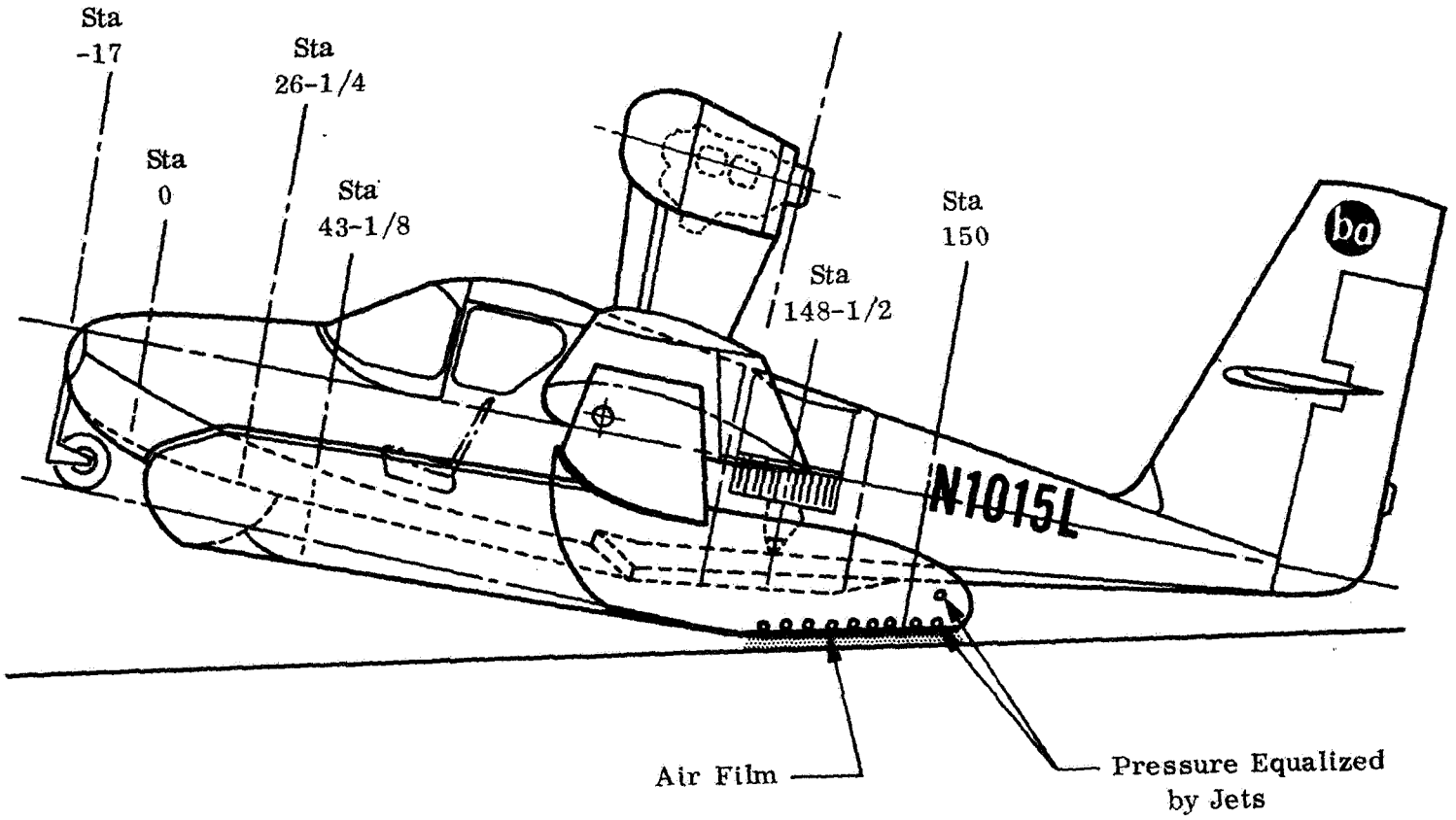

Fig. 13. Air Lubrication Effects

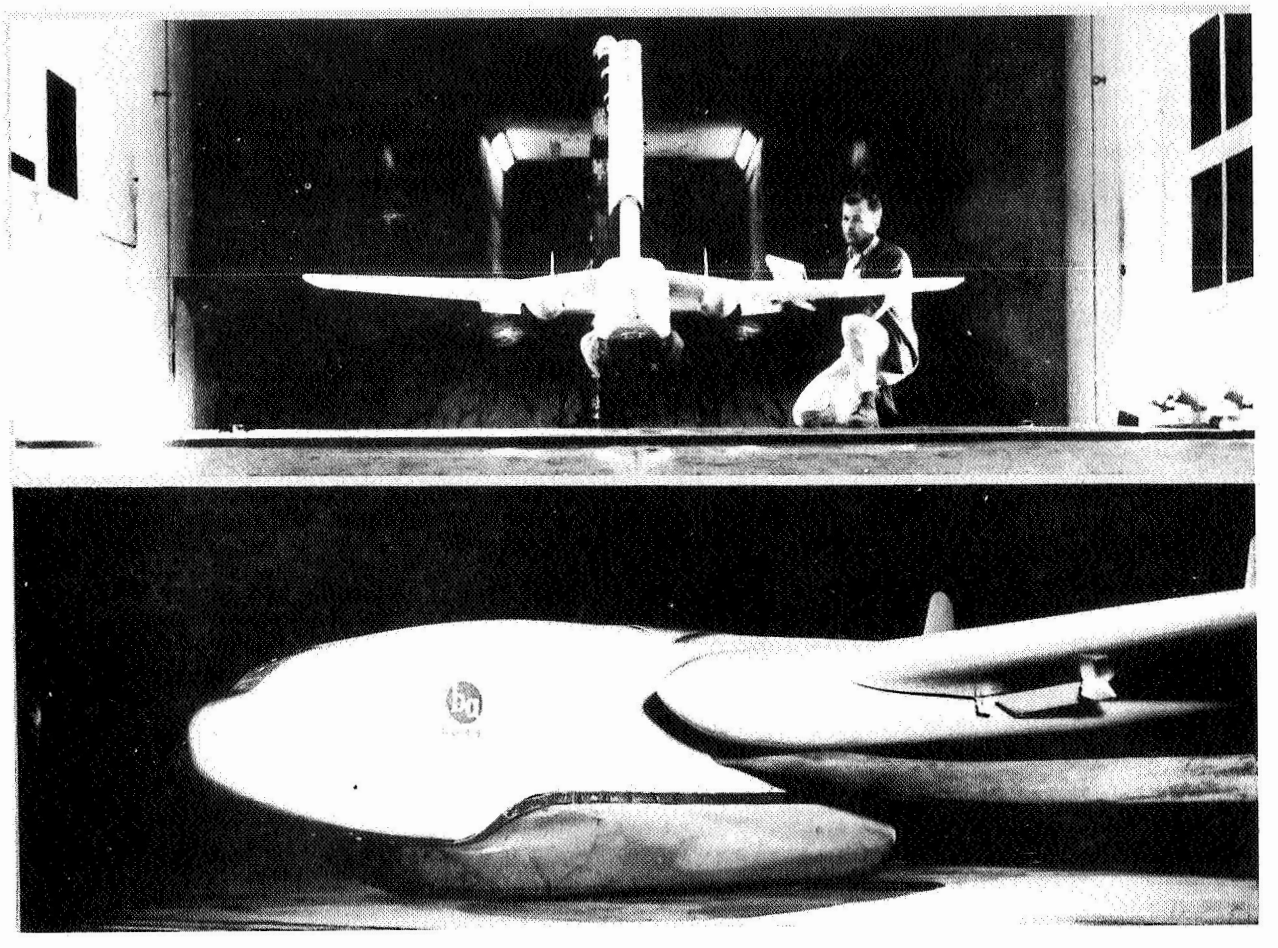

Fig. 14. 1/12-Scale Quasi-Dynamic Model of C-119 in Langley Wind Tunnel

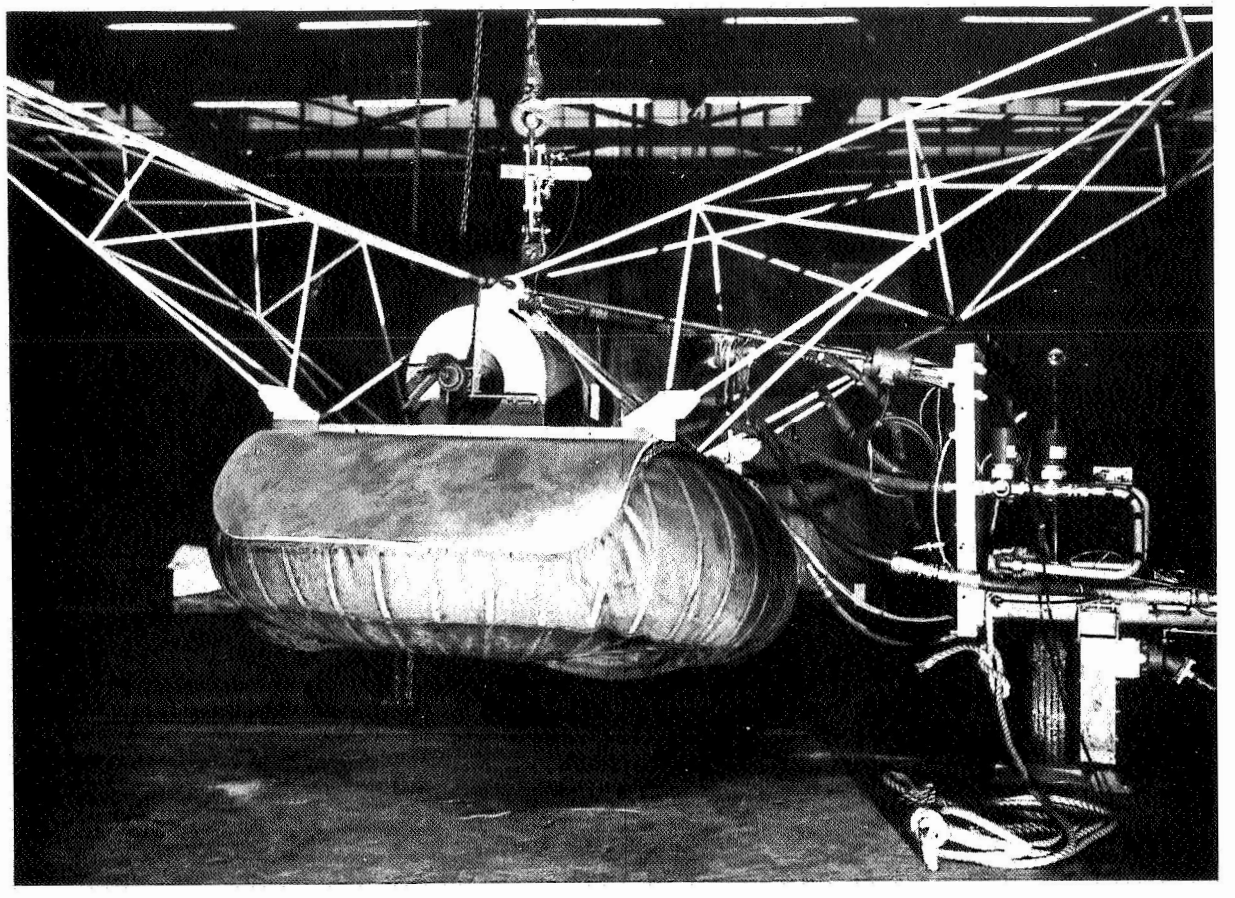

Fig. 15. C-119 Trunk Model Ready for Drop Test

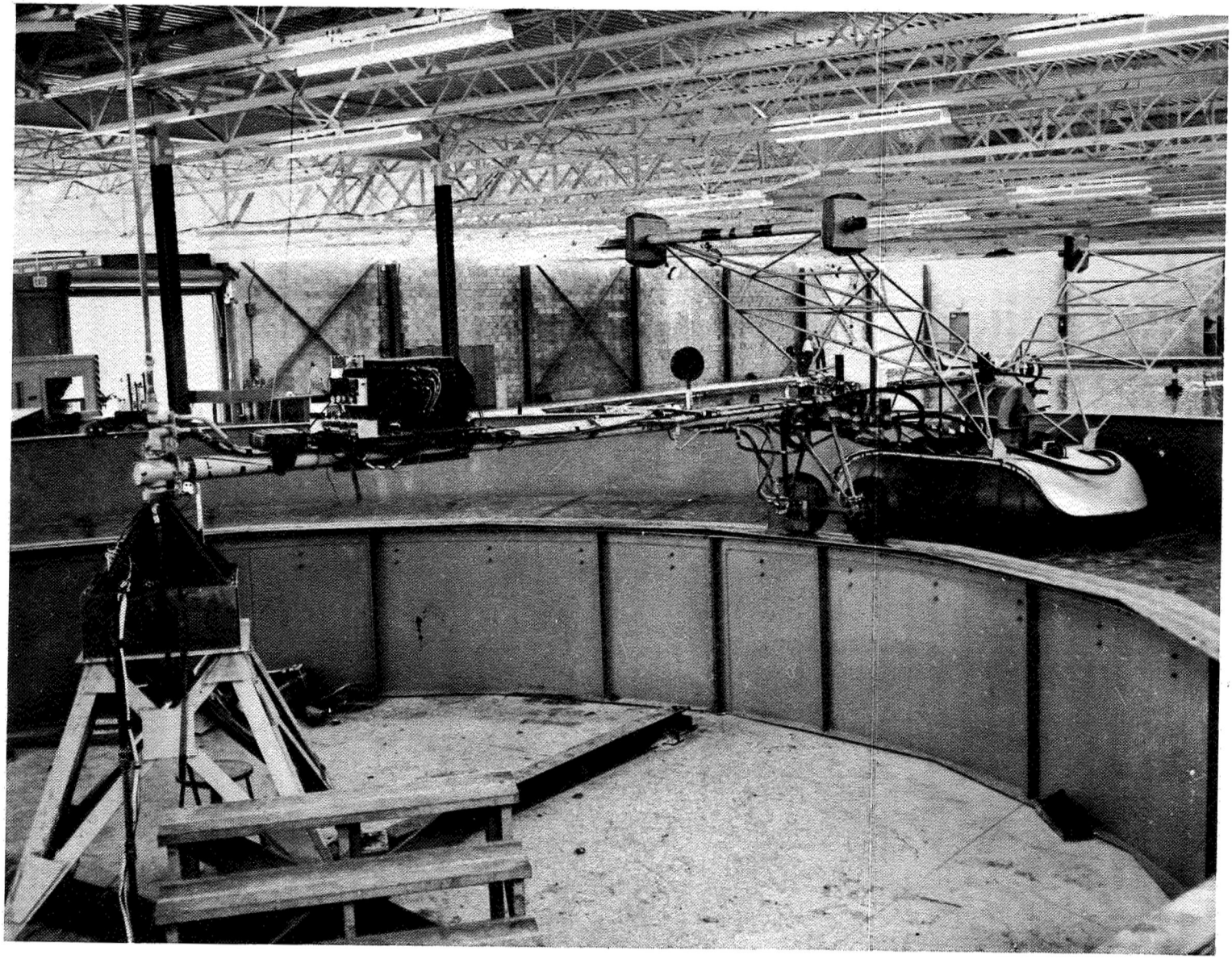

Fig. 16. C-119 Trunk and Brake Model on Whirling Arm

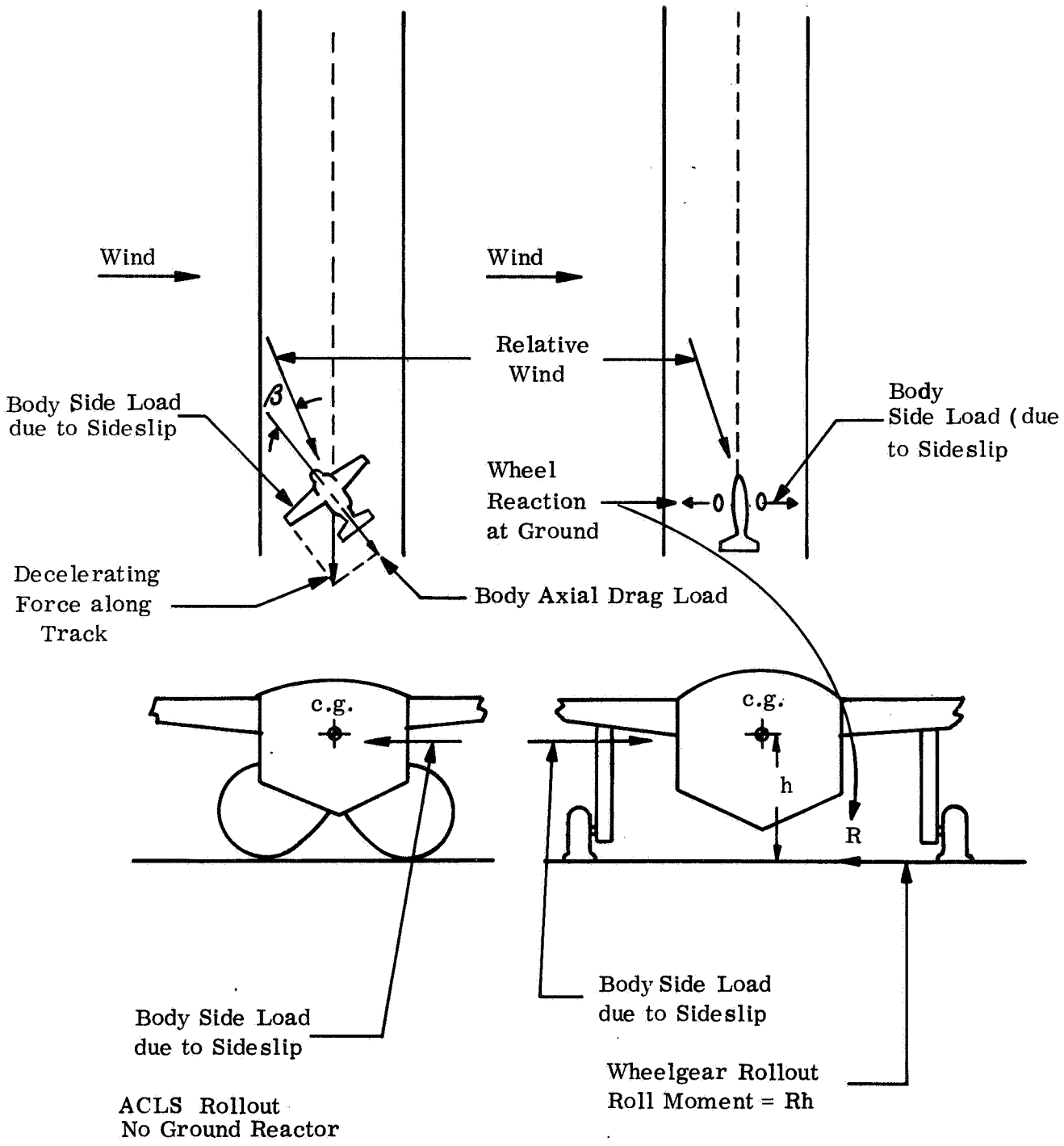

Fig. 17. Crosswind Landing Rollout Comparison

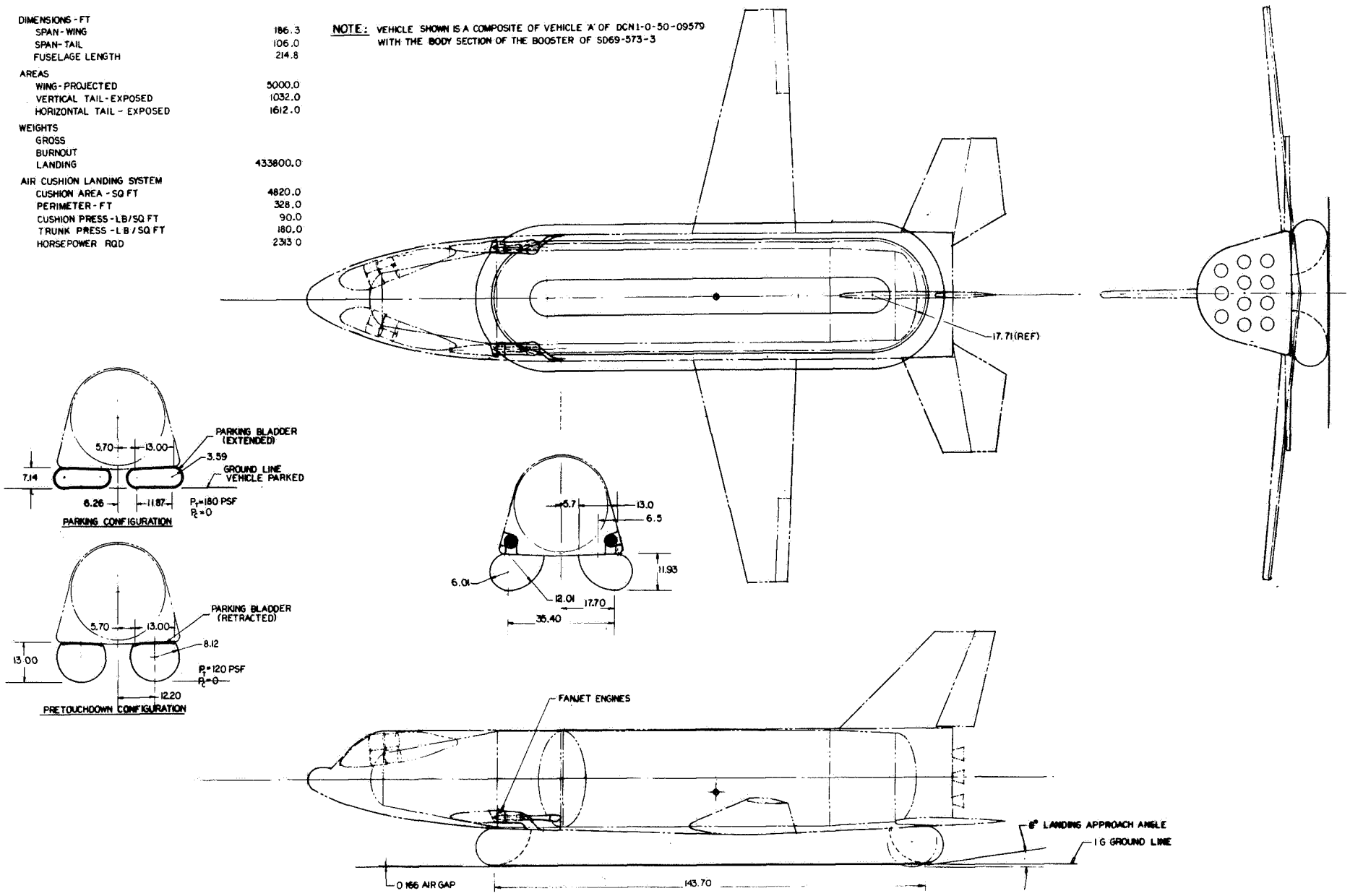

Fig. 18. Booster with Low Pressure ACLS (Configuration 005)

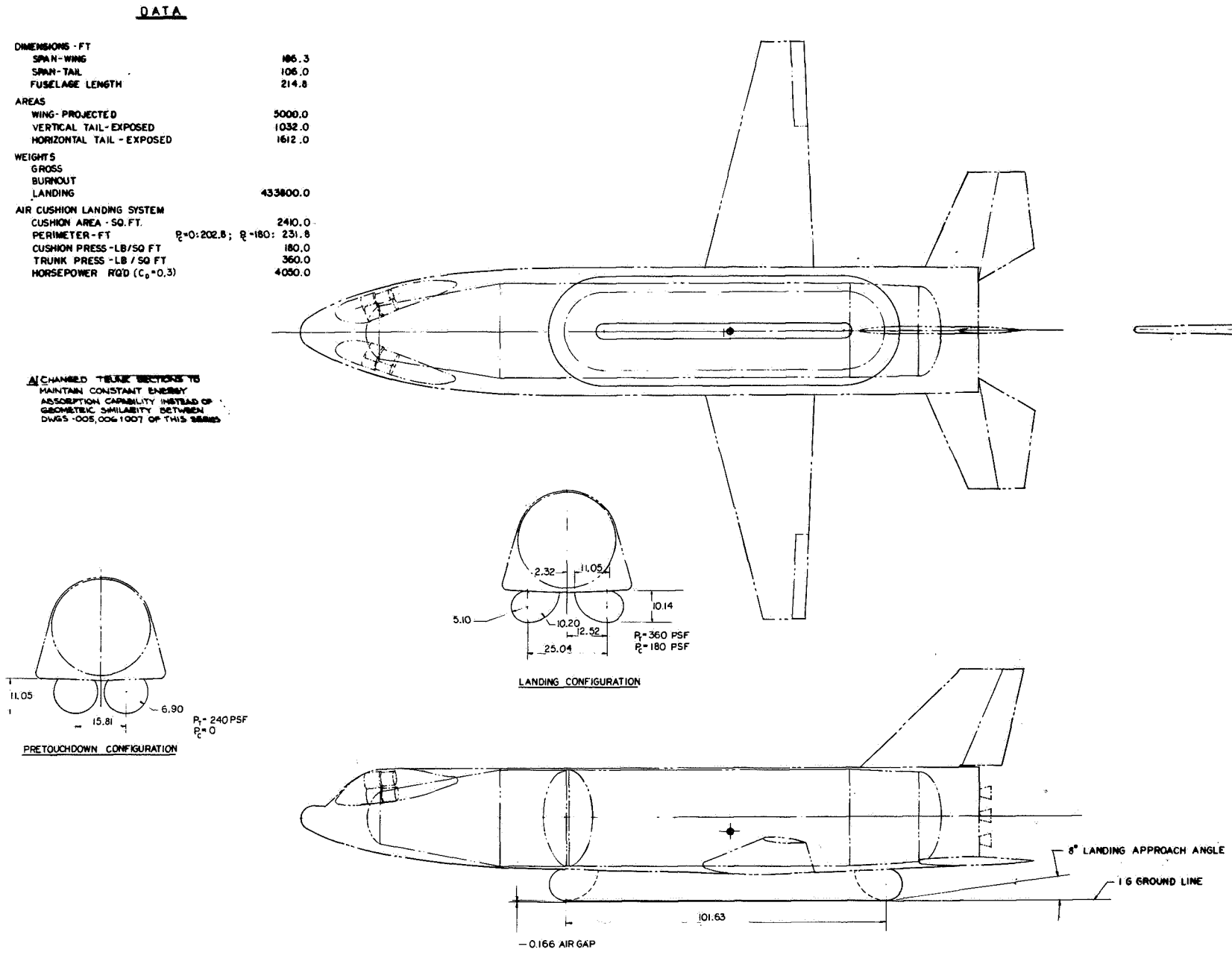

Fig. 19. Booster with Medium Pressure ACLS (Configuration 006A)

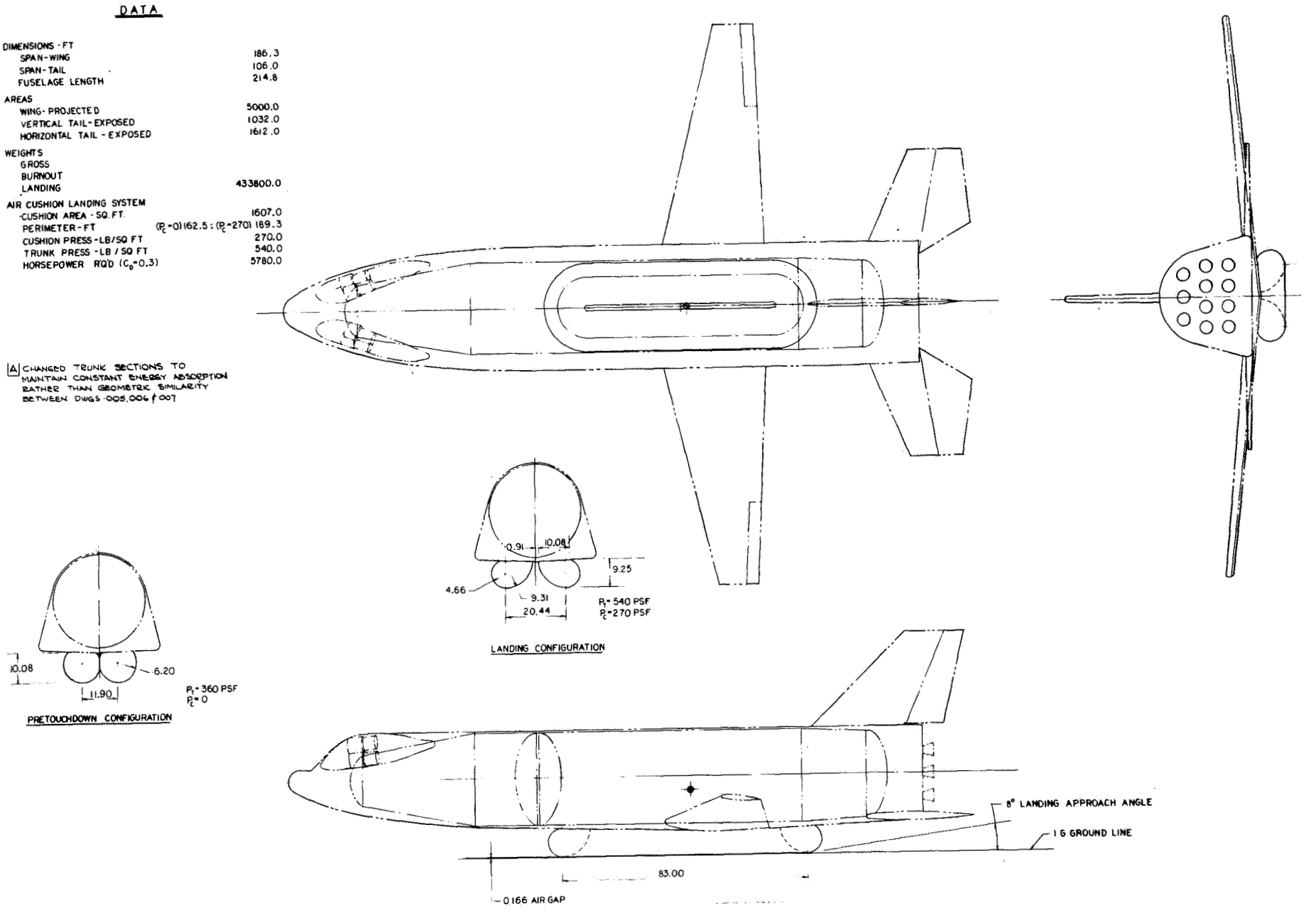

Fig. 20. Booster with High Pressure ACLS (Configuration 007A)

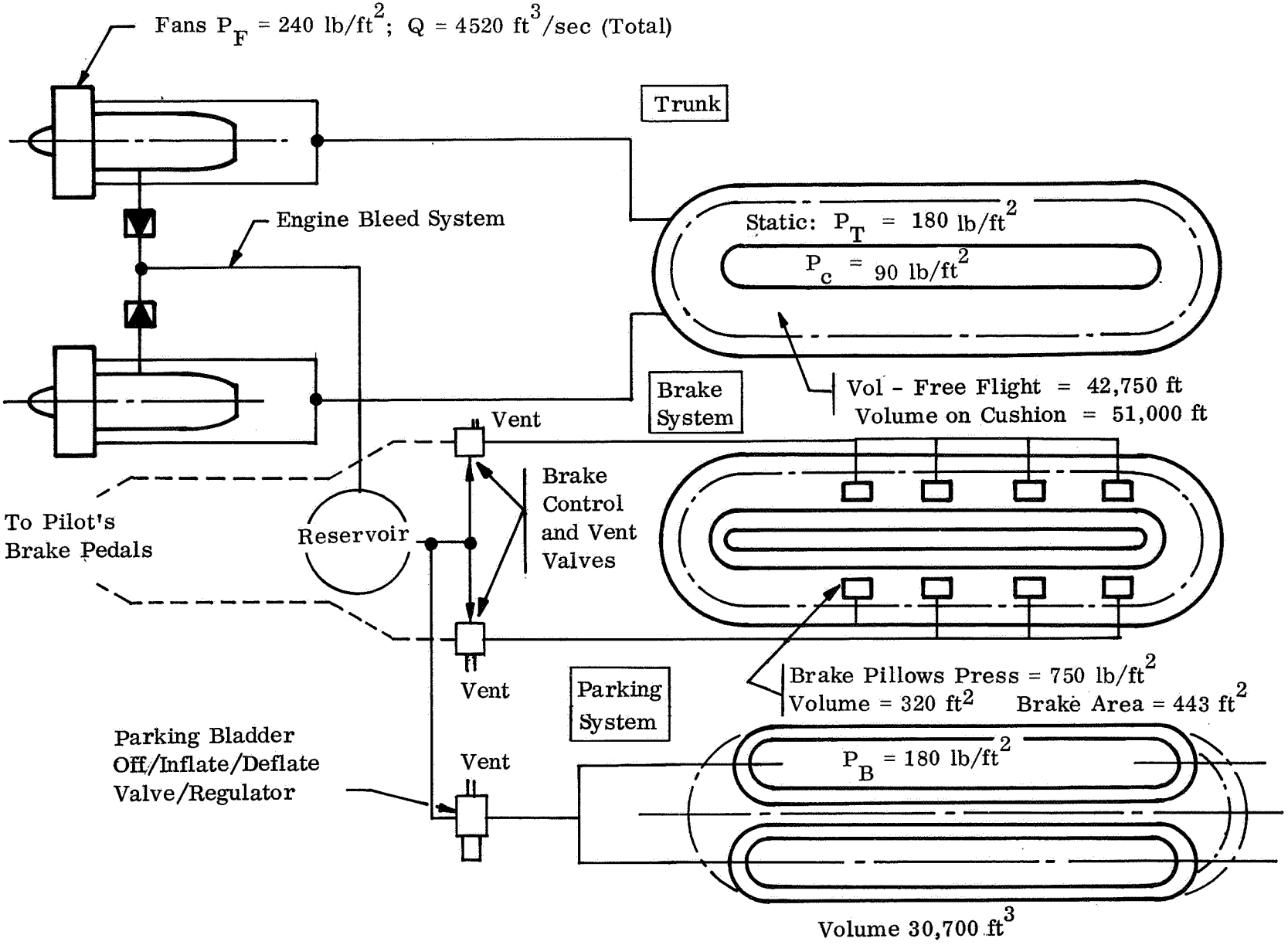

Fig. 21. Shuttle Booster ACLS System Schematic

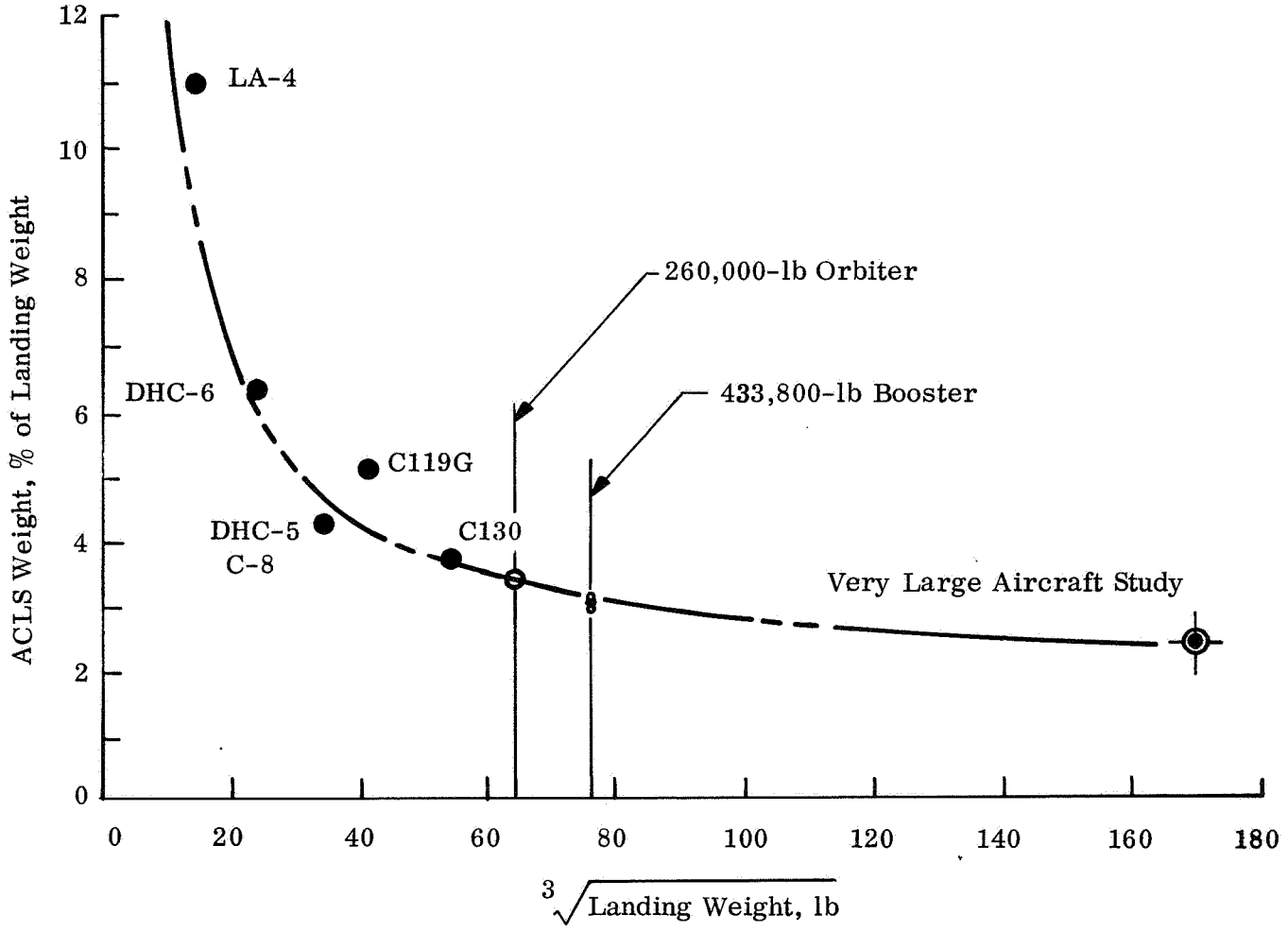

Fig. 22. ACLS Weight vs Vehicle Landing Weight

DATA

DIMENSIONS - FT	
SPAN - WING - TIP TO TIP	101.0
OVERALL LENGTH - NOSE TO WING TIP	179.5
FUSELAGE LENGTH - NOSE TO FIXED ENG. EXIT	160.0
MAX BODY WIDTH	70.0
MAX BODY HEIGHT	27.0
AREAS - SQ. FT.	
PLANFORM	5720.0
VERTICAL TAIL - BOTH FINS	1540.0
ELEVON	1350.0
WEIGHTS - LB	
LAUNCH	978 269.0
ENTRY	265893.0
LANDING	259501.0
AIR CUSHION LANDING SYSTEM	
CUSHION AREA - SQ. FT	1445.0
CUSHION PRESS - LB/SQ FT	180.0
TRUNK PRESS - LB/SQ FT	360.0
PERIMETER - FT (STATIC)	151.2
HORSEPOWER RQ'D (C_p = 0.3)	2630.0

NOTE:
VEHICLE SHOWN IS THAT OF LOCKHEED SK5-100769
OF REPORT LSMC-A959837

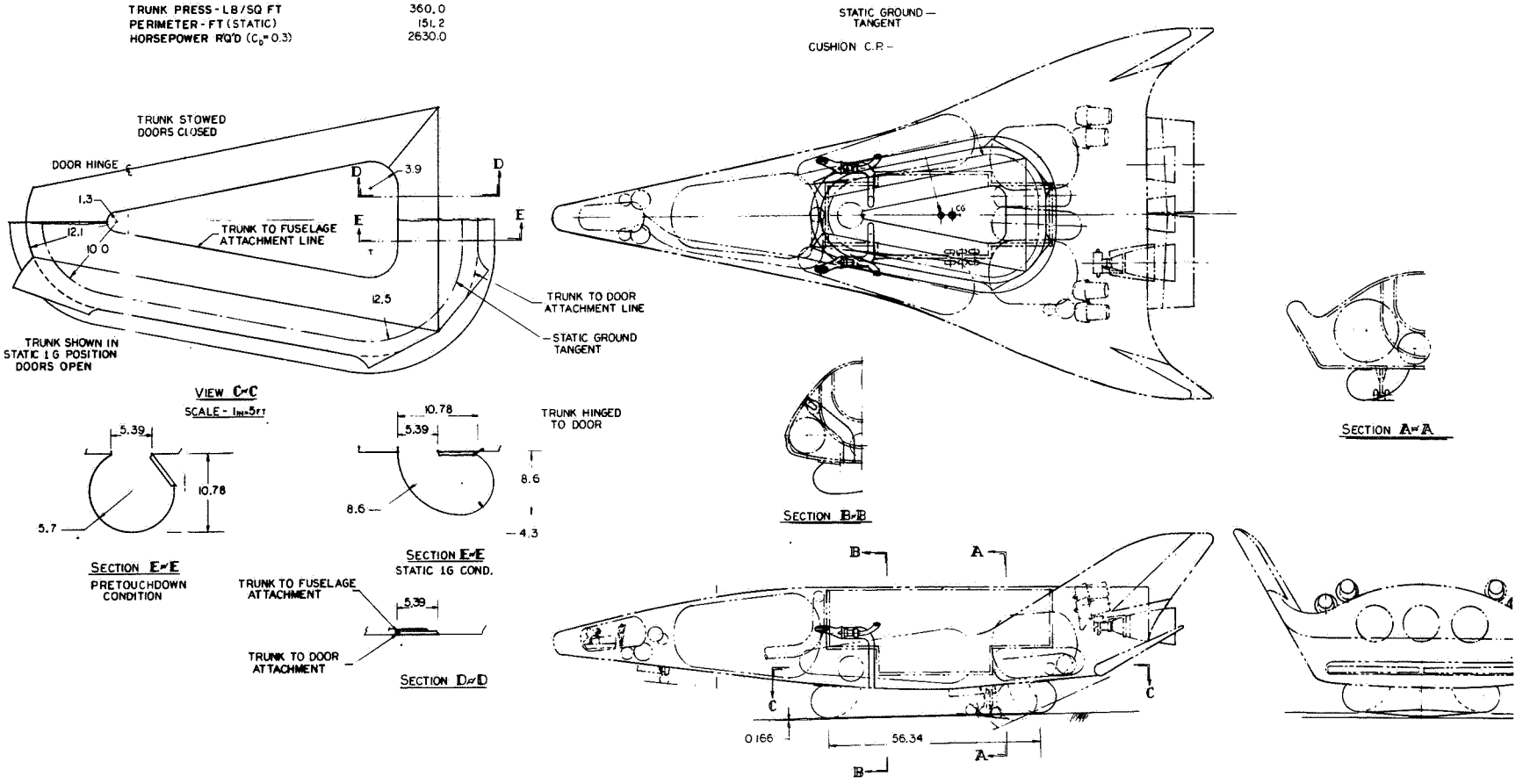

Fig. 23. Orbiter with Medium Pressure ACLS (Configuration 008A)

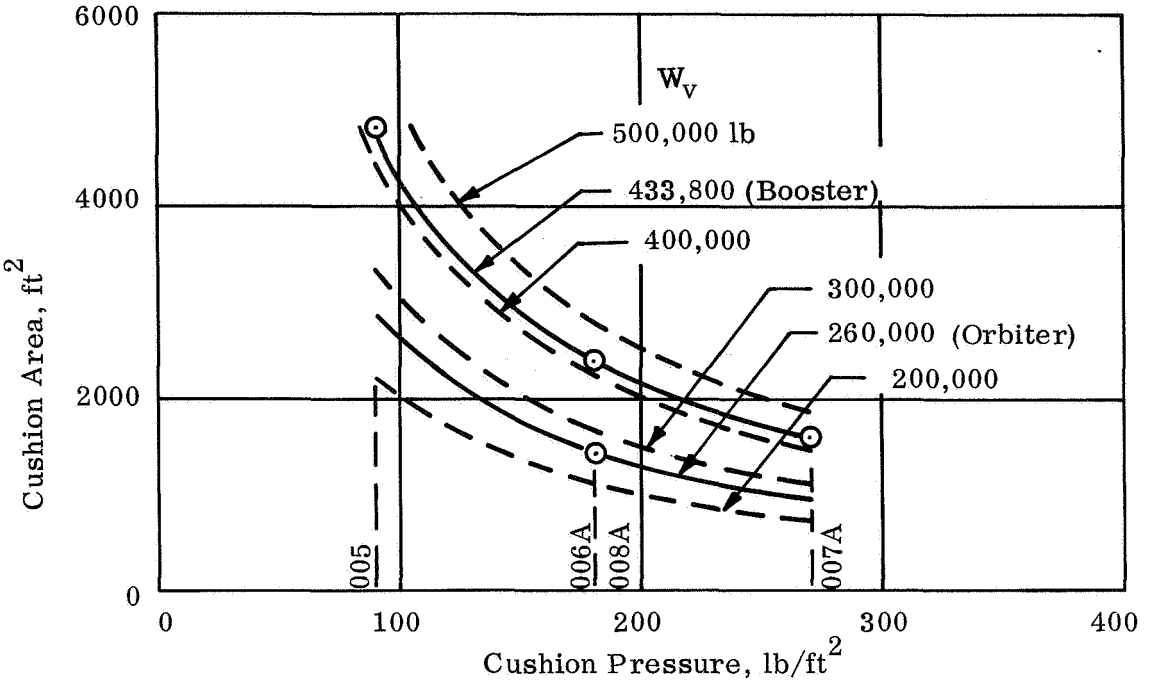

Fig. 24. Cushion Area vs Cushion Pressure

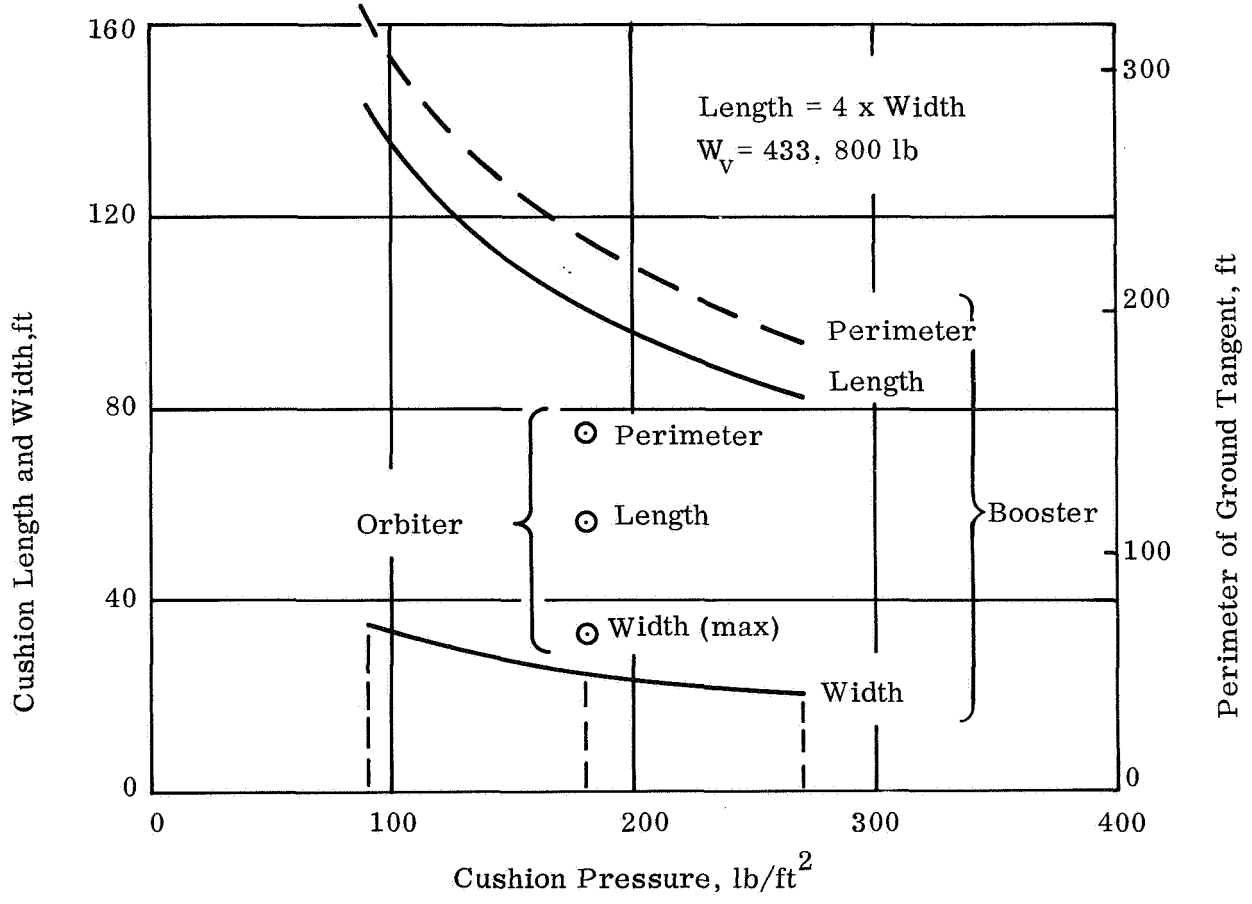

Fig. 25. Cushion Dimensions vs Cushion Pressure

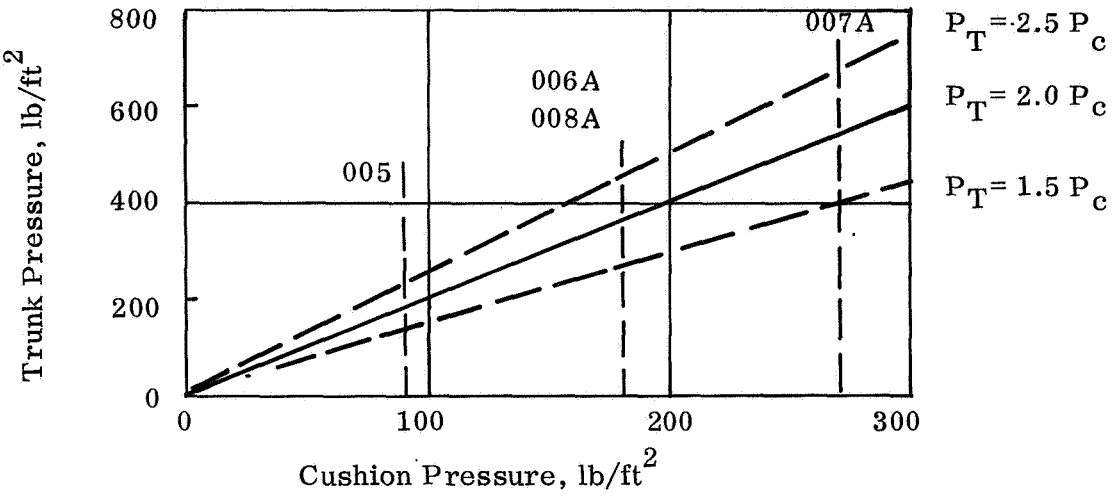

Fig. 26. Trunk Pressure vs Cushion Pressure

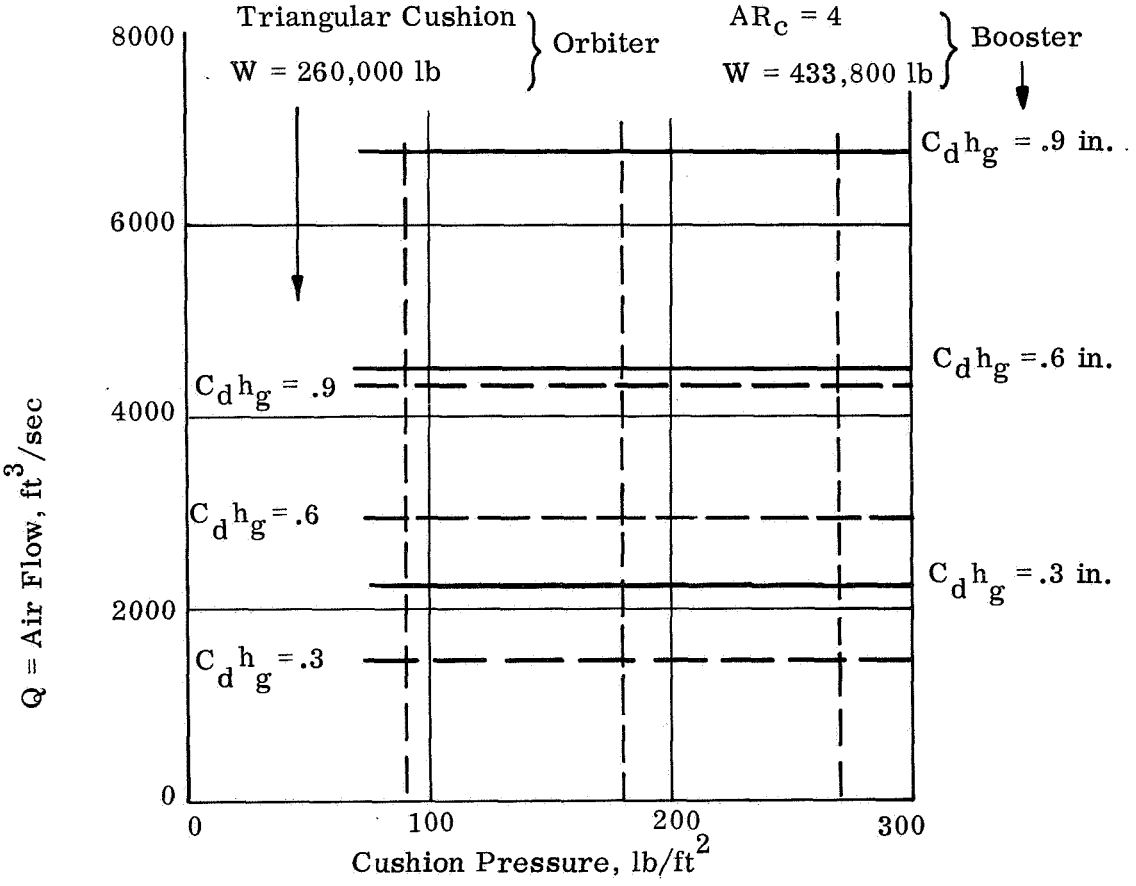

Fig. 27. Air Flow vs Cushion Pressure

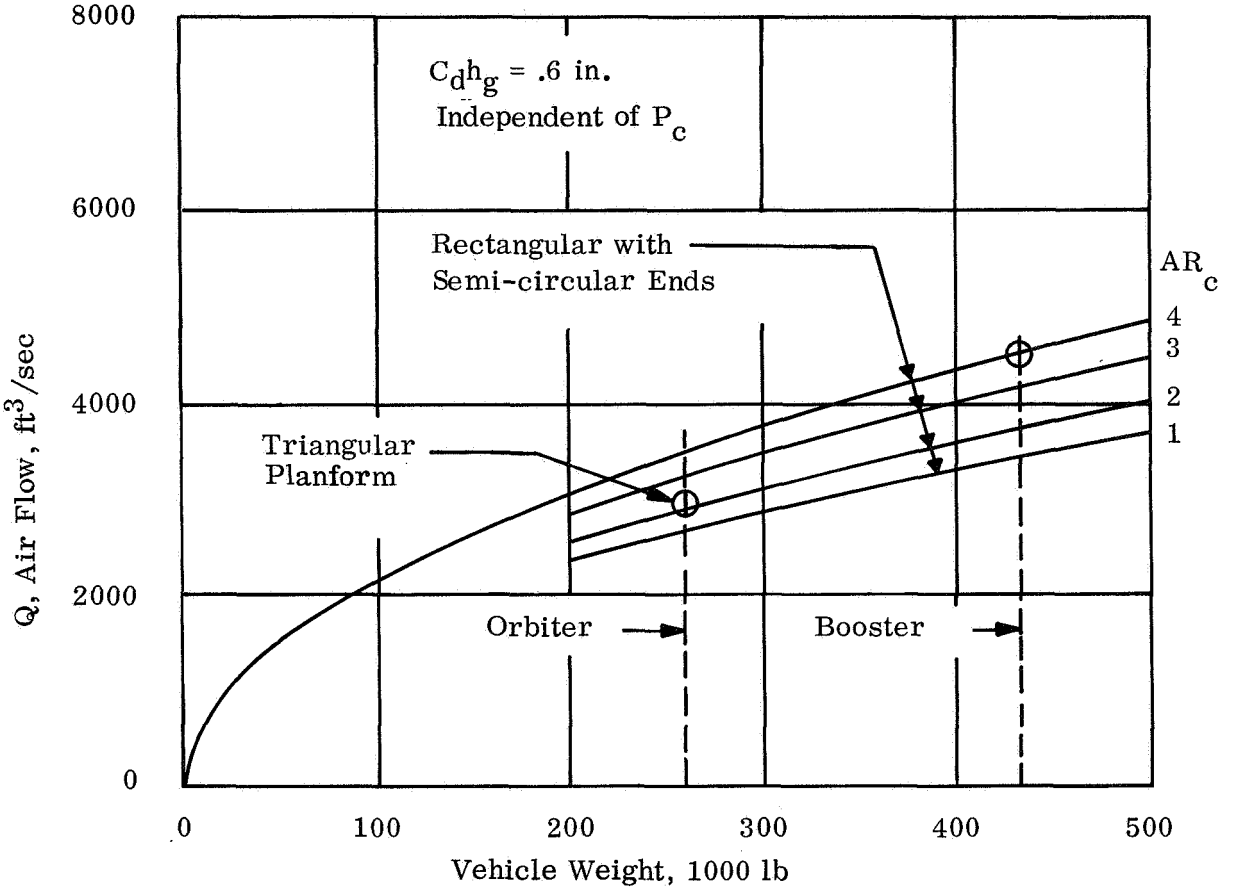

Fig. 28. Air Flow vs Vehicle Weight

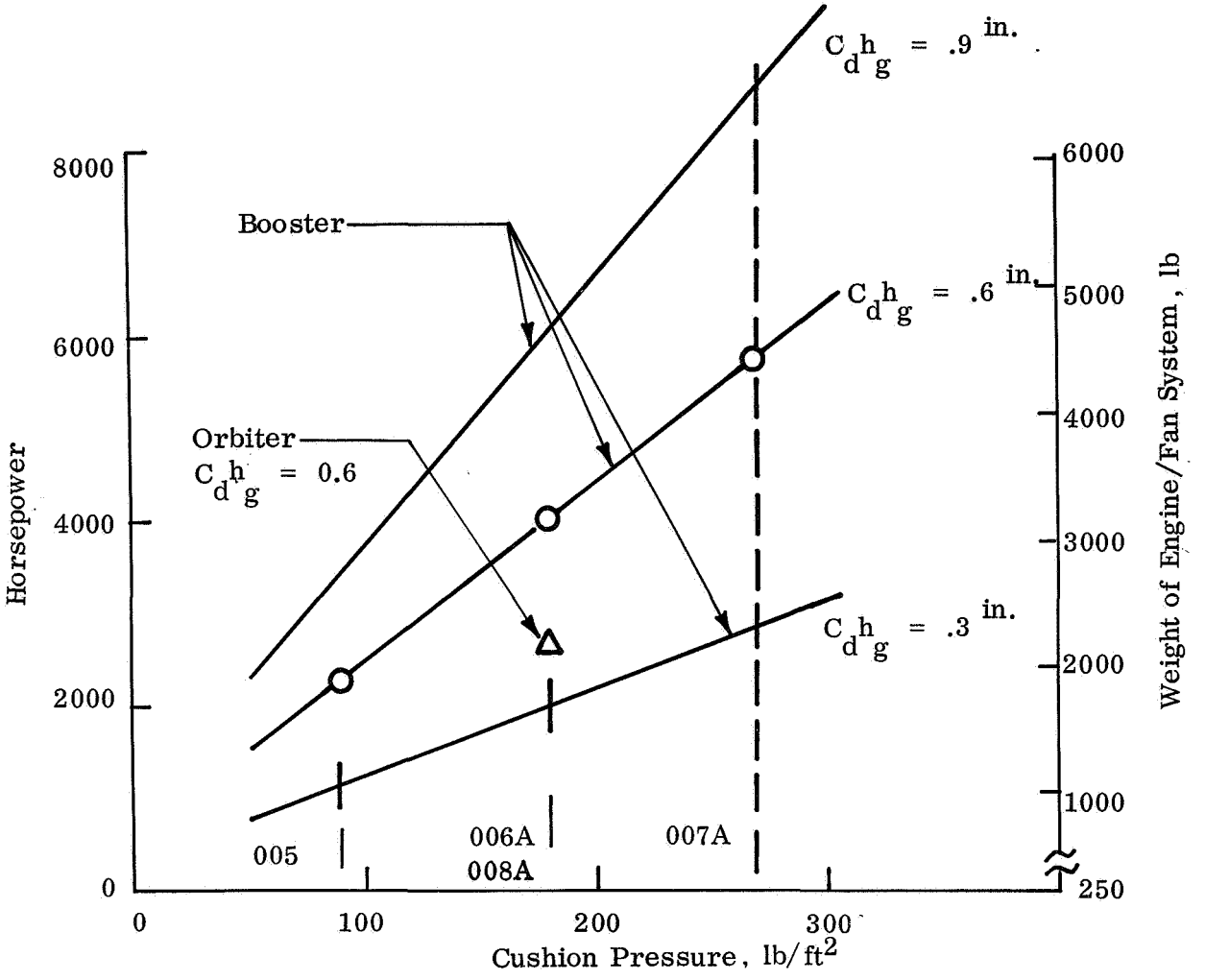

Fig. 29. ACLS Horsepower vs Cushion Pressure

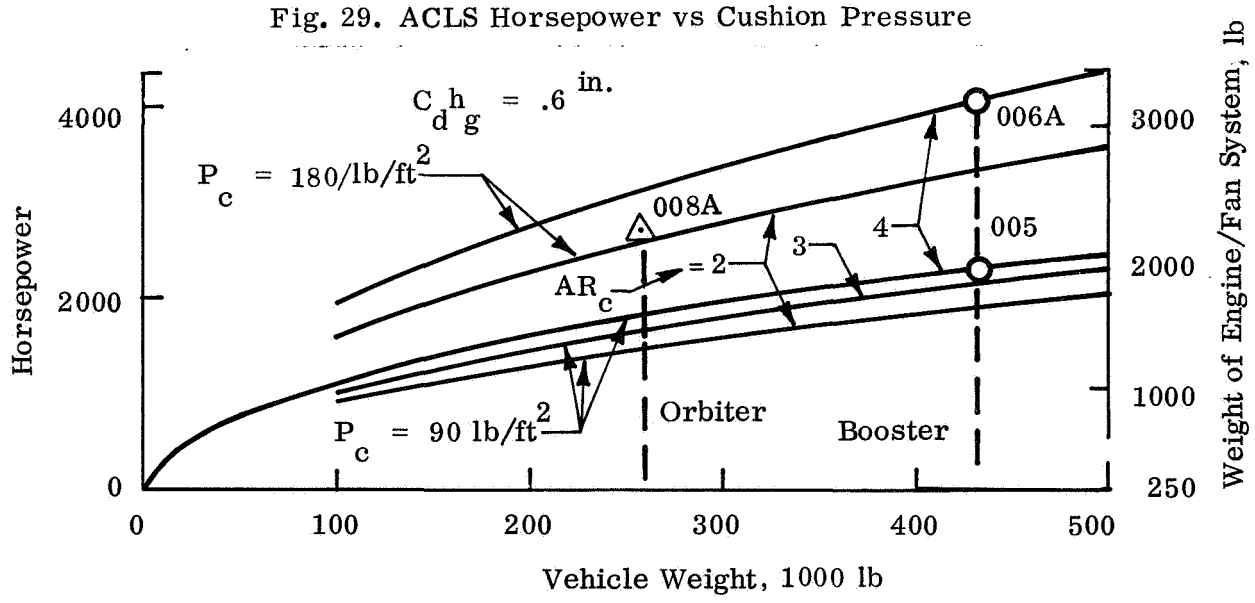

Fig. 30. ACLS Horsepower vs Vehicle Weight

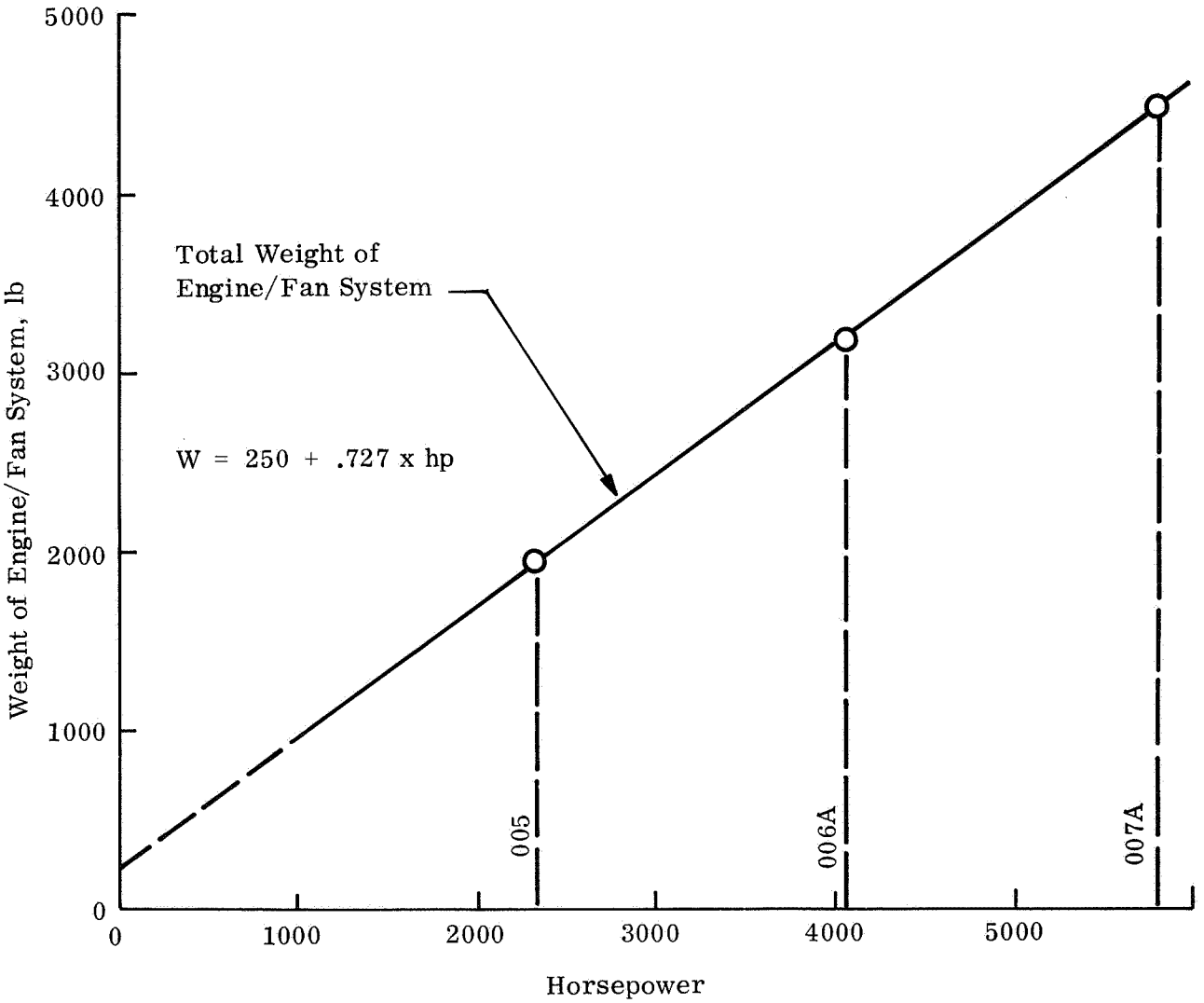

Fig. 31. Weight of ACLS Engine/Fan System vs Horsepower

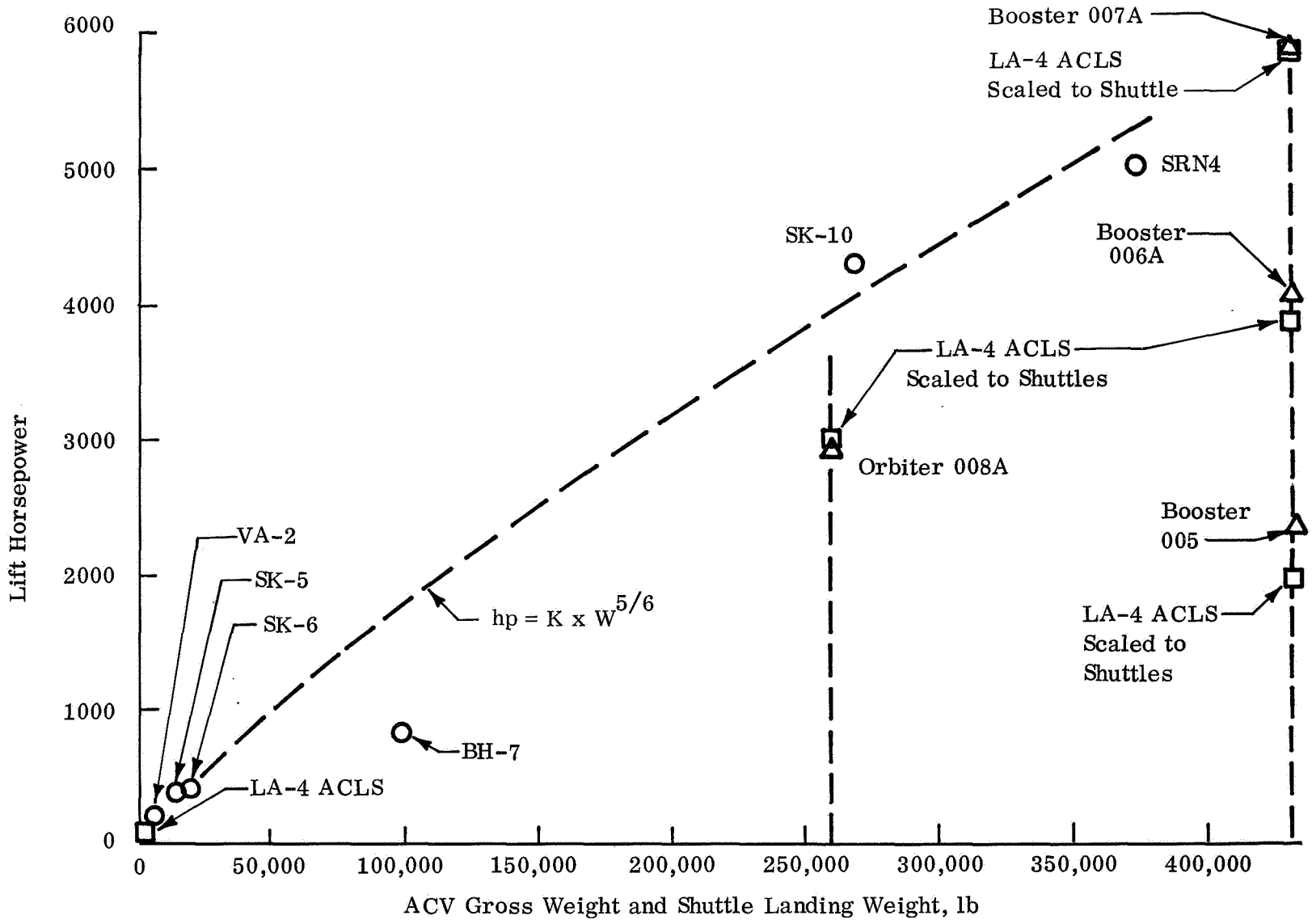

Fig. 32. Comparison of Lift Horsepower of Shuttle ACLS and Air Cushion Vehicles

W_v = 433,800 lb

AR_c = 4

$C_d h_g$ = 0.6 in.

P_c = 90 lb/ft^2

ΔP = 60 lb/ft^2

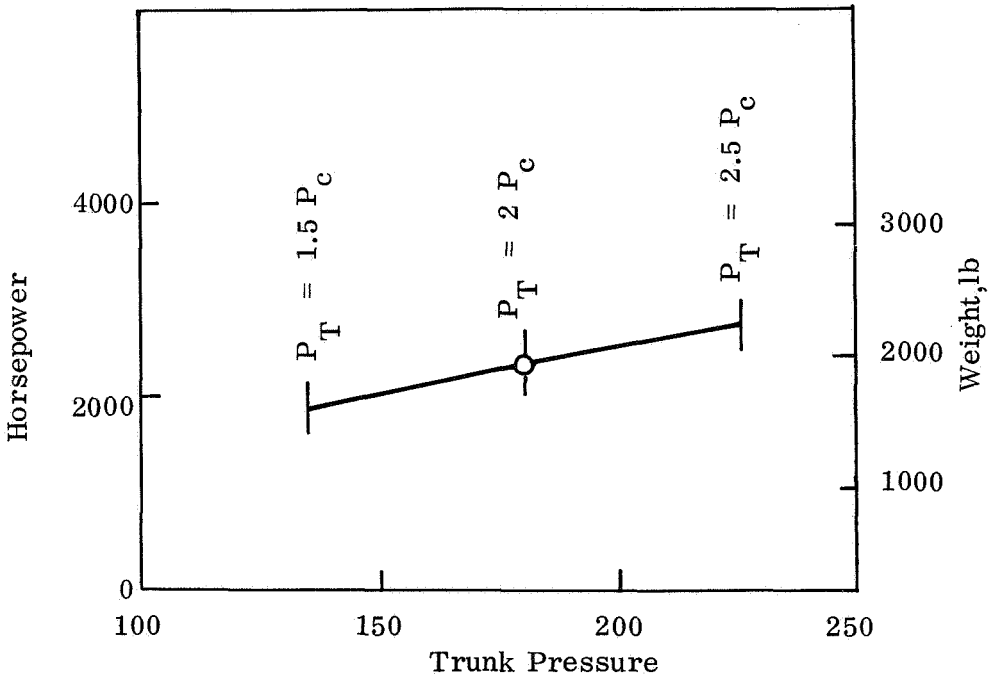

Fig. 33. Booster ACLS Horsepower vs Trunk Pressure

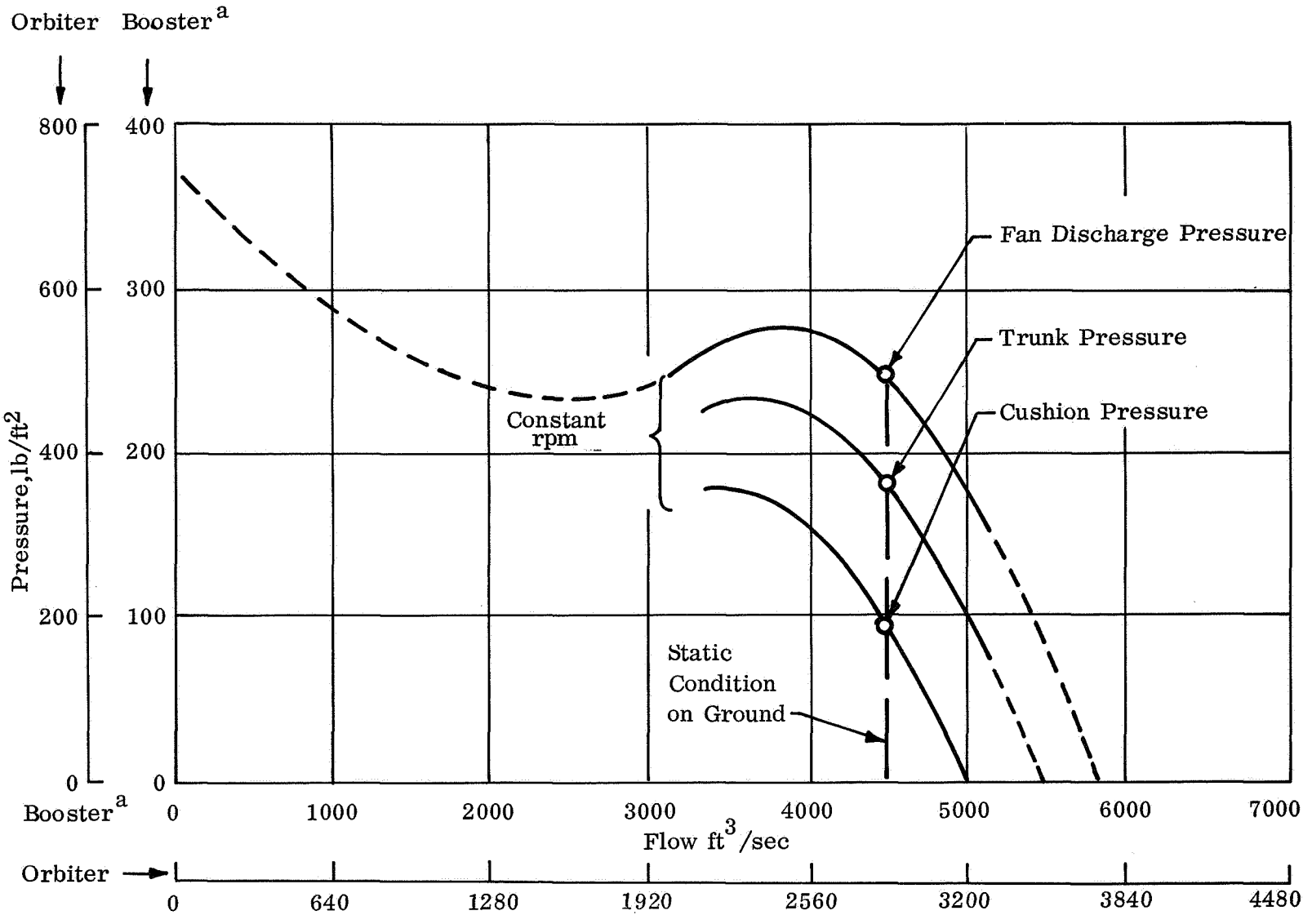

[a] Low Pressure ACLS

Fig. 34. ACLS Pressures vs Flow

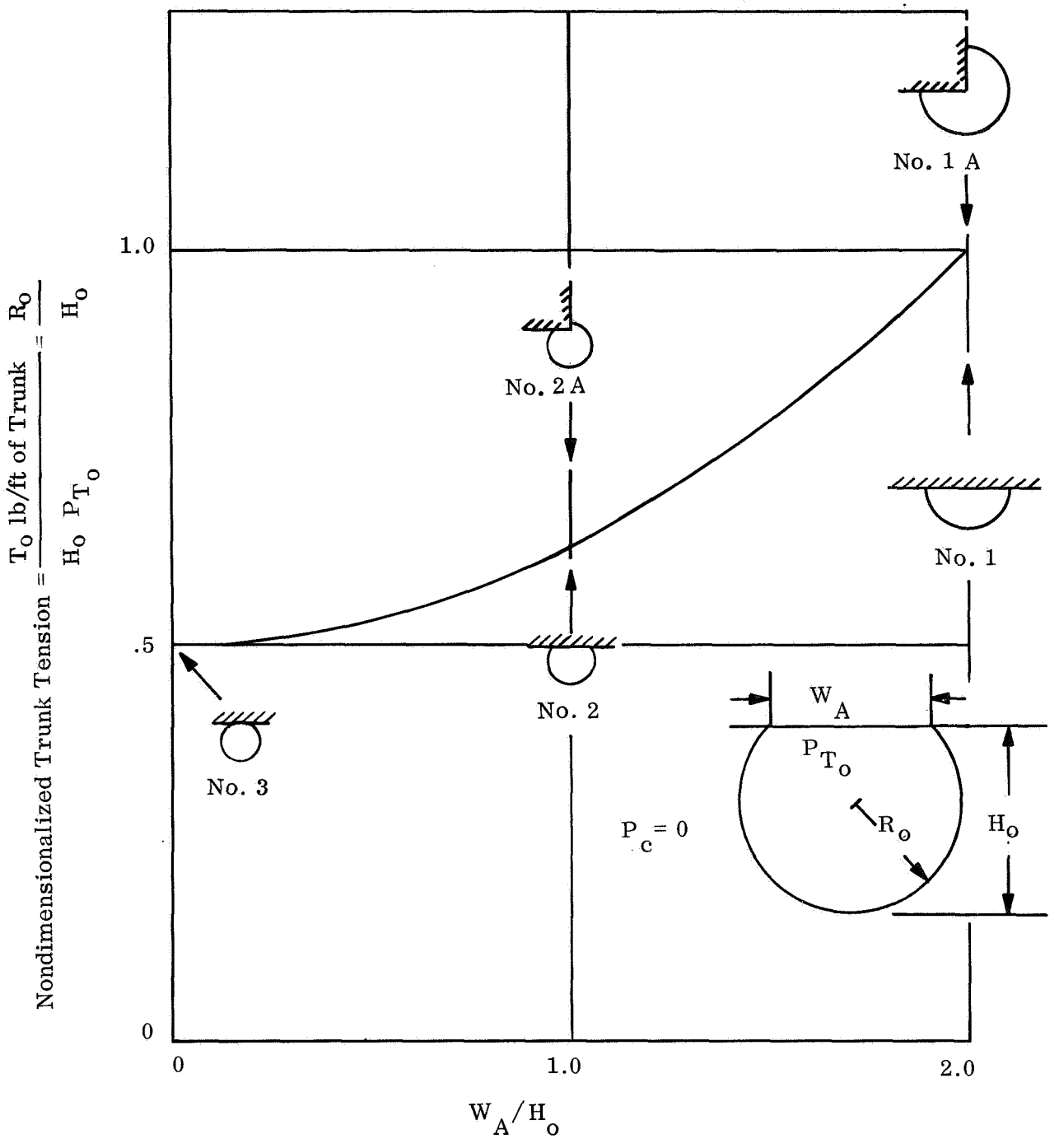

Fig. 35. Effect of Trunk Cross Section on Tension, $P_c = 0$

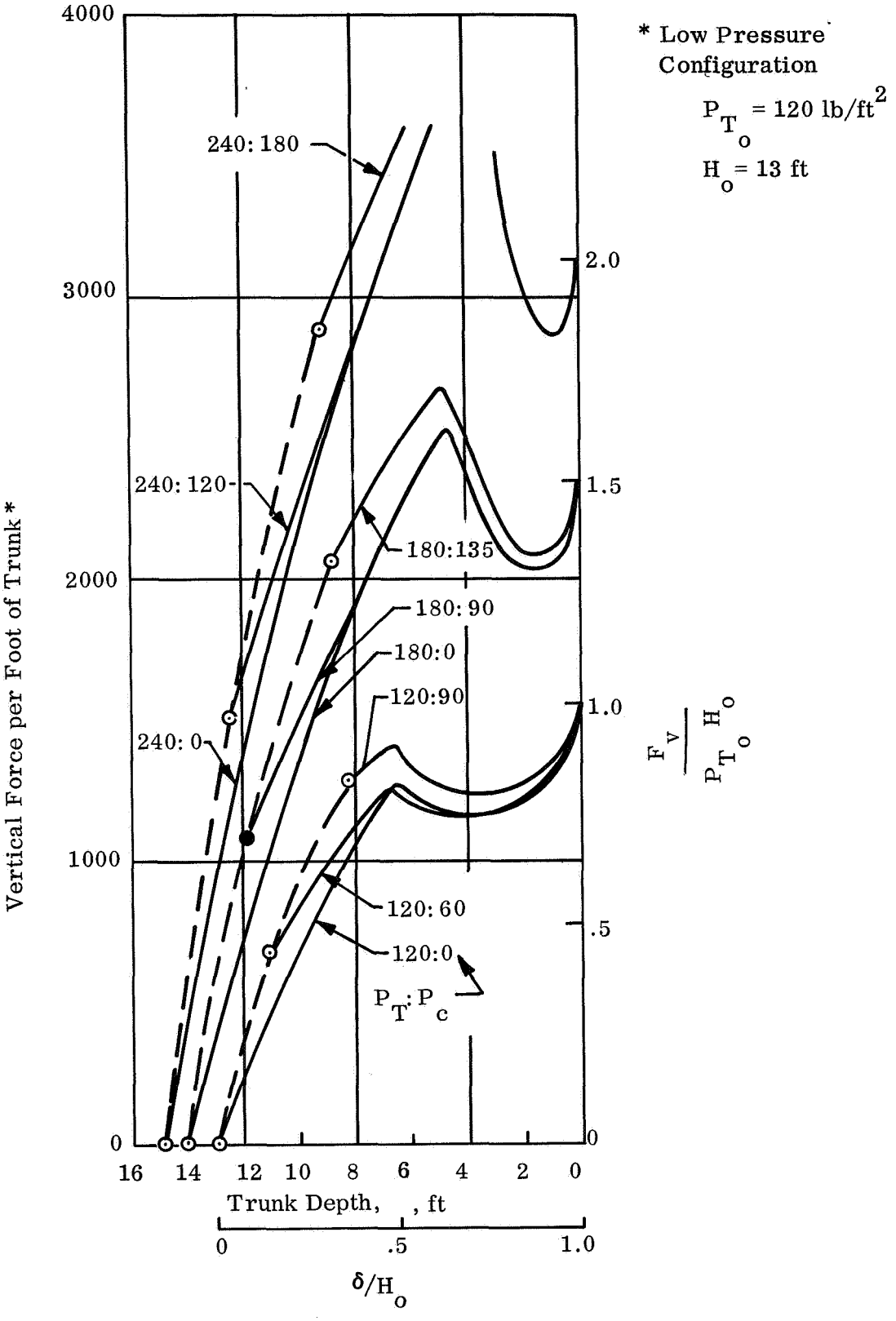

Fig. 36. Vertical Force vs Trunk Depth for Booster ACLS

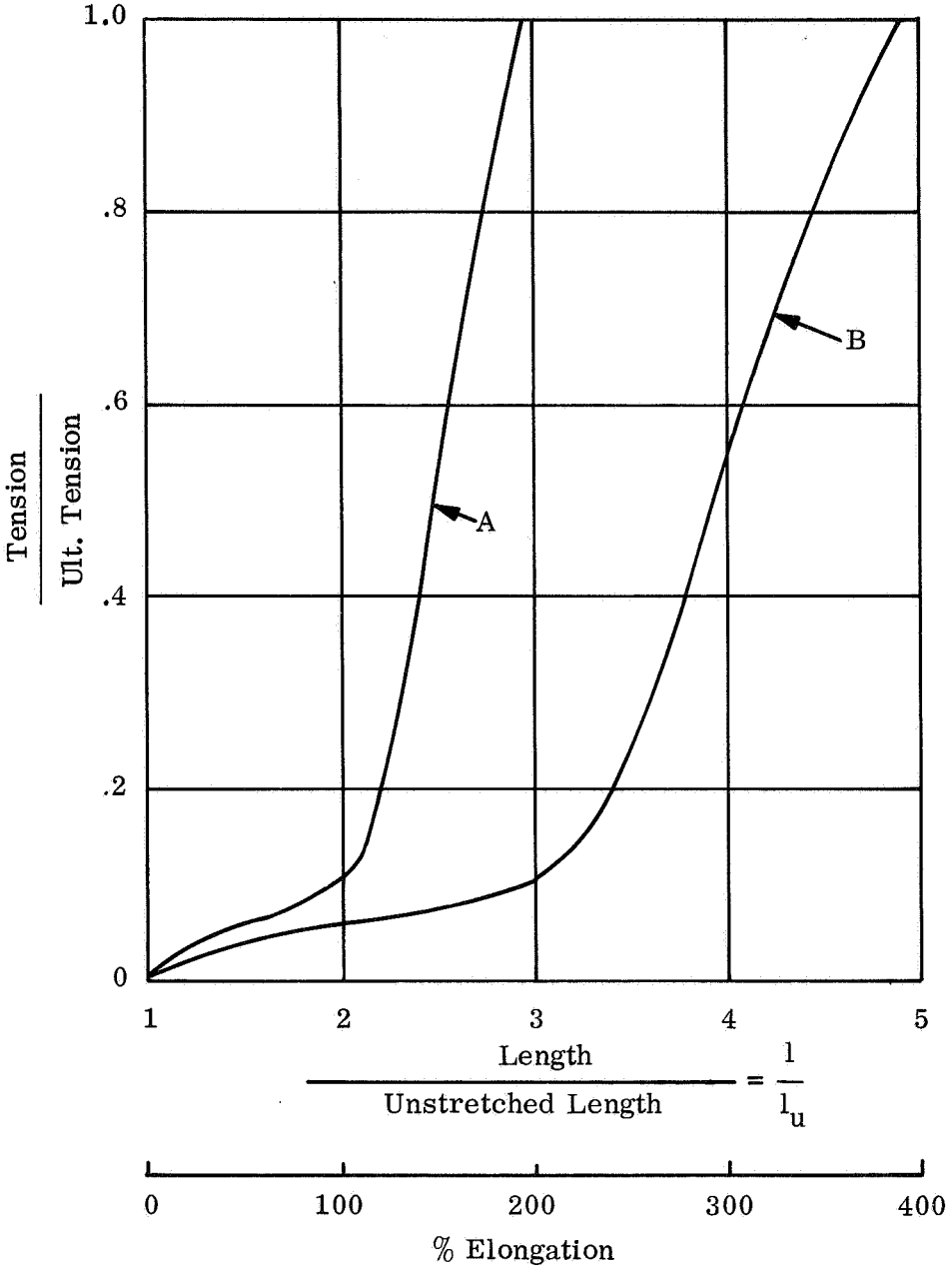

Fig. 37. Nondimensional Tension vs Elongation of Trunk Materials

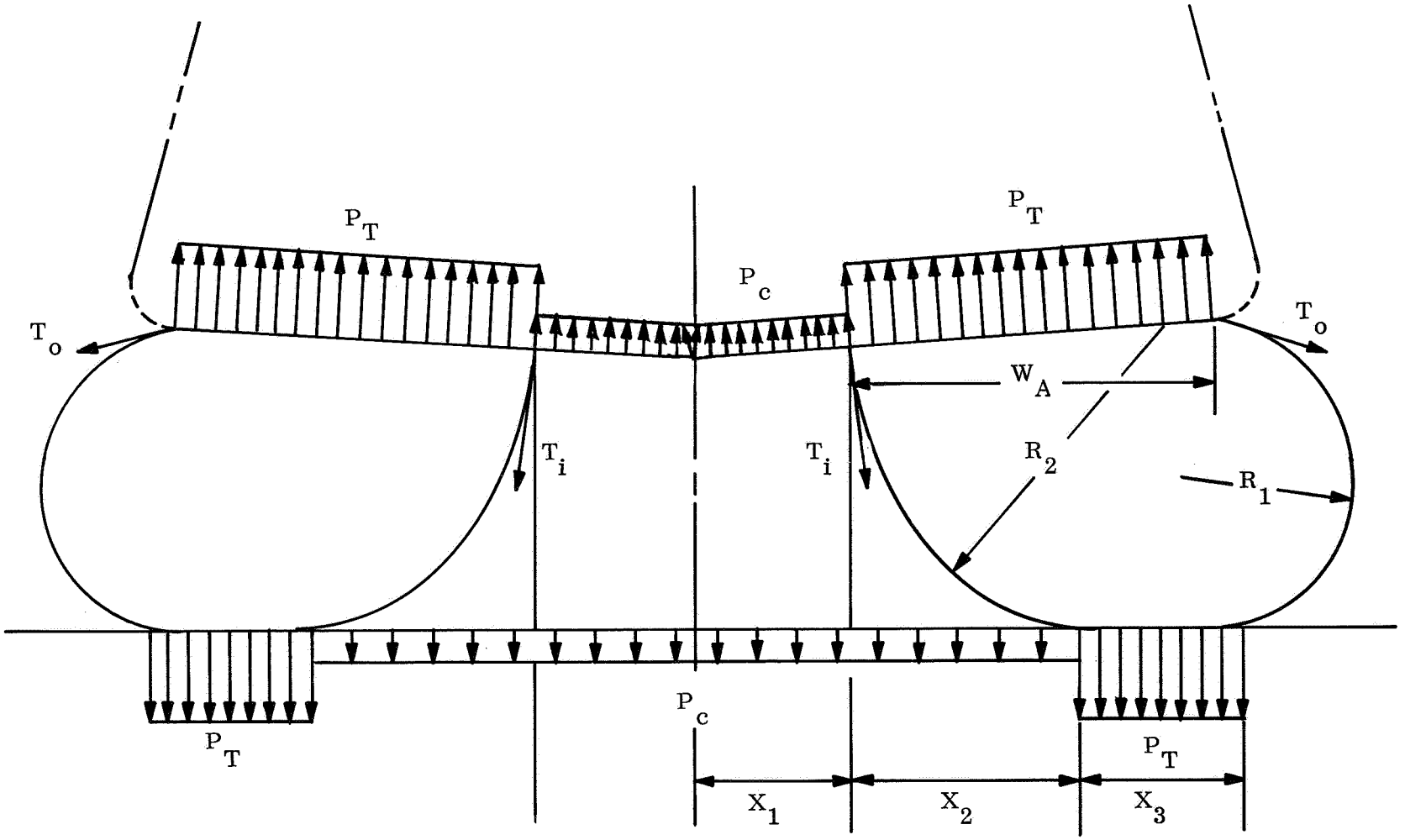

Fig. 38. ACLS Pressures and Tensions

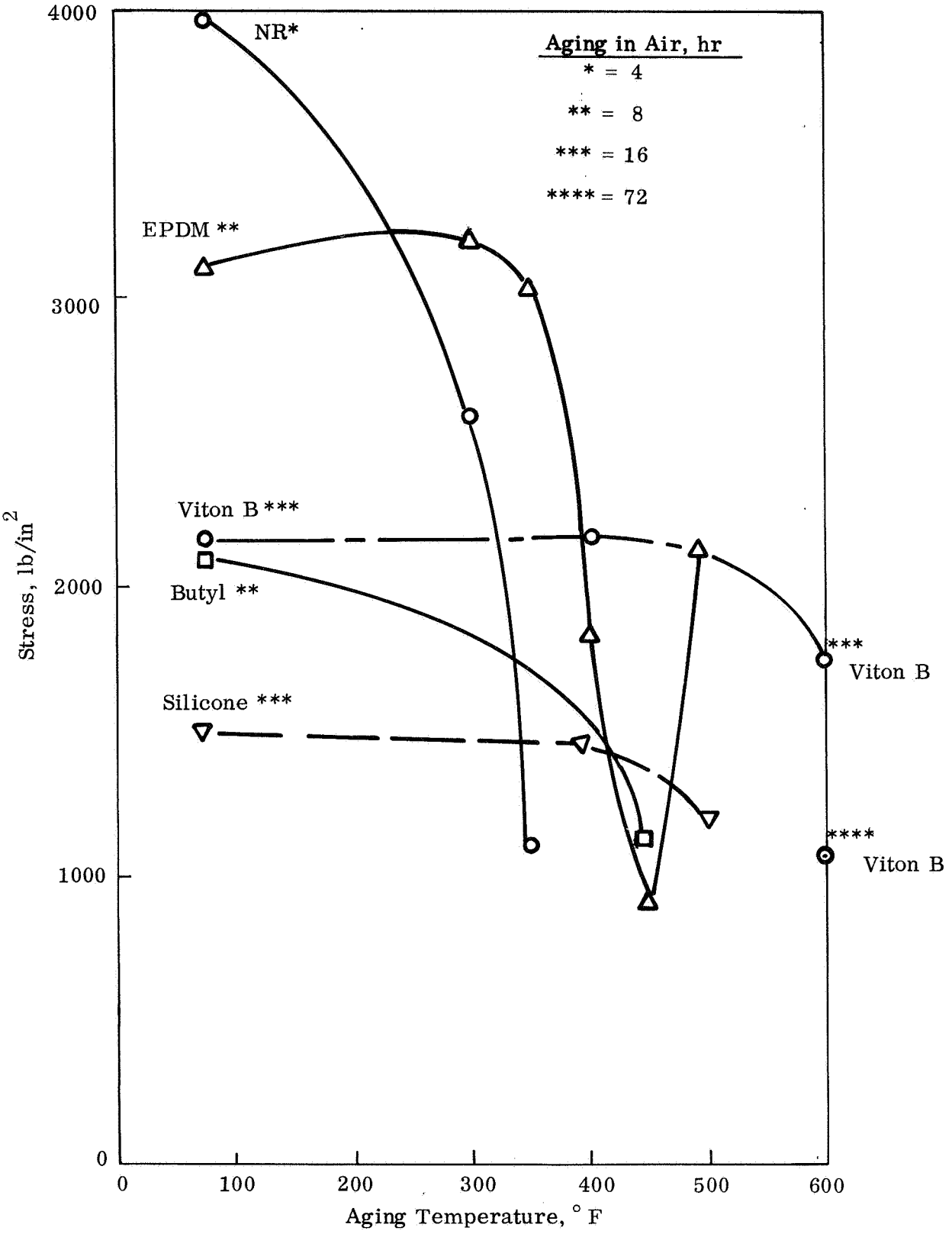

Fig. 39. Room Temperature Tensile Strength of High Temperature Compounds

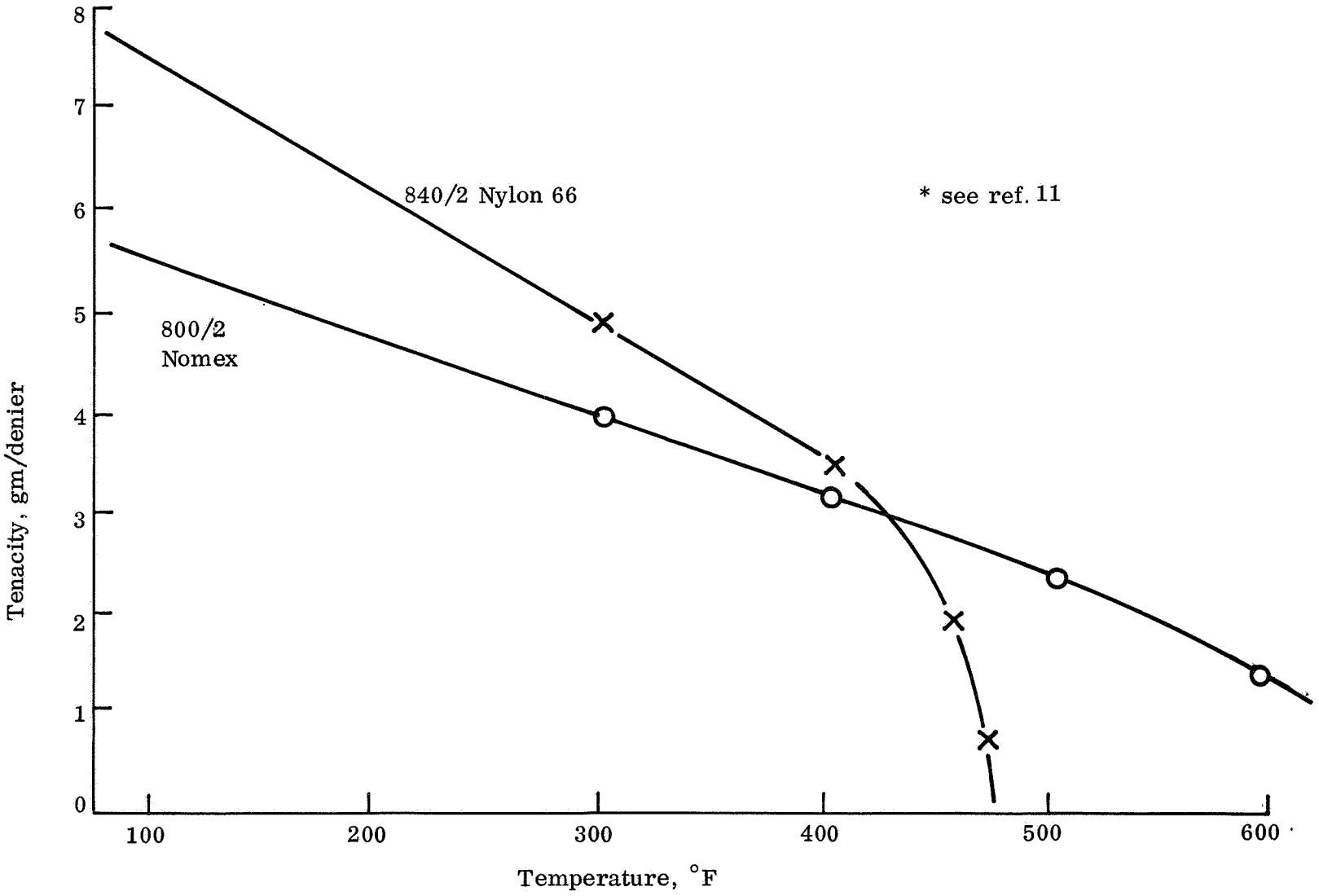

Fig. 40. Effect of Temperature On Tenacity of Nylon 66 and Nomex Fibers* - Exposure Time = 1 Minute

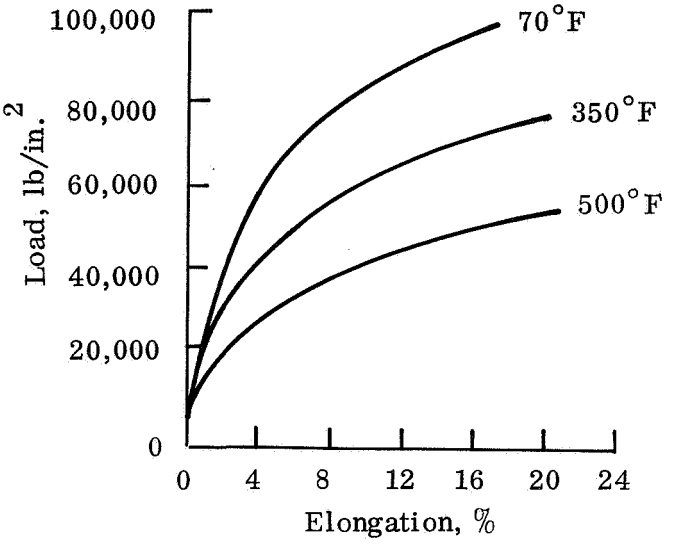

Fig. 41. Nomex High Temperature Resistant Nylon Stress-Strain Curves at Various Temperatures

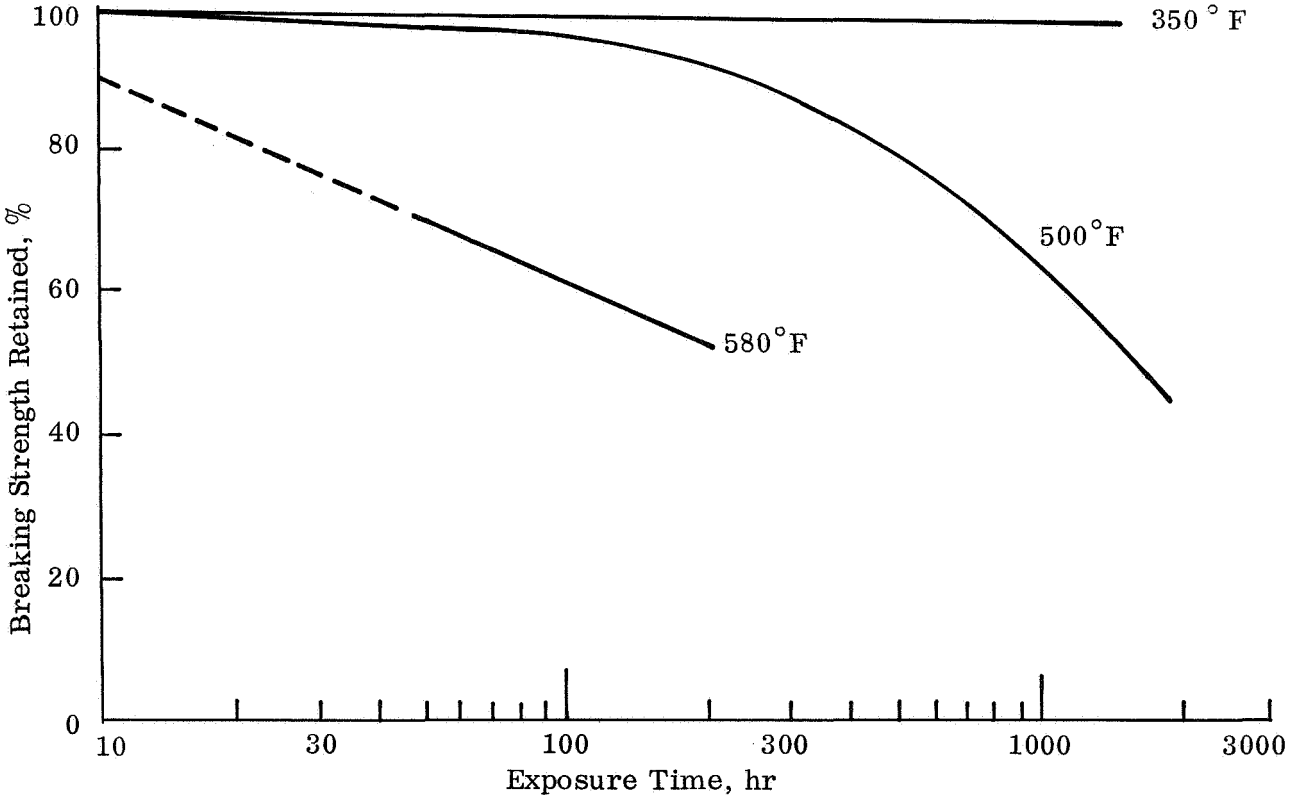

Fig. 42. Strength Retained by Nomex After Exposure to Hot, Dry Air; Specimens Tested at 70°F, 65% R.H.

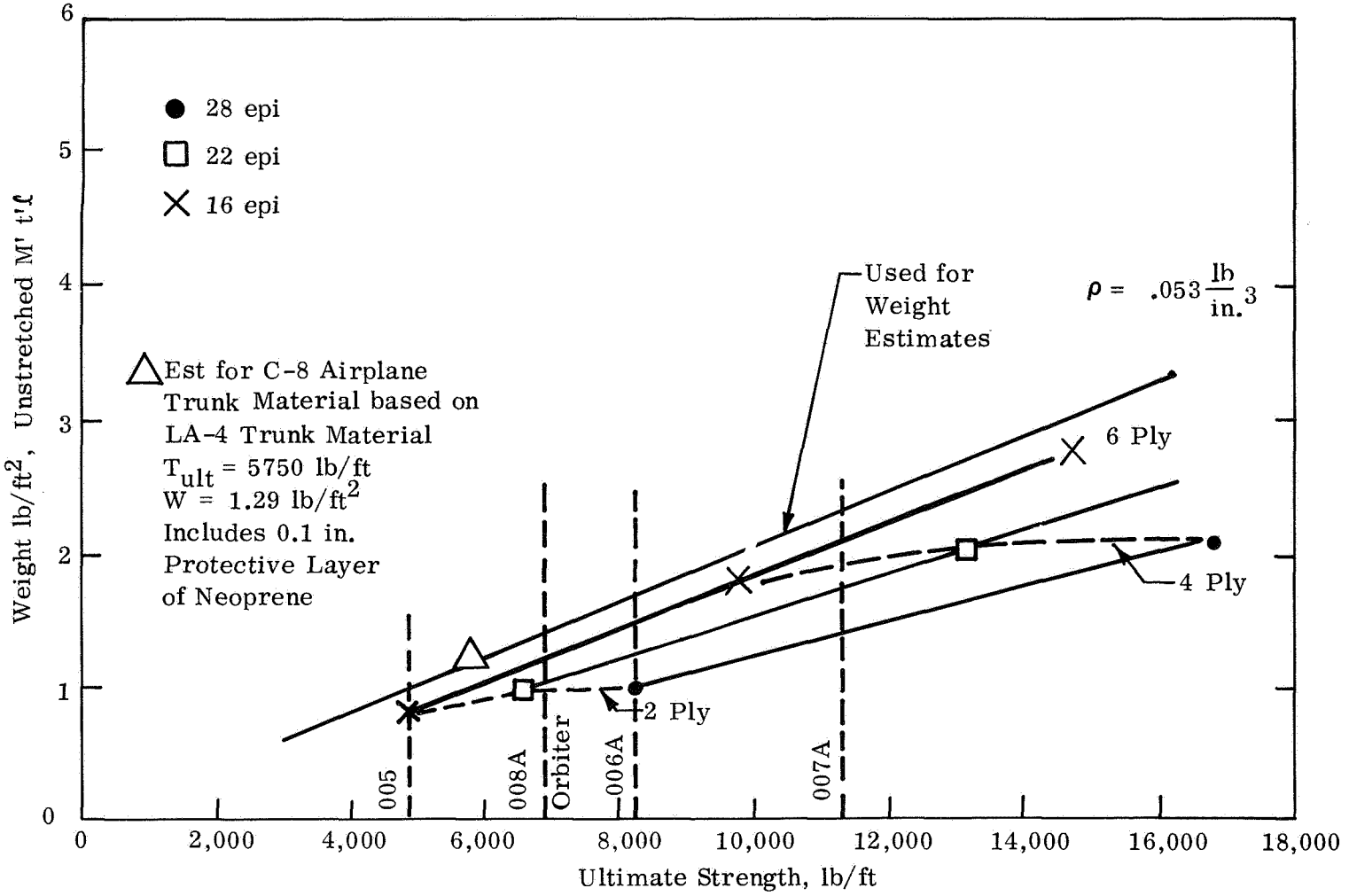

Fig. 43. Trunk Material Weight vs Ultimate Strength
(without Thermal Protection)

(ref. 5 MDC-E0056 - Vol. II, fig. 5.4-1)

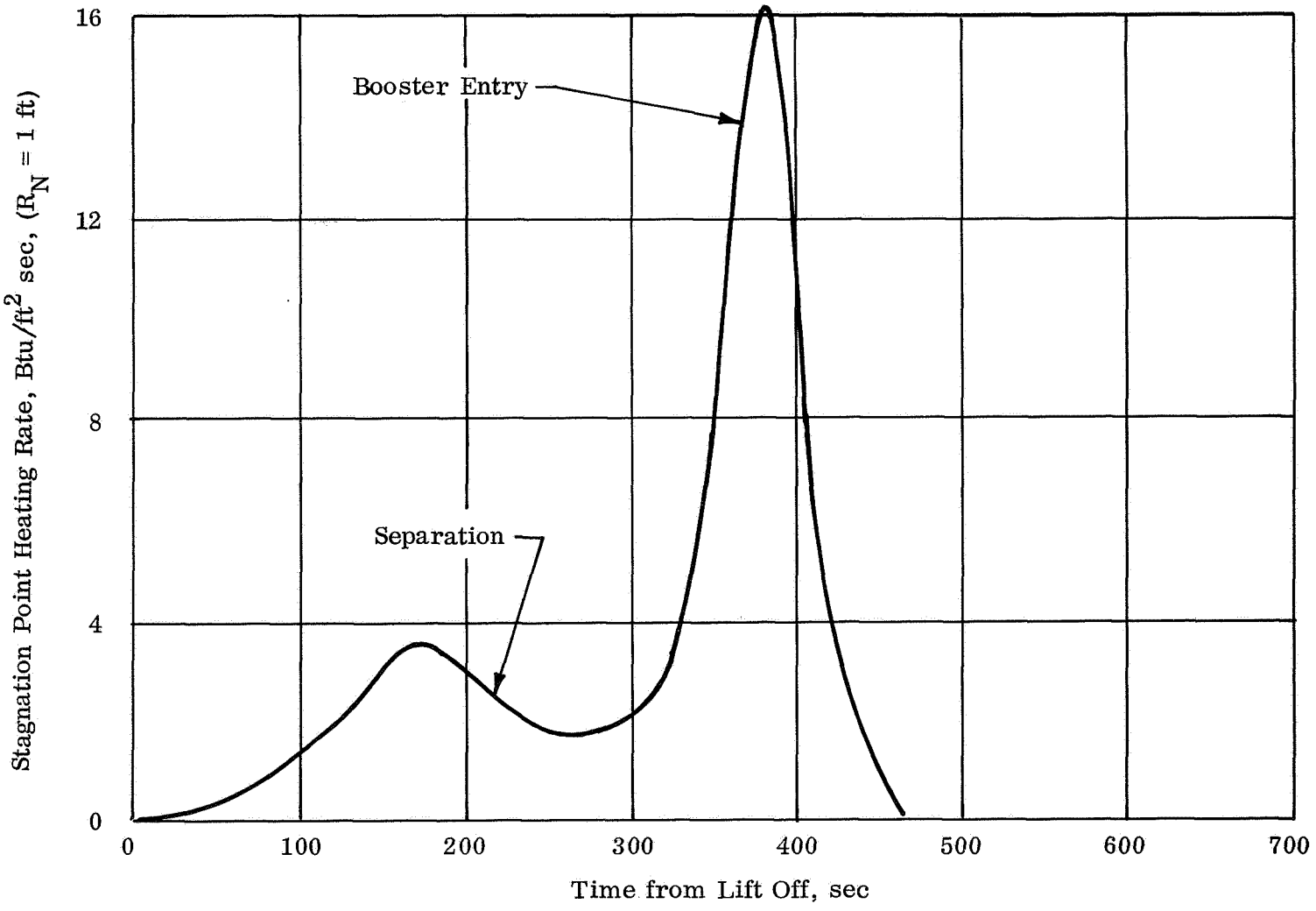

Fig. 44. Design Heating Rate History for the Booster
(Stagnation Point; R_N = 1 ft)

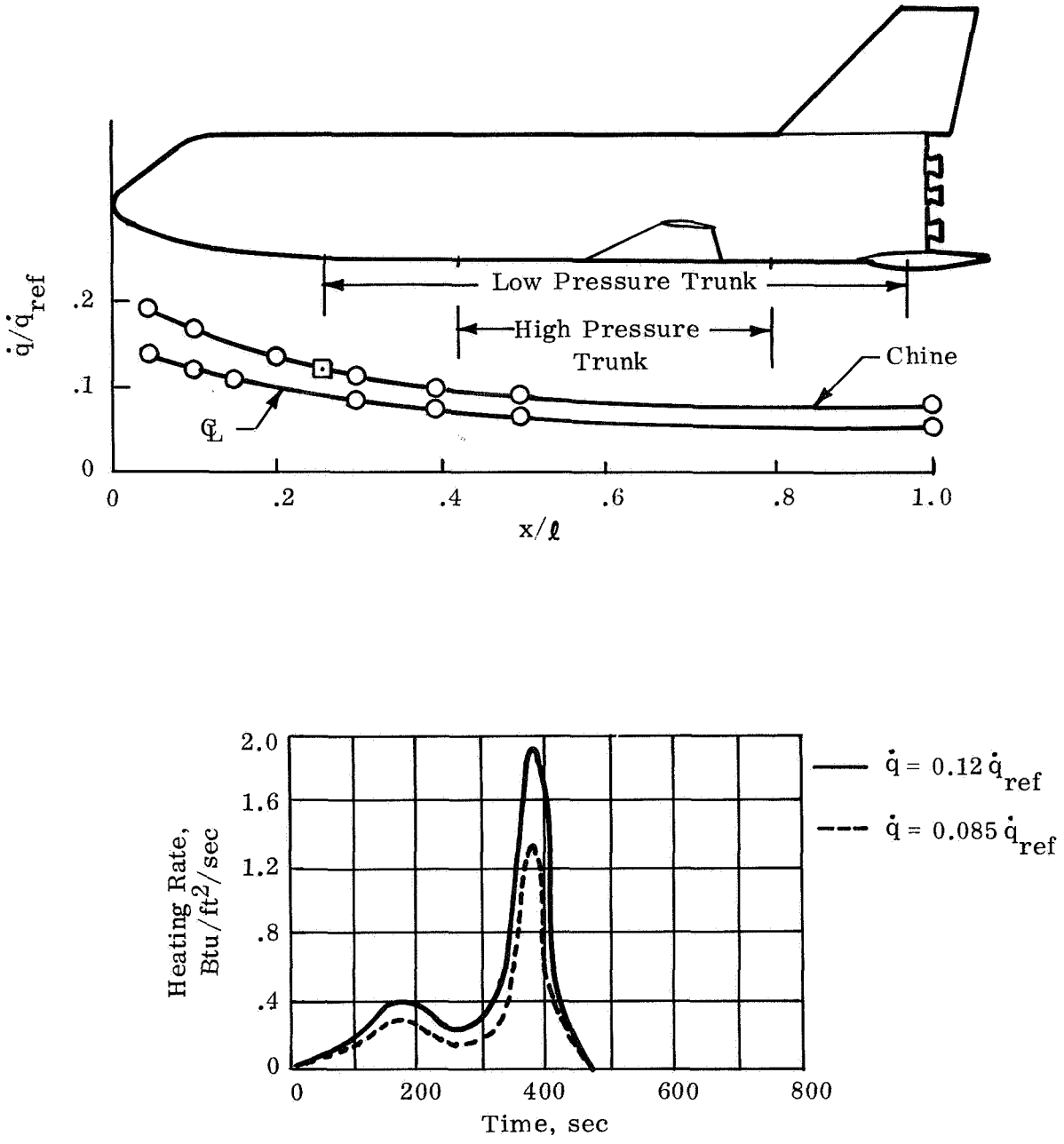

Fig. 45. Booster Lower Surface Heating Rates
(Based on McDonnell-Douglas Report, MDC-E 0056)

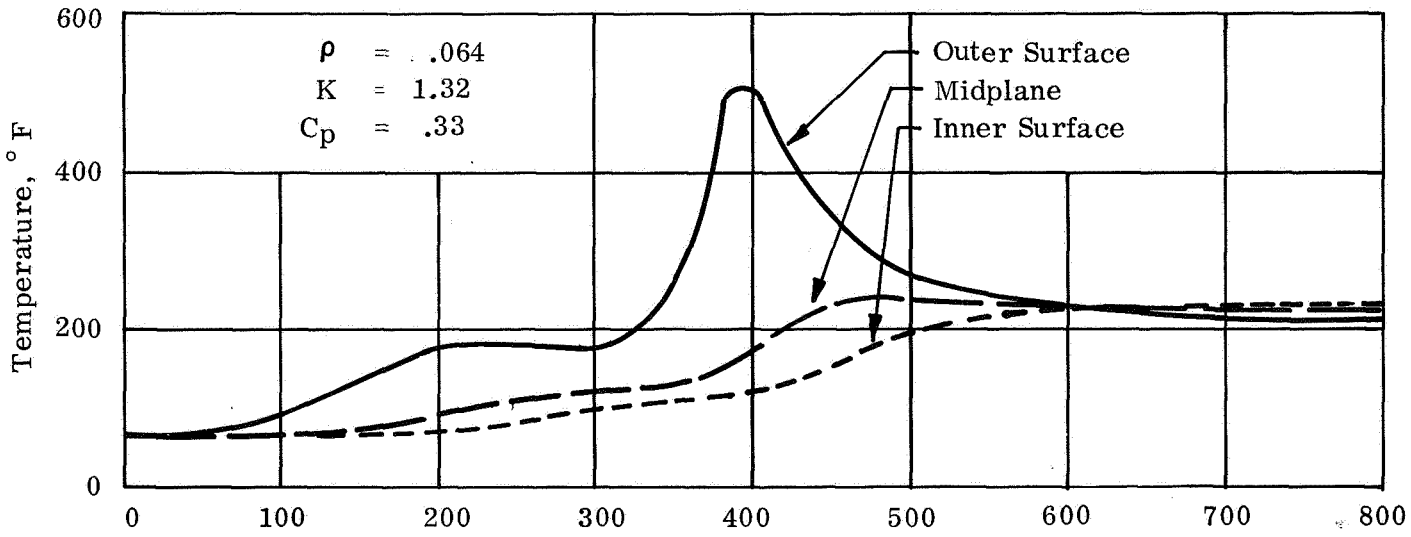

Fig. 46. Transient Temperature Distribution through .3 in. Thick Booster Trunk, Material (a)

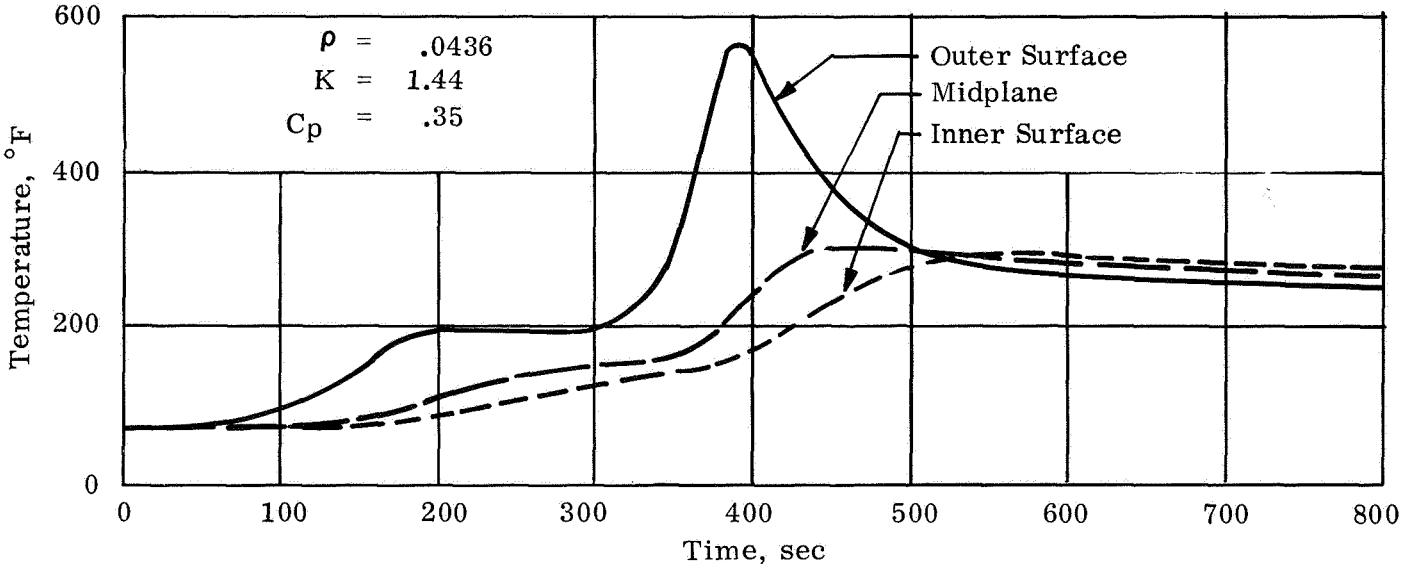

Fig. 47. Transient Temperature Distribution through .3 in. Thick Booster Trunk, Material (b)

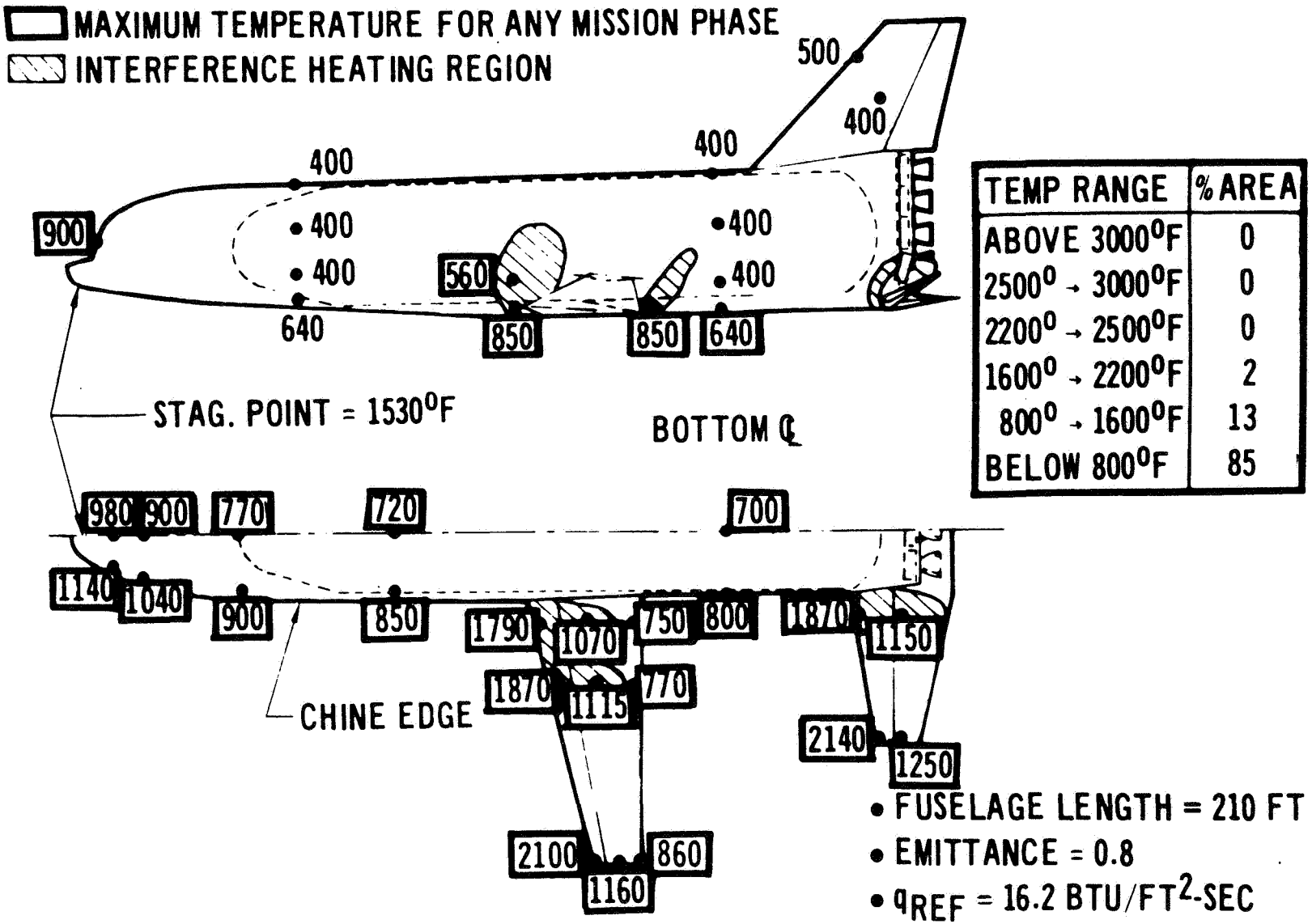

TEMP RANGE	%AREA
ABOVE 3000°F	0
2500° → 3000°F	0
2200° → 2500°F	0
1600° → 2200°F	2
800° → 1600°F	13
BELOW 800°F	85

(ref. 5 Report MDC E0056, Vol II, 15 Dec 1969)

Fig. 48. Booster Temperature, $\alpha = 60^\circ$ Entry

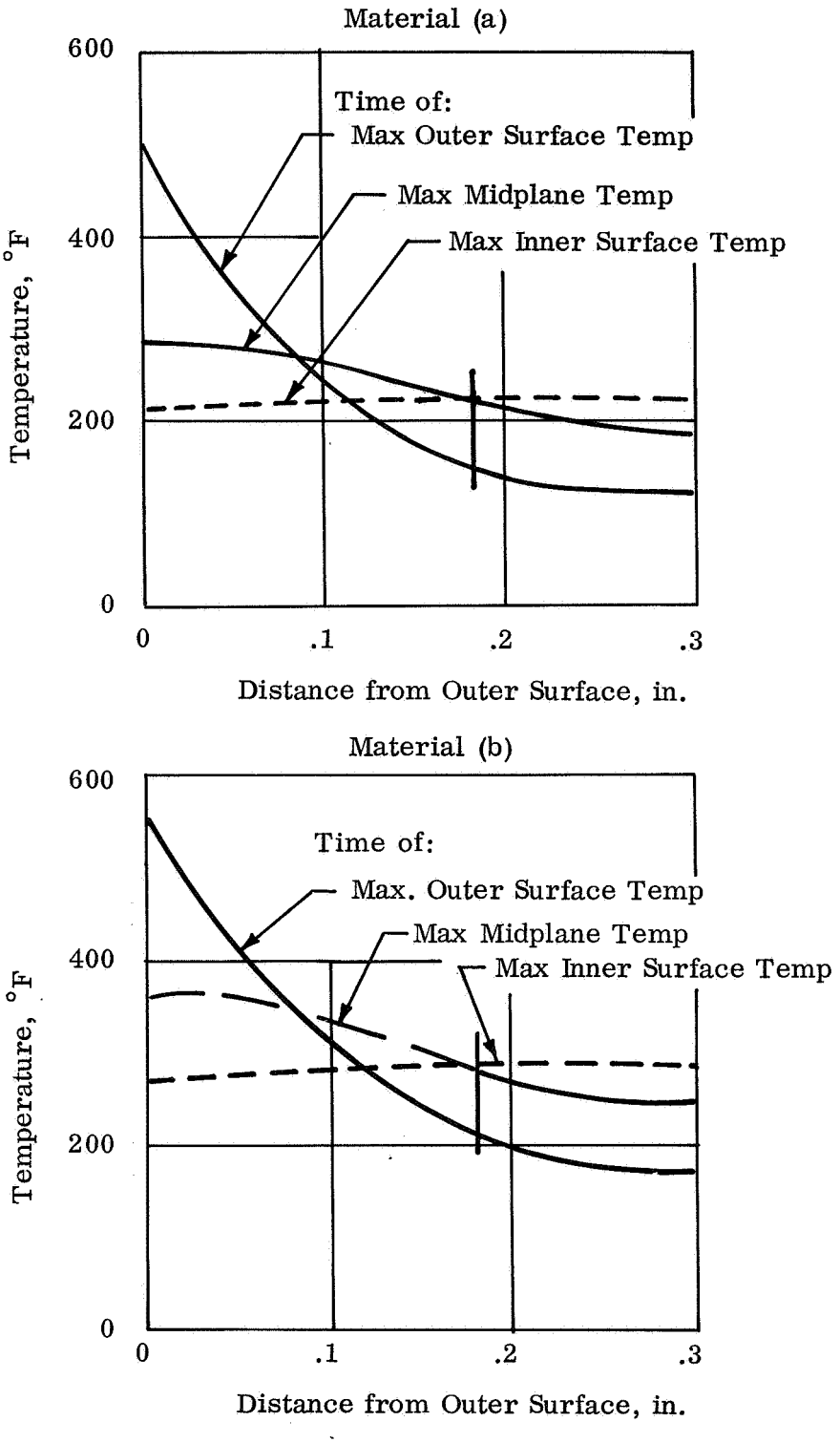

Fig. 49. Temperature Gradients through .3 in. Thick Trunks at Selected Times

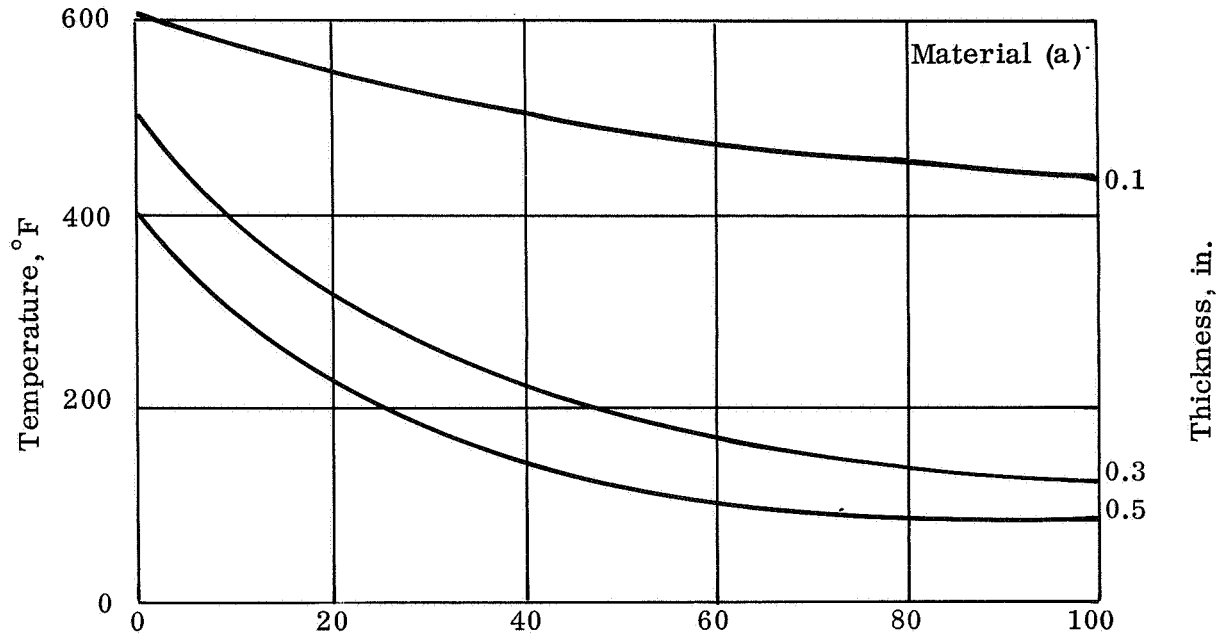

Fig. 50. Effect of Trunk Thickness on Temperature Gradients at Time of Maximum Outer Surface Temperature

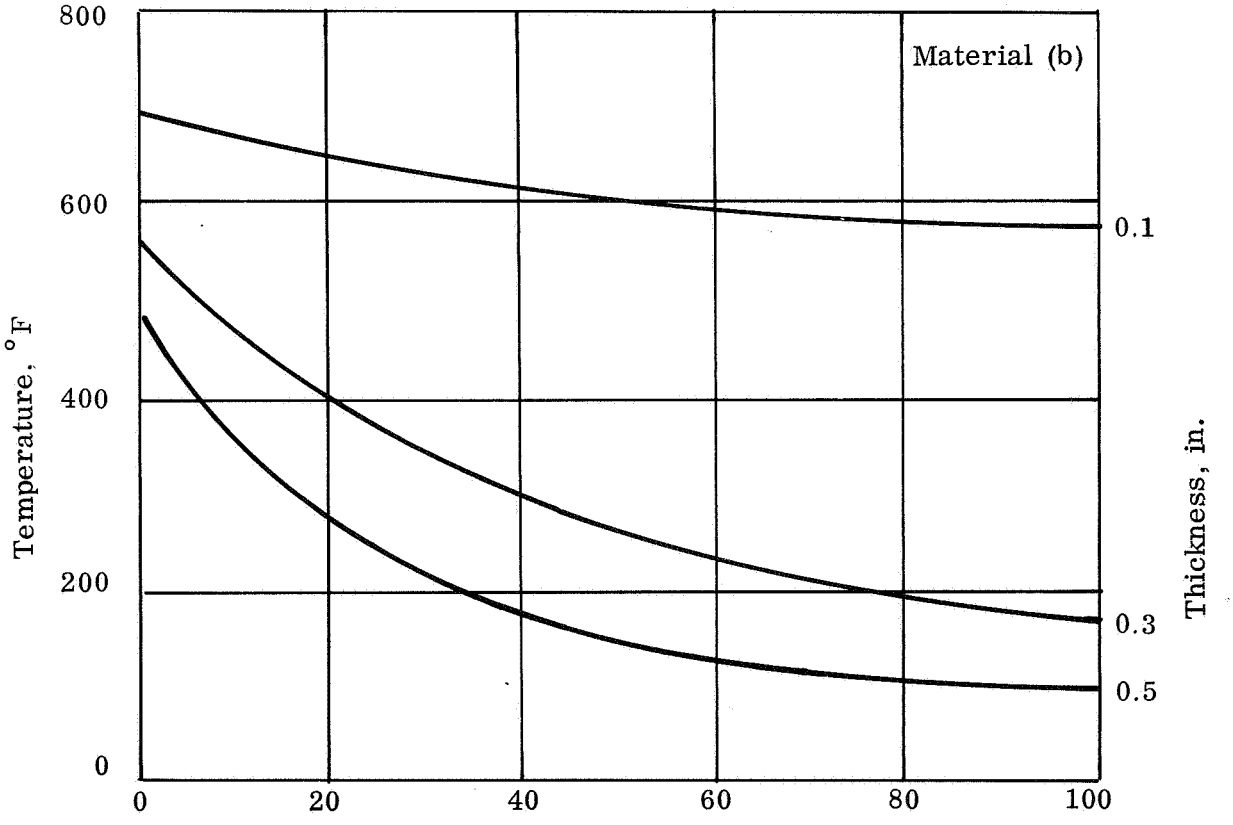

Fig. 51. Effect of Trunk Thickness on Temperature Gradients at Time of Maximum Outer Surface Temperature

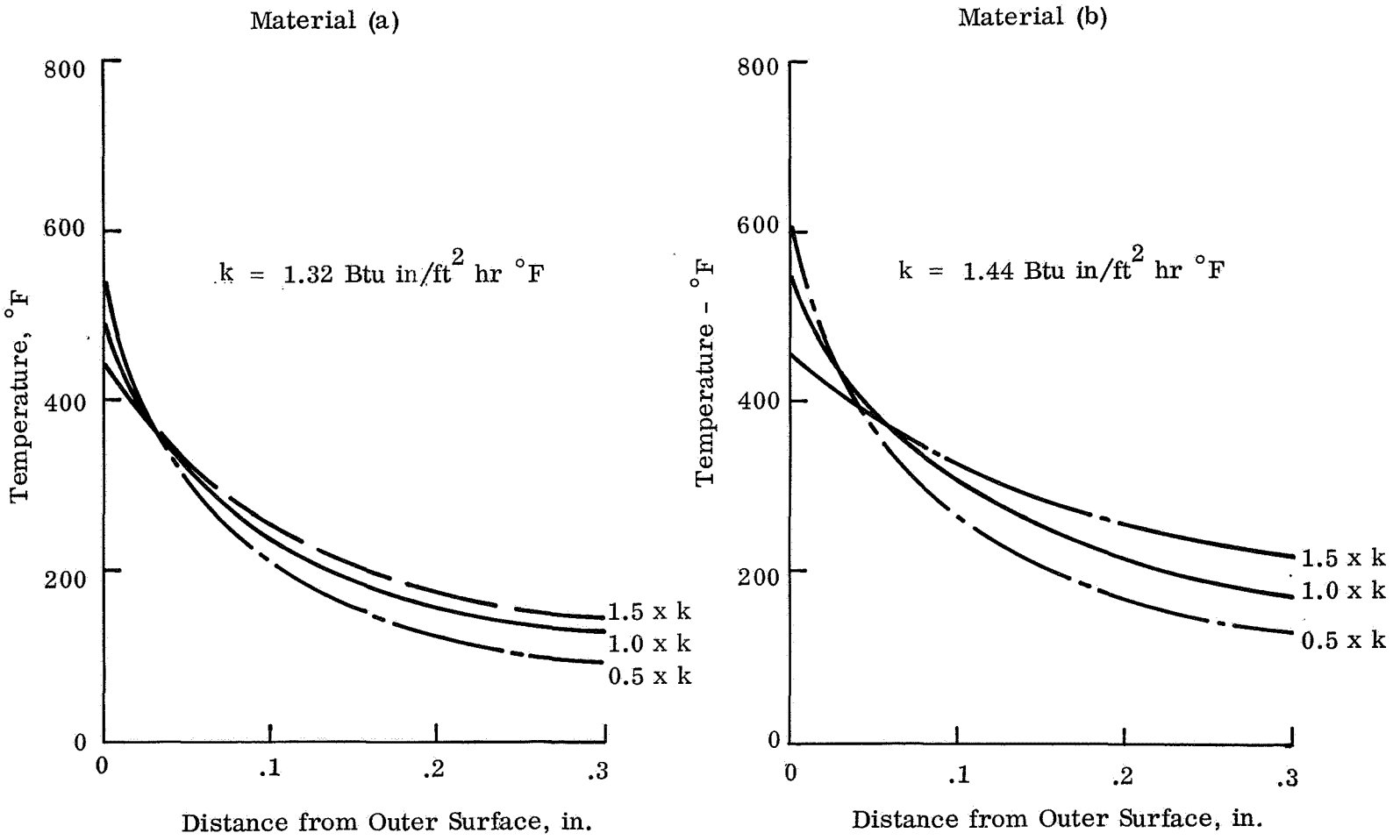

Fig. 52. Effect of Thermal Conductivity on Temperature Gradients through .3 in. Thick Trunks at Time of Maximum Outer Surface Temperature

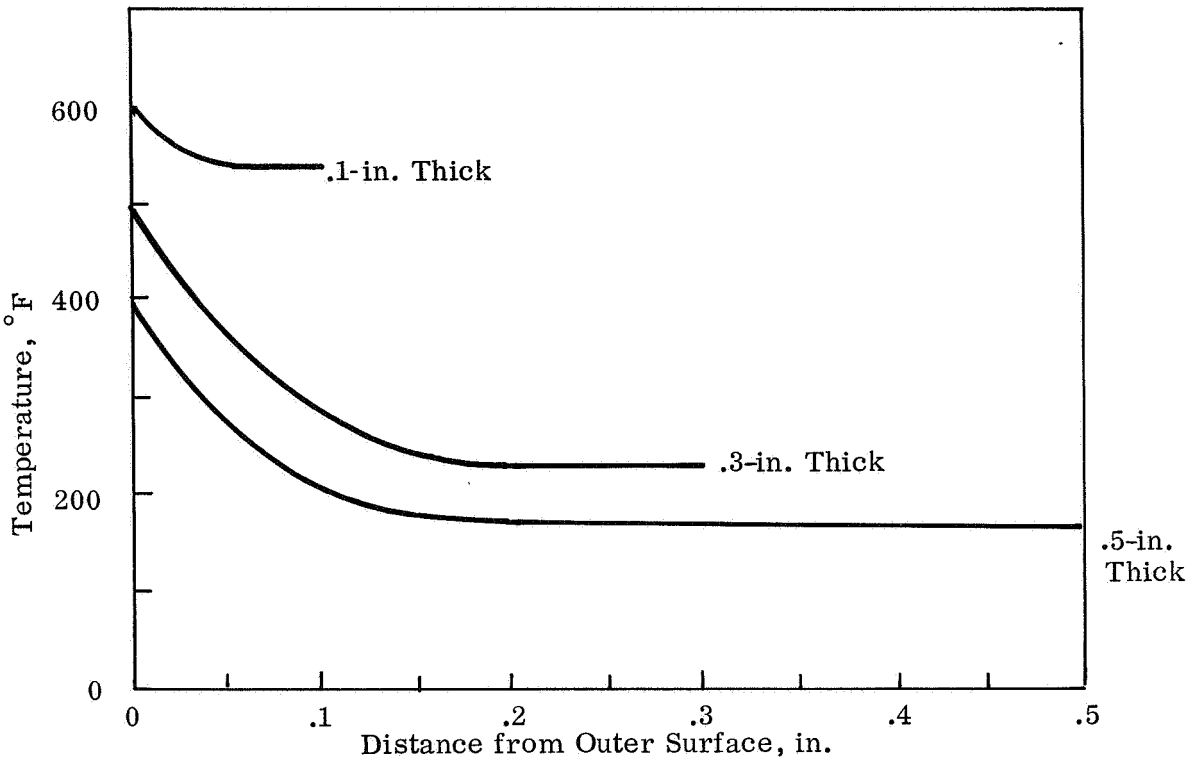

Fig. 53. Maximum Temperature Attained through the Thickness vs Distance from Outer Surface, Material (a)

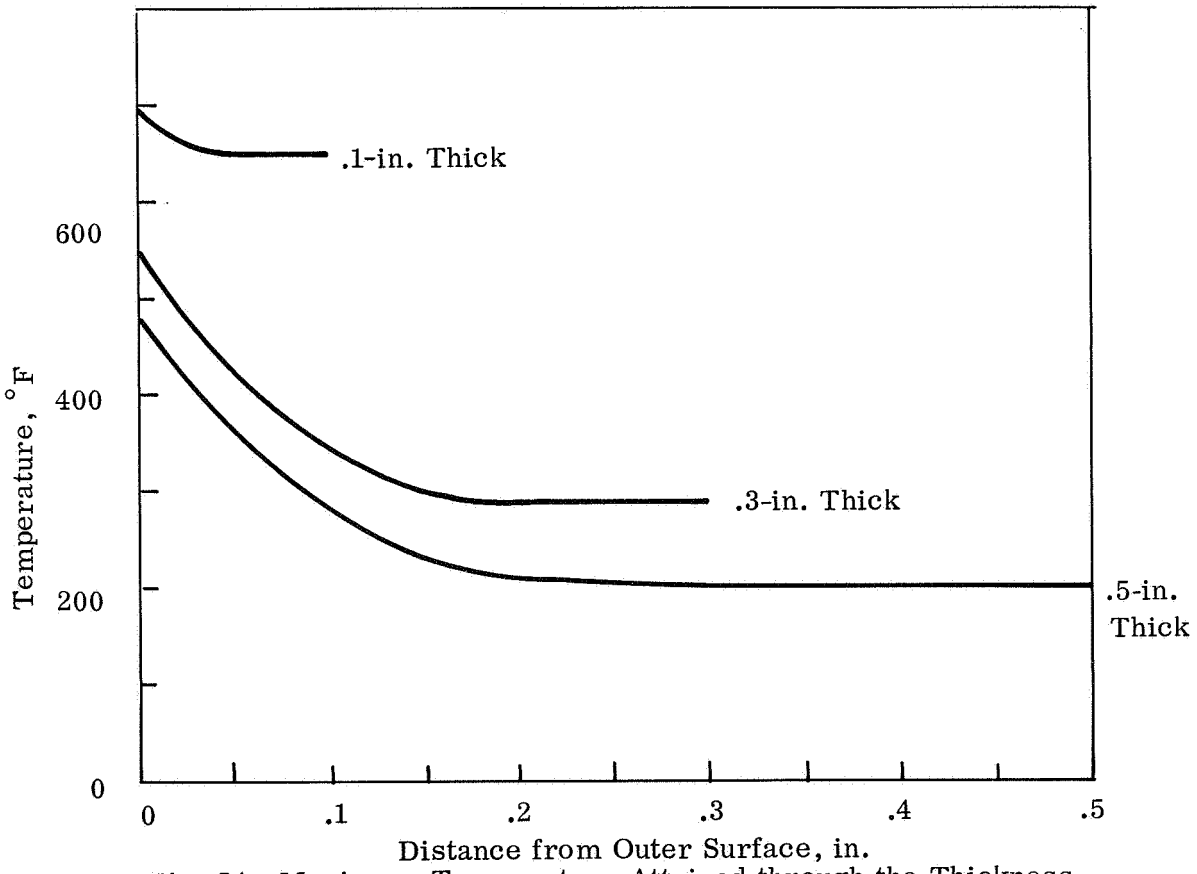

Fig. 54. Maximum Temperature Attained through the Thickness vs Distance from Outer Surface, Material (b)

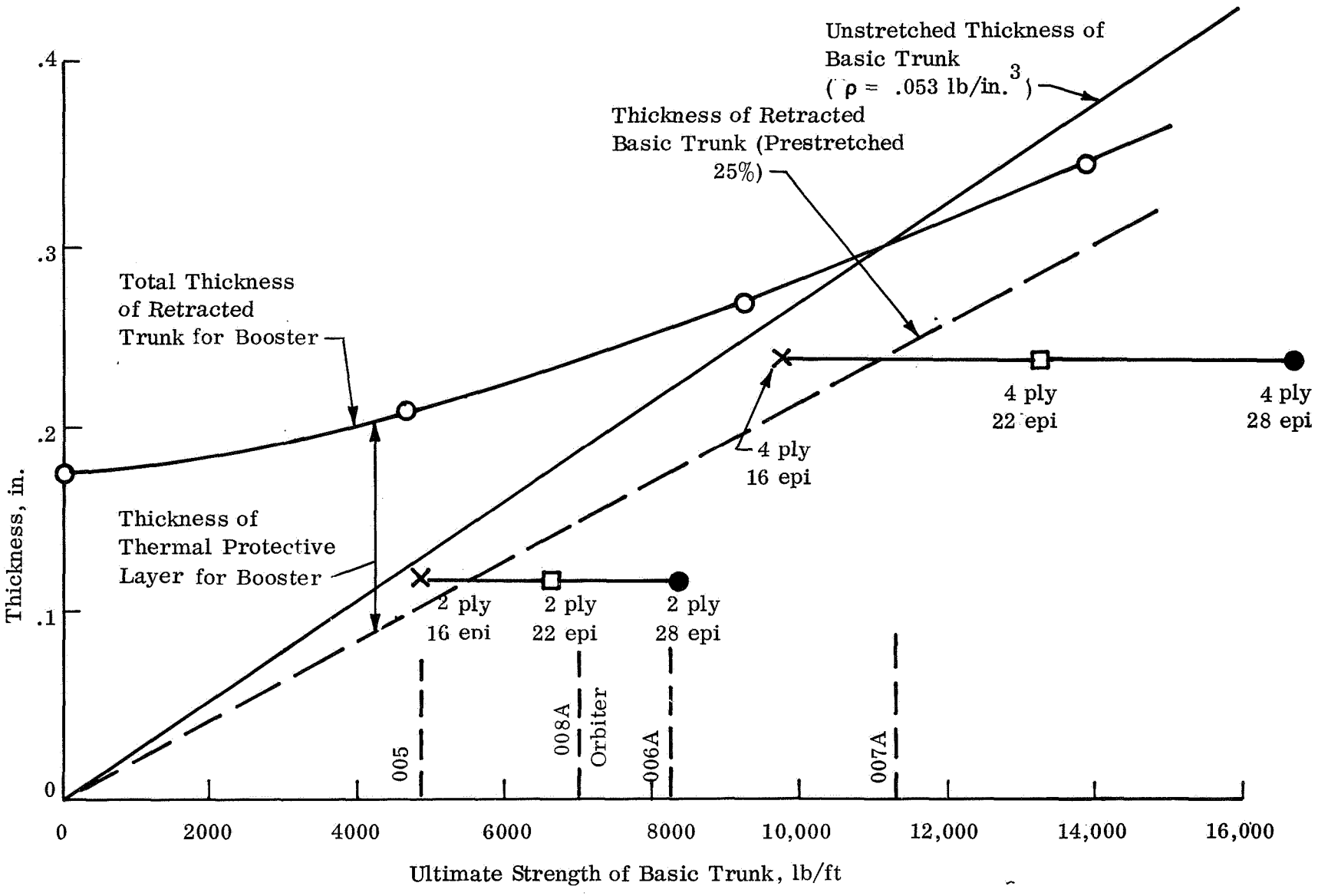

Fig. 55 . Trunk Material Thickness vs Ultimate Strength

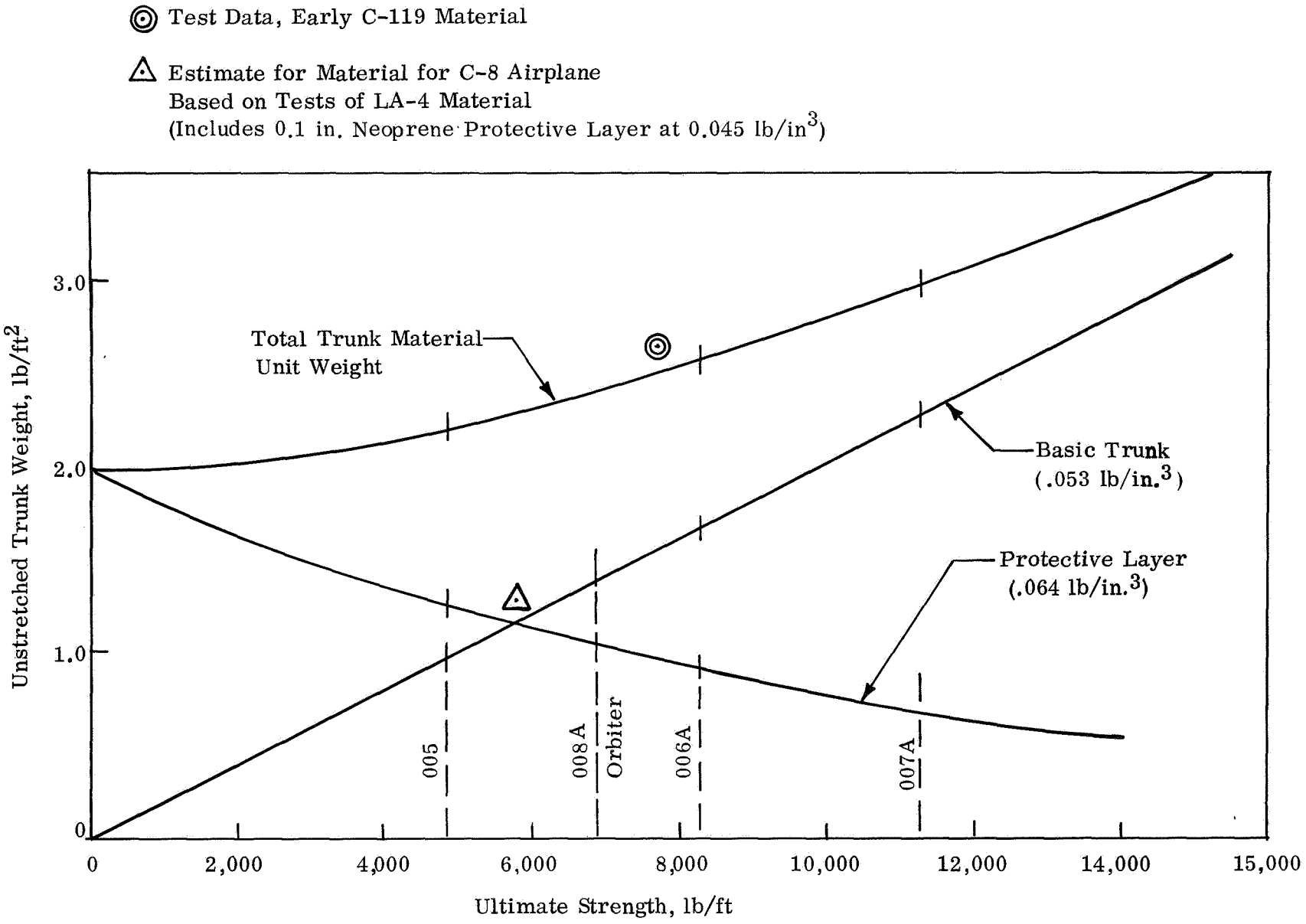

Fig. 56. Trunk Material Unit Weight vs Ultimate Strength

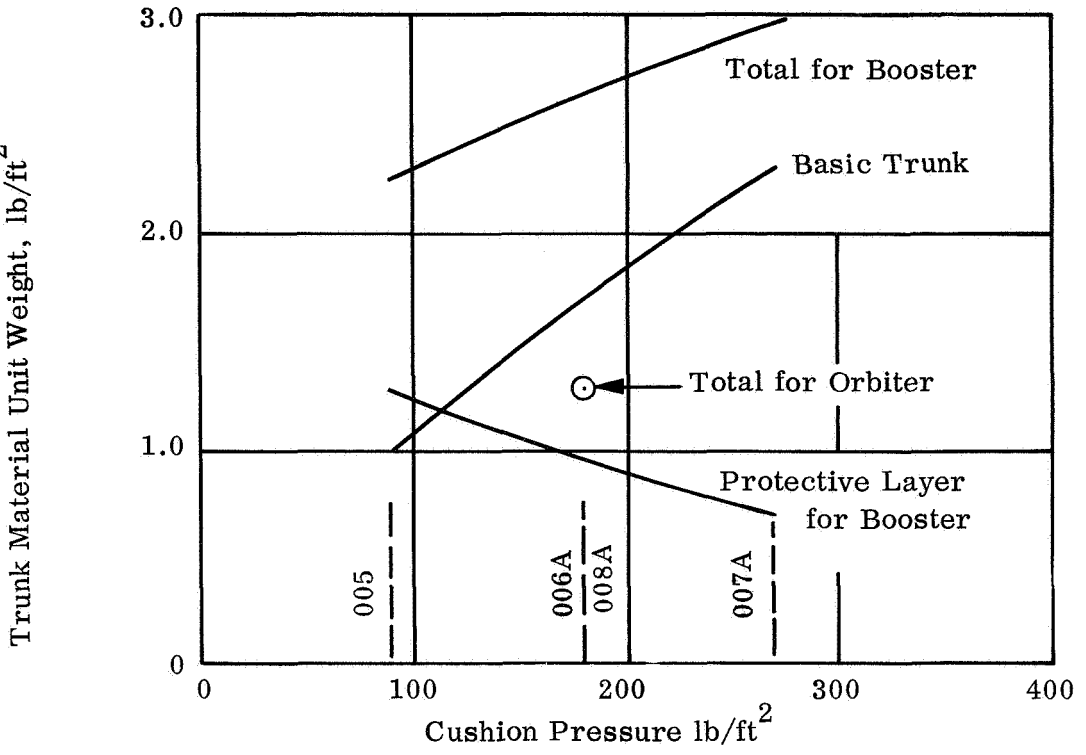

Fig. 57. Trunk Material Unit Weight versus Cushion Pressure

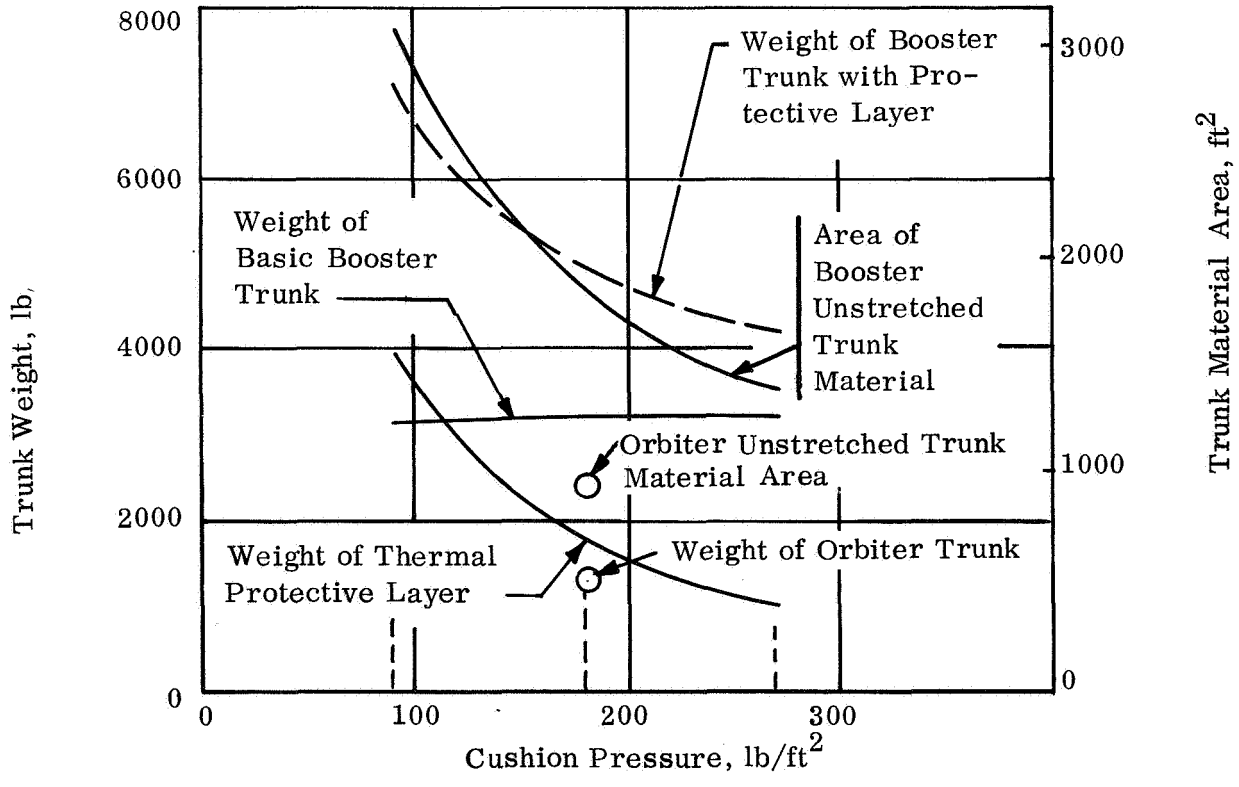

Fig. 58. Trunk Weight versus Cushion Pressure

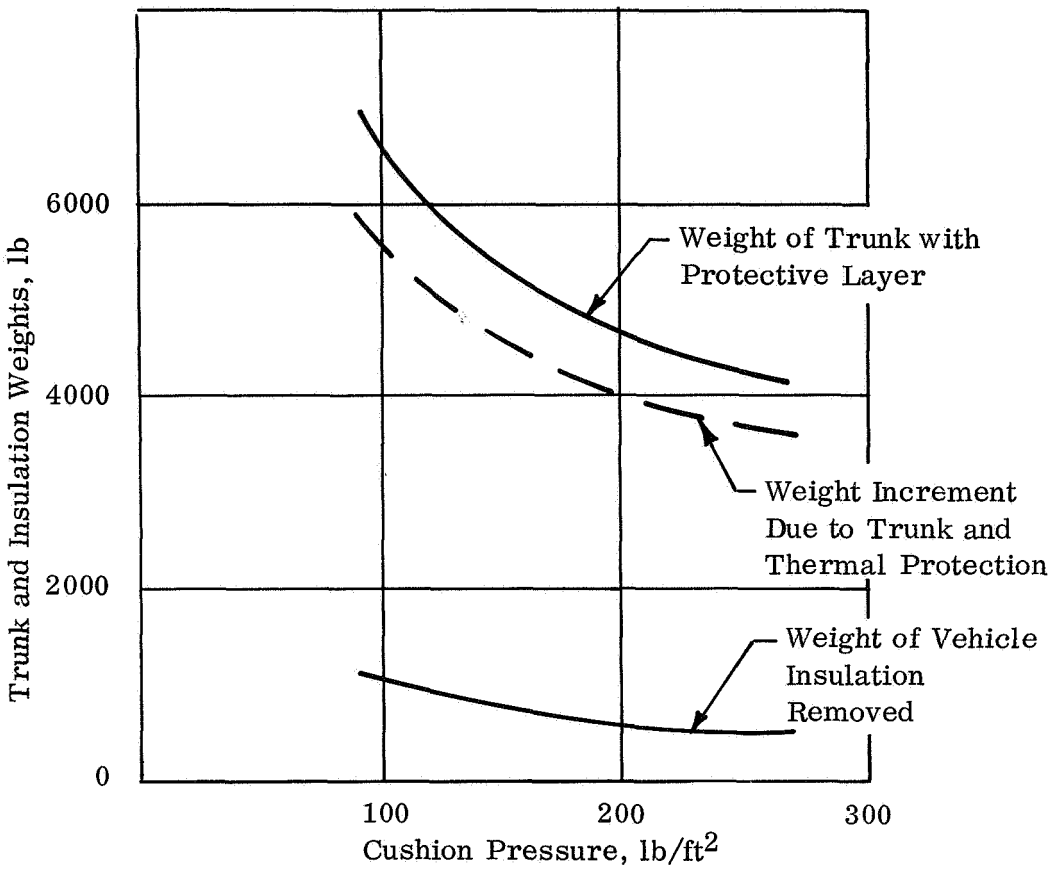

Fig. 59. Weight Increment Due to Booster Trunk vs Cushion Pressure

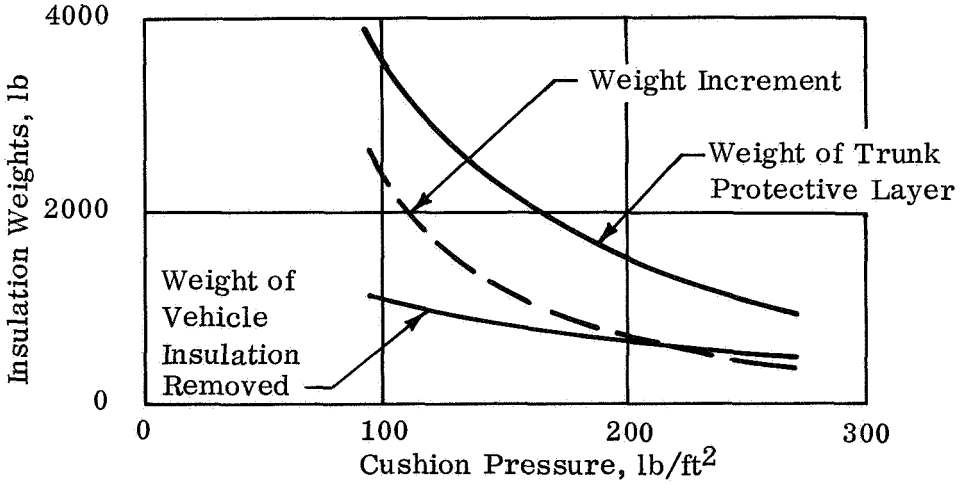

Fig. 60. Booster ACLS Thermal Protection Weight Increment vs Cushion Pressure

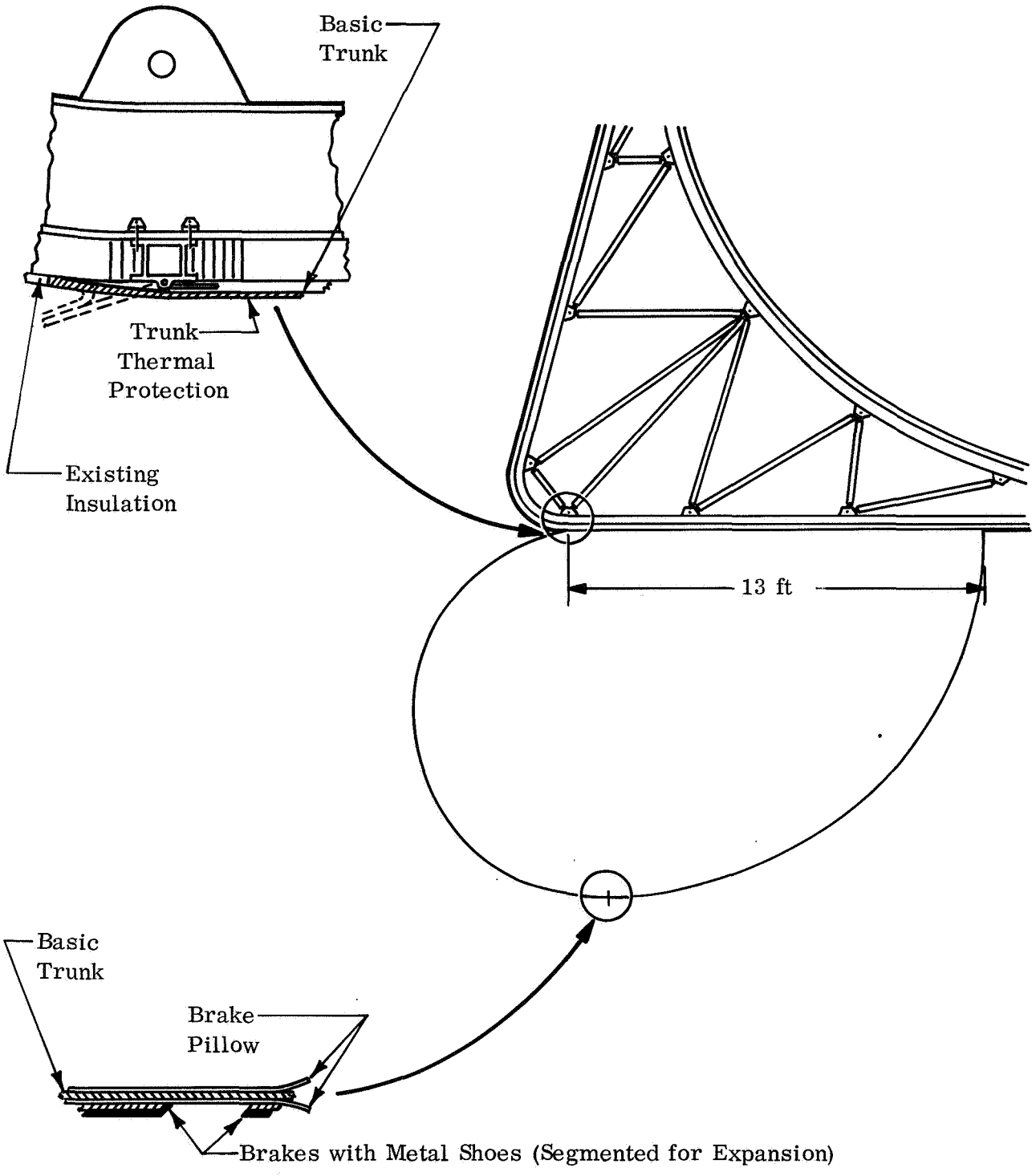

Fig. 61. Trunk Details

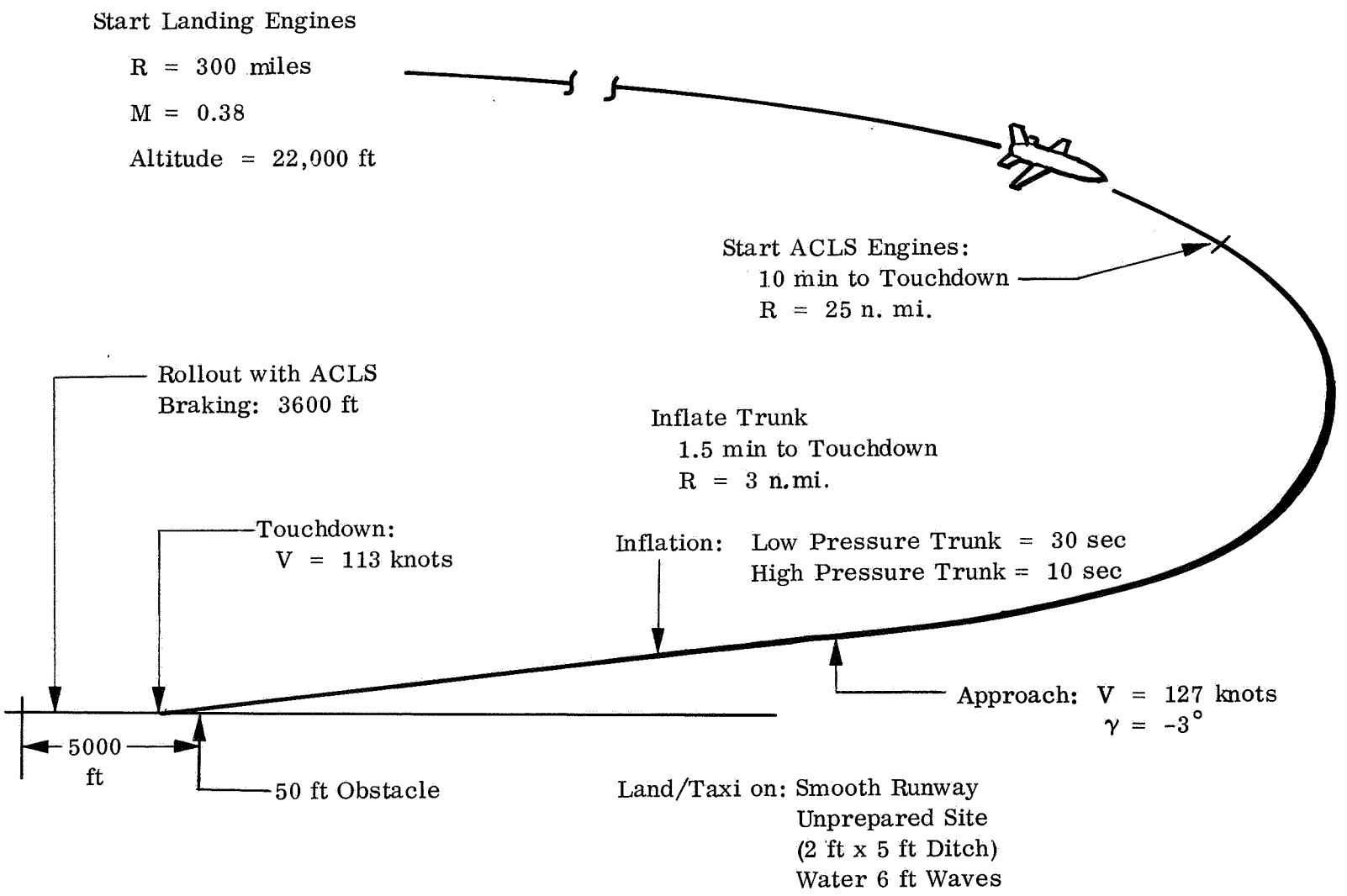

Fig. 62. Approach, Landing, and Braking with ACLS

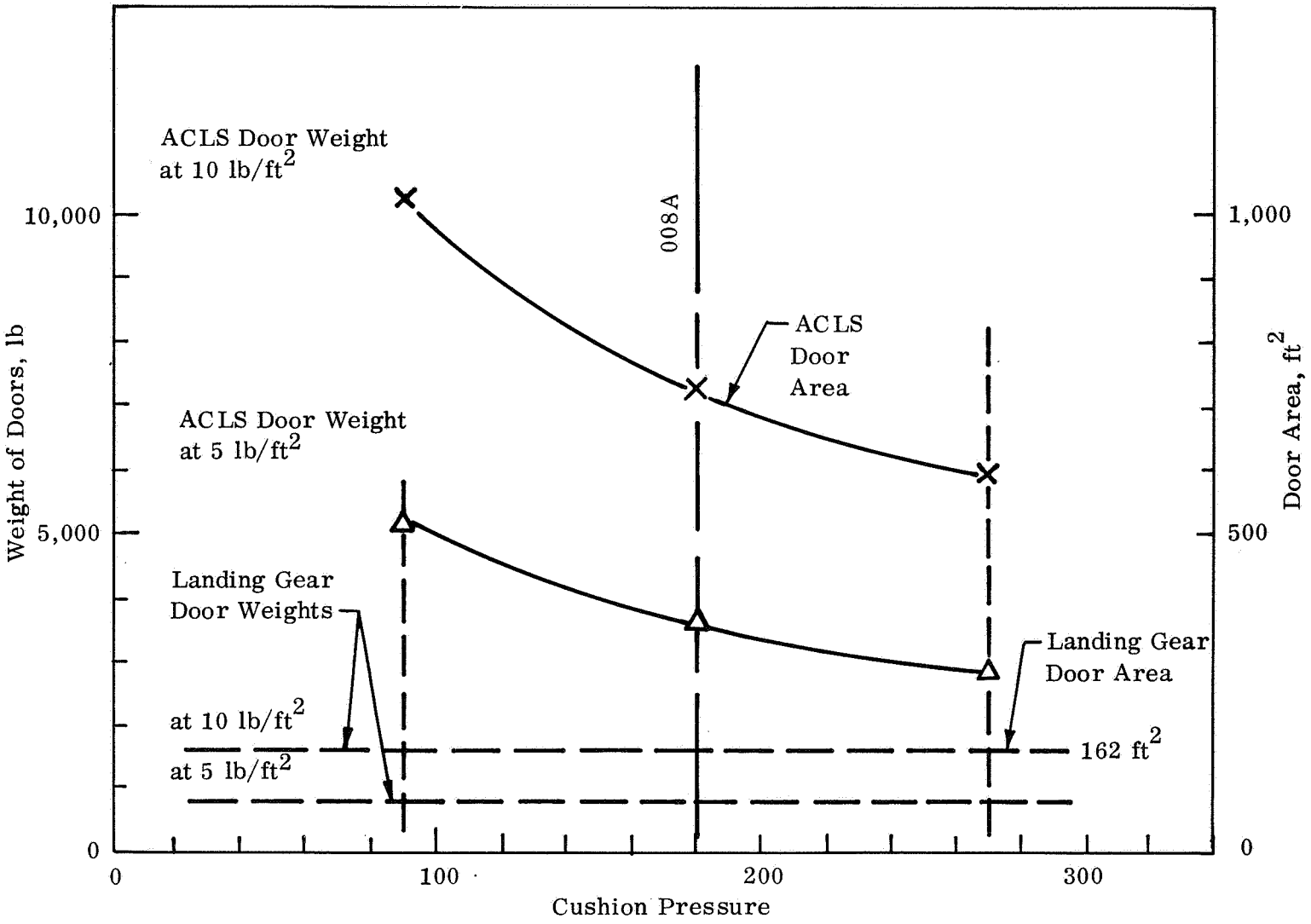

Fig. 63. Orbiter Trunk Protection Door Weight versus Cushion Pressure

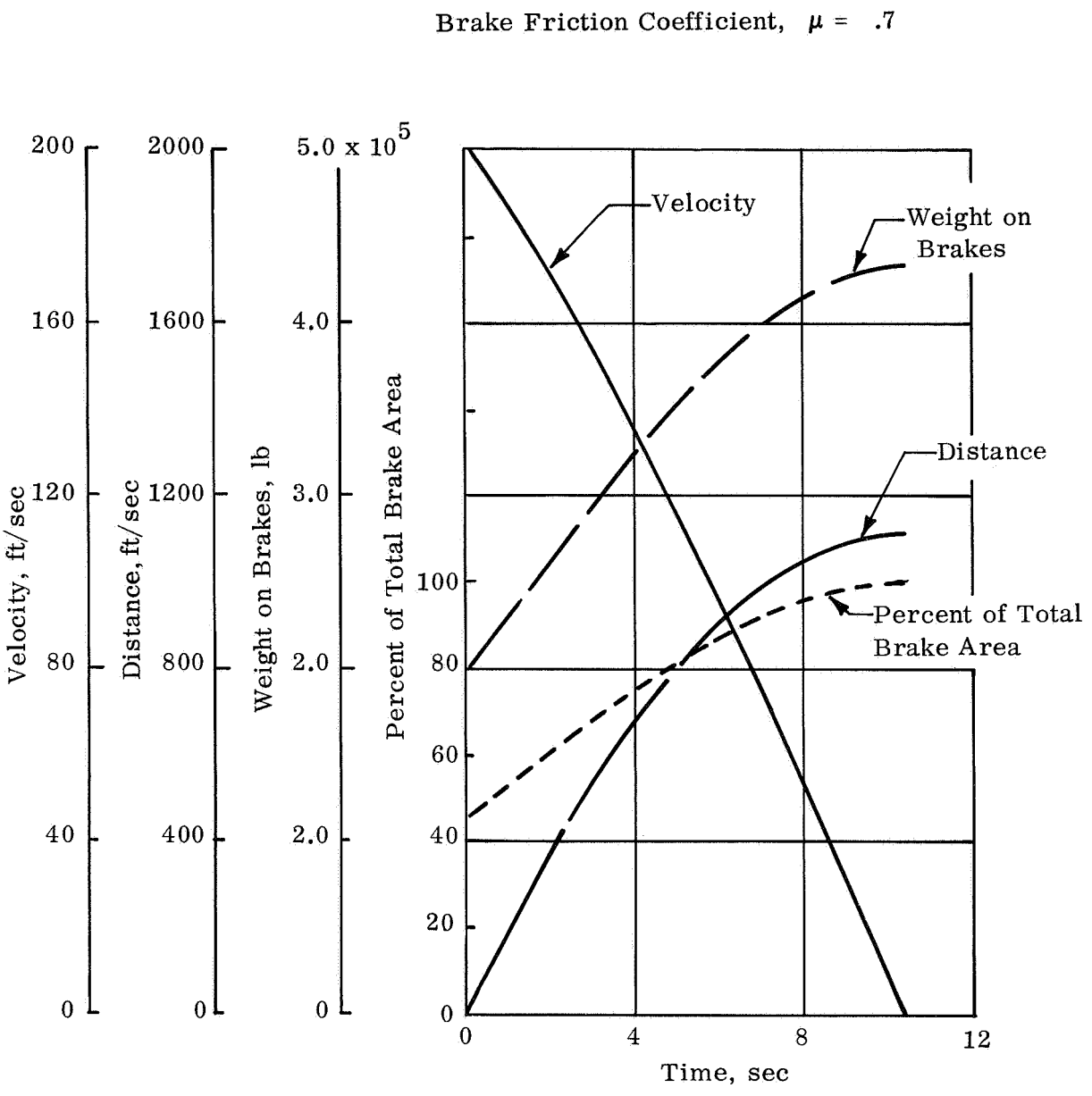

Fig. 64. Time Histories of Braking Parameters with $\mu = .70$

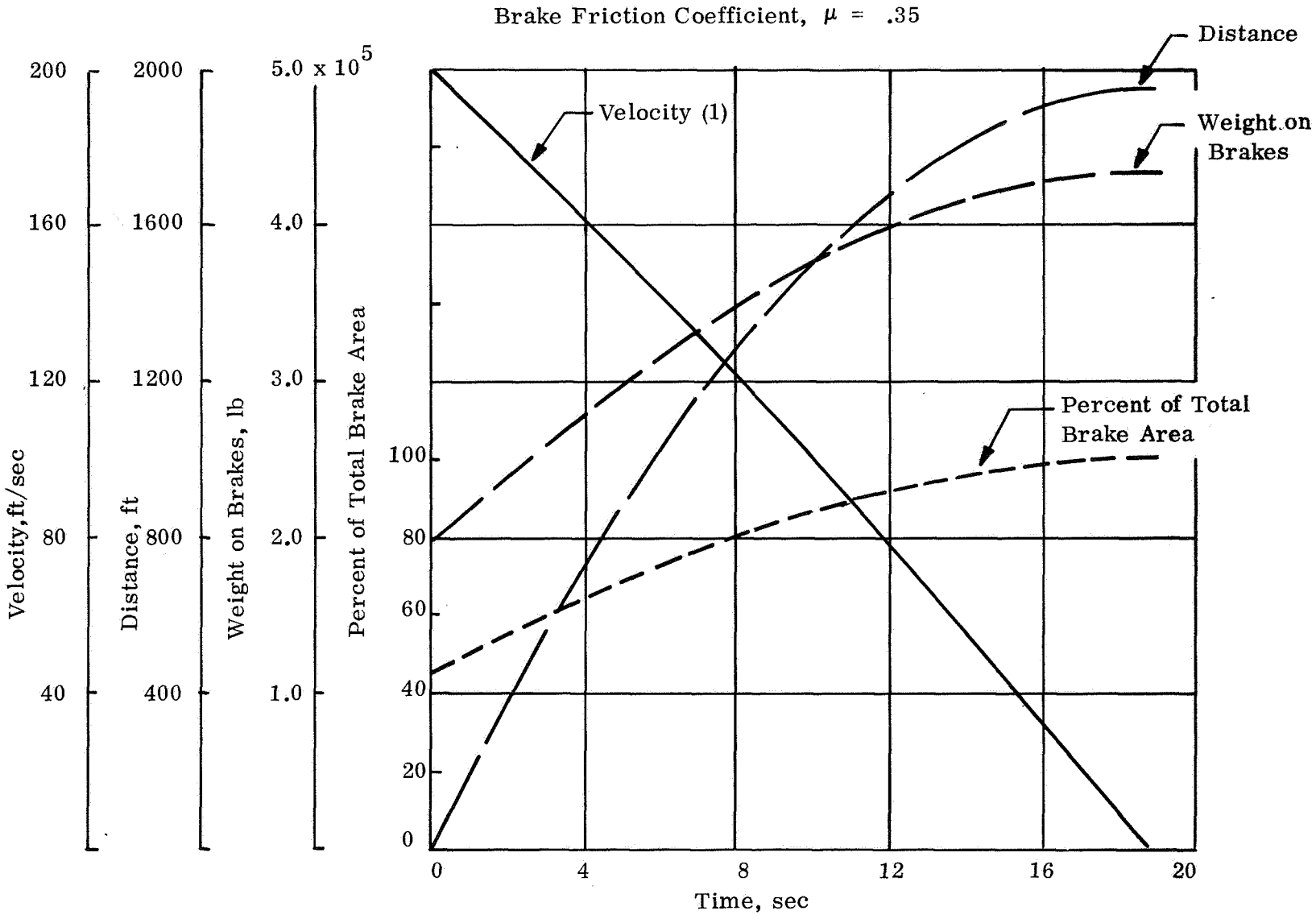

Fig. 65. Time Histories of Braking Parameters with μ = .35

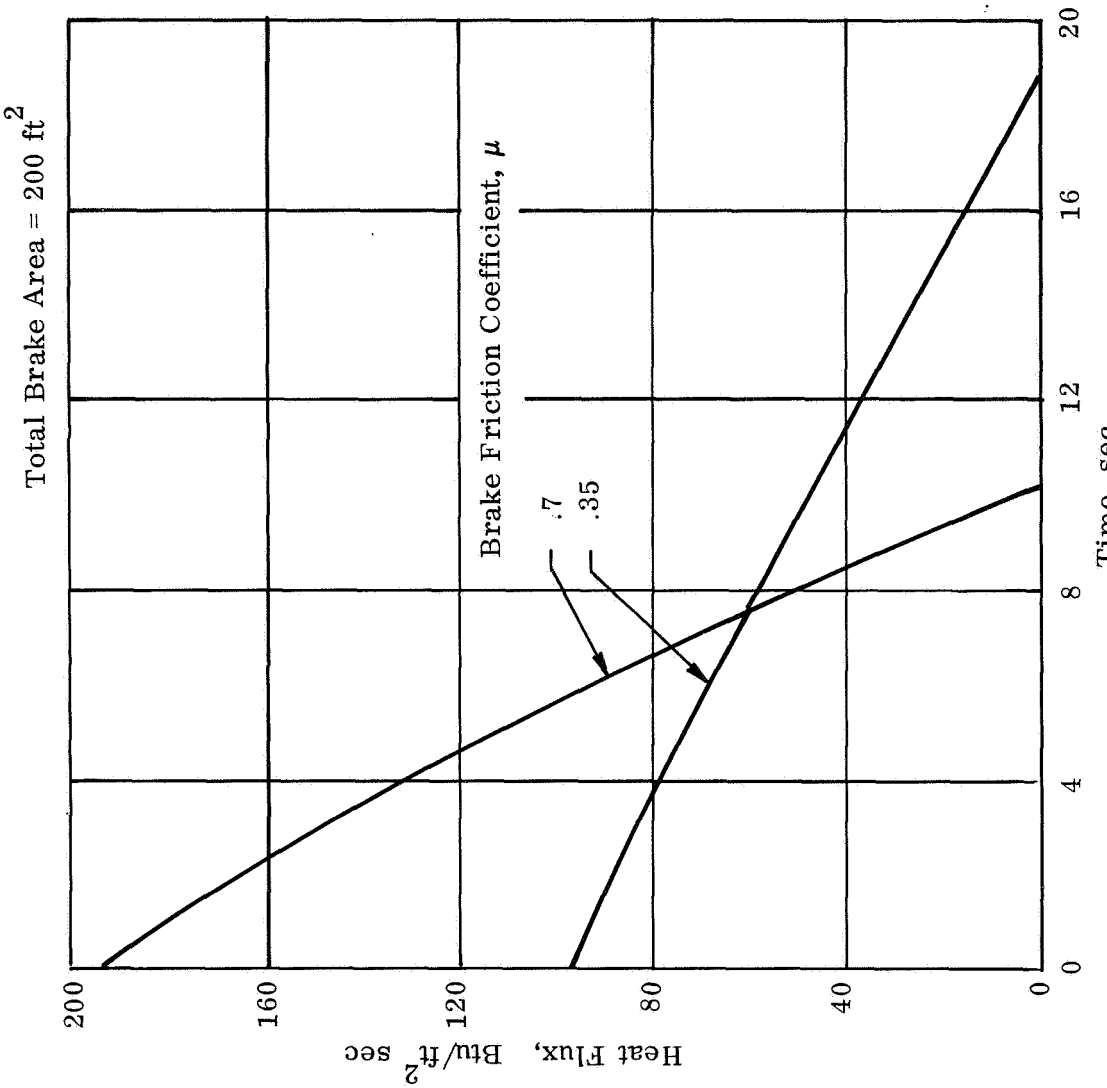

Fig. 66. Heat Flux to the Brakes vs Time

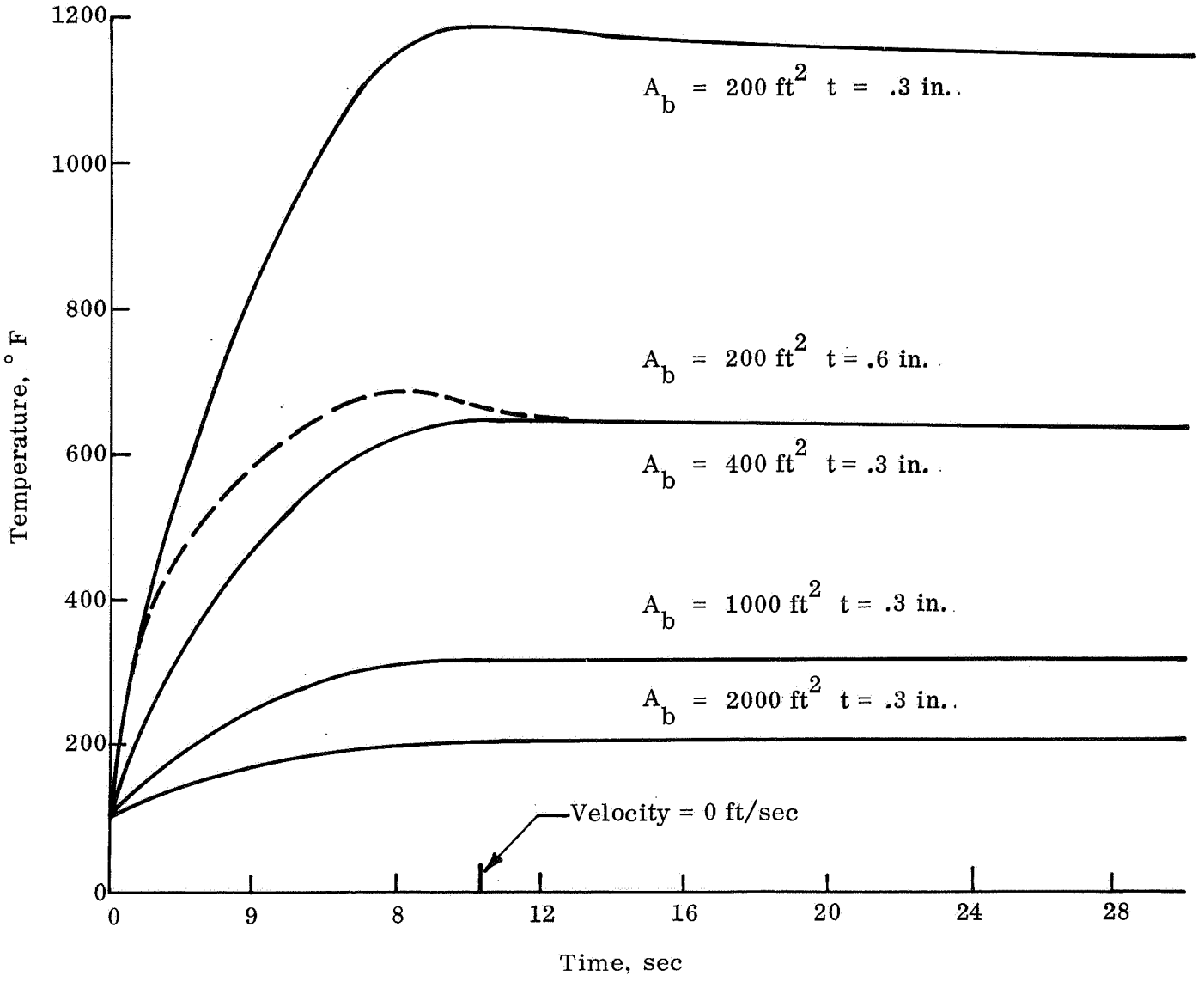

Fig. 67. Brake Temperature vs Time with μ = .7

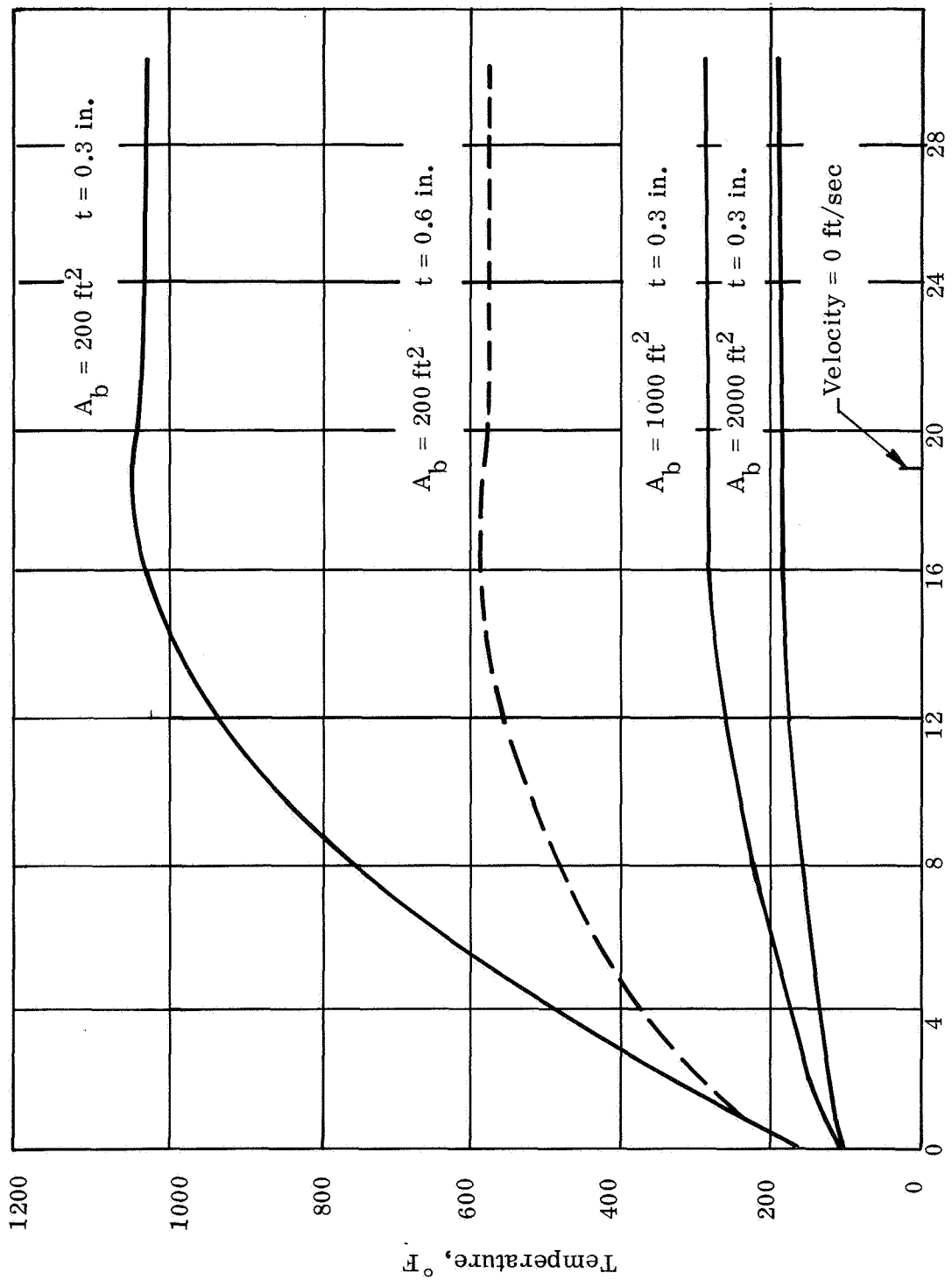

Fig. 68 . Brake Temperature vs Time with μ = .35

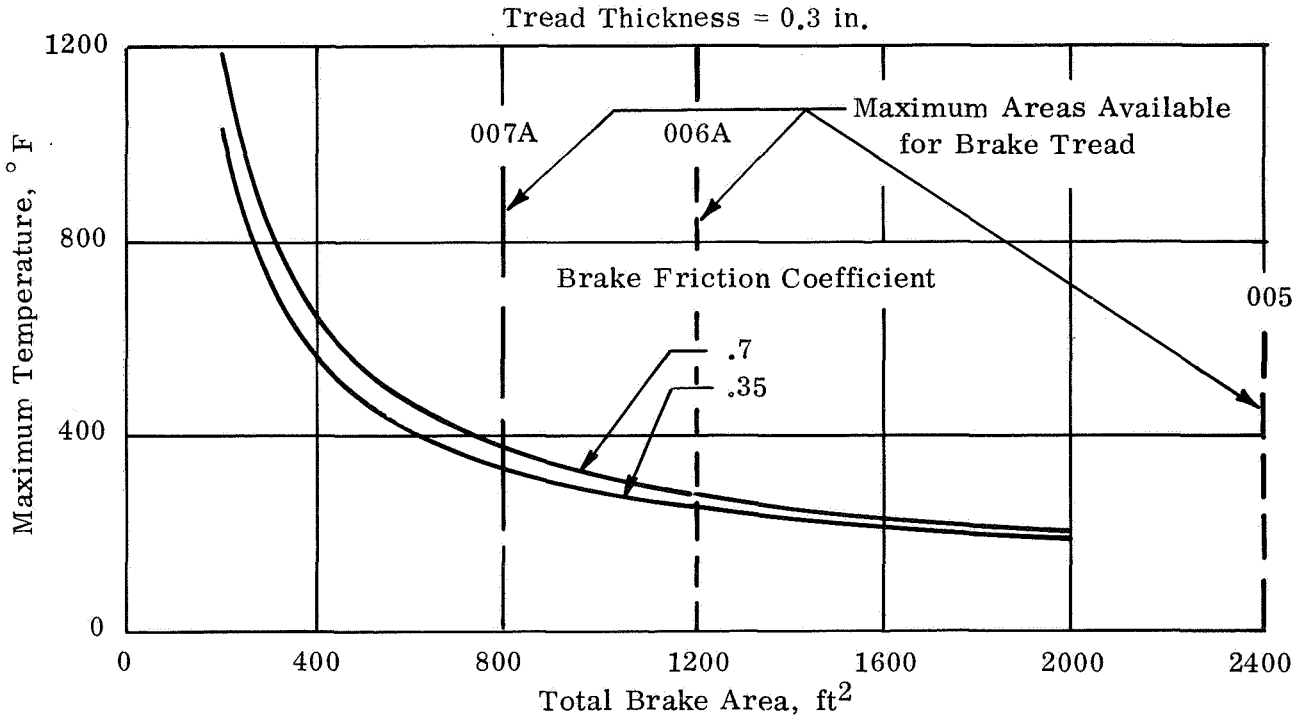

Fig. 69. Maximum Brake Temperatures vs Brake Area

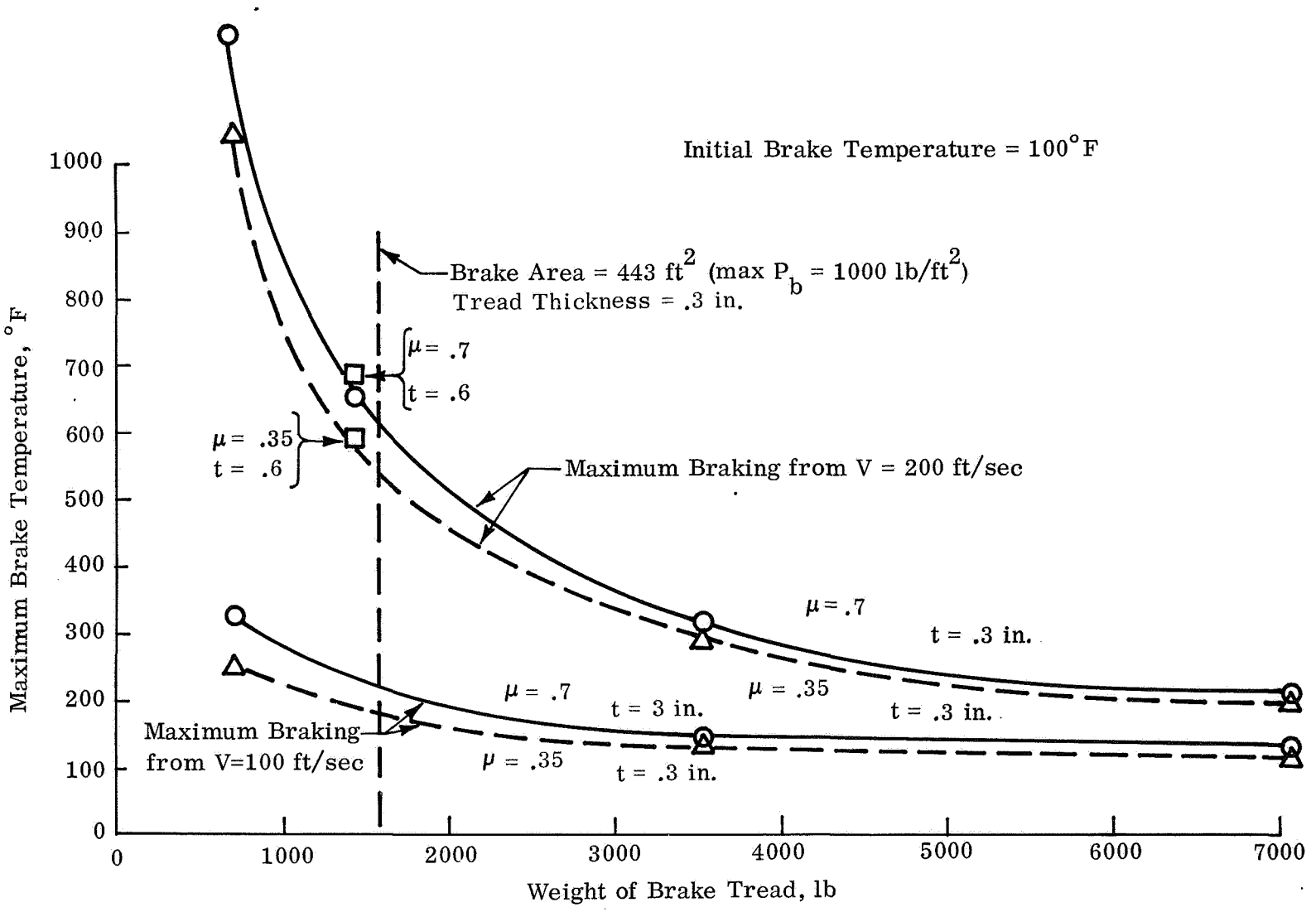

Fig. 70. Maximum Brake Tread Temperature vs Tread Weight

This fig. assumes maximum braking with cushion pressure of zero

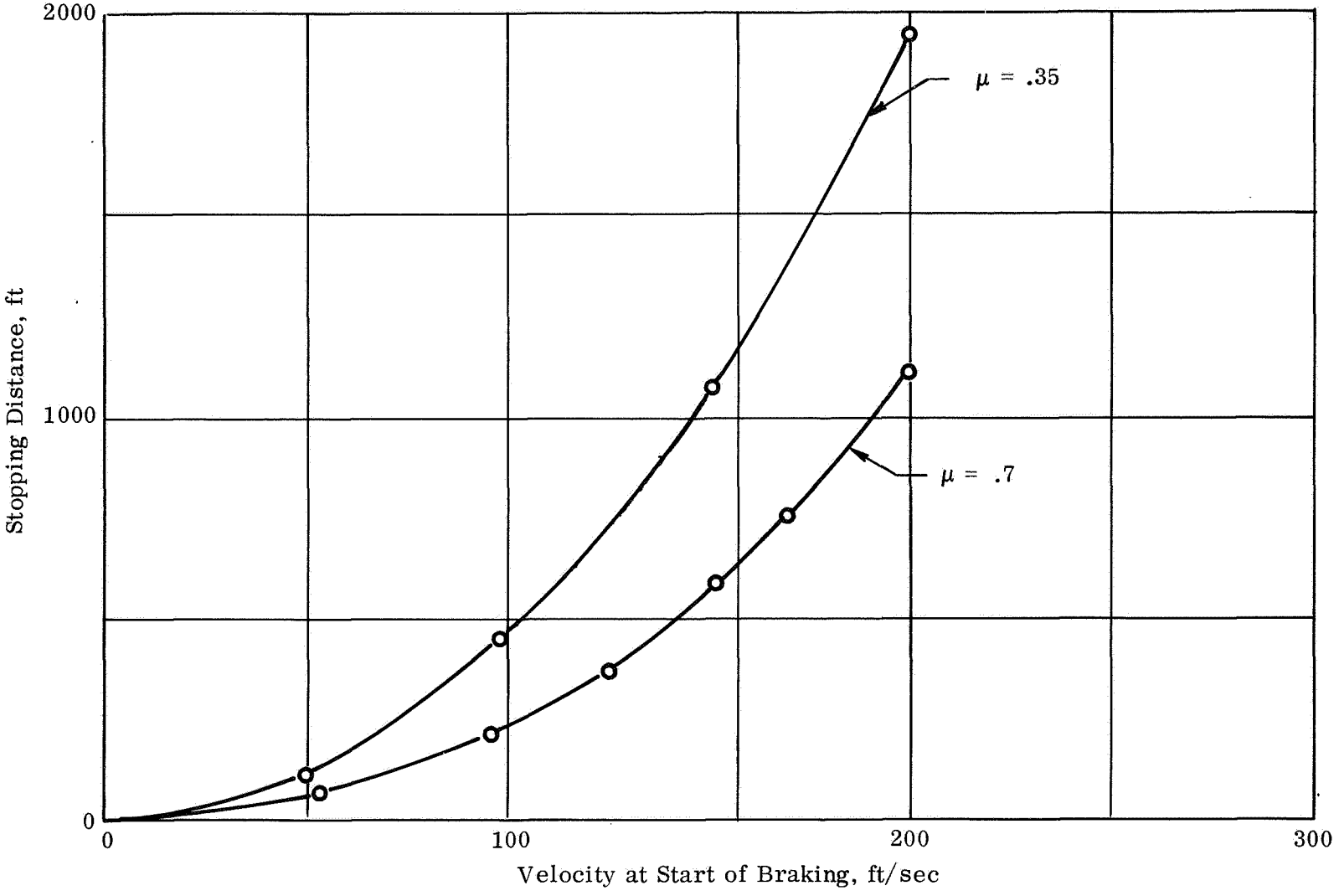

Fig. 71. Minimum Booster Stopping Distance vs Velocity at Start of Braking

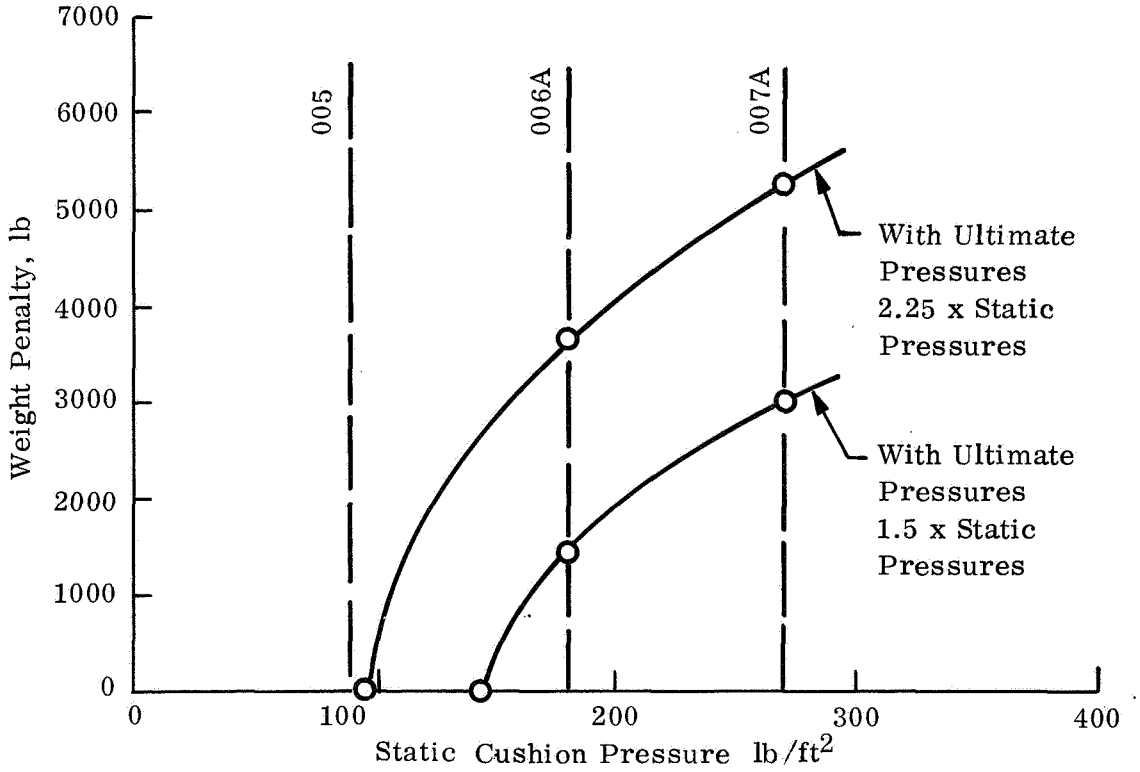

Fig. 72. Effect of ACLS on Booster Structure Weight

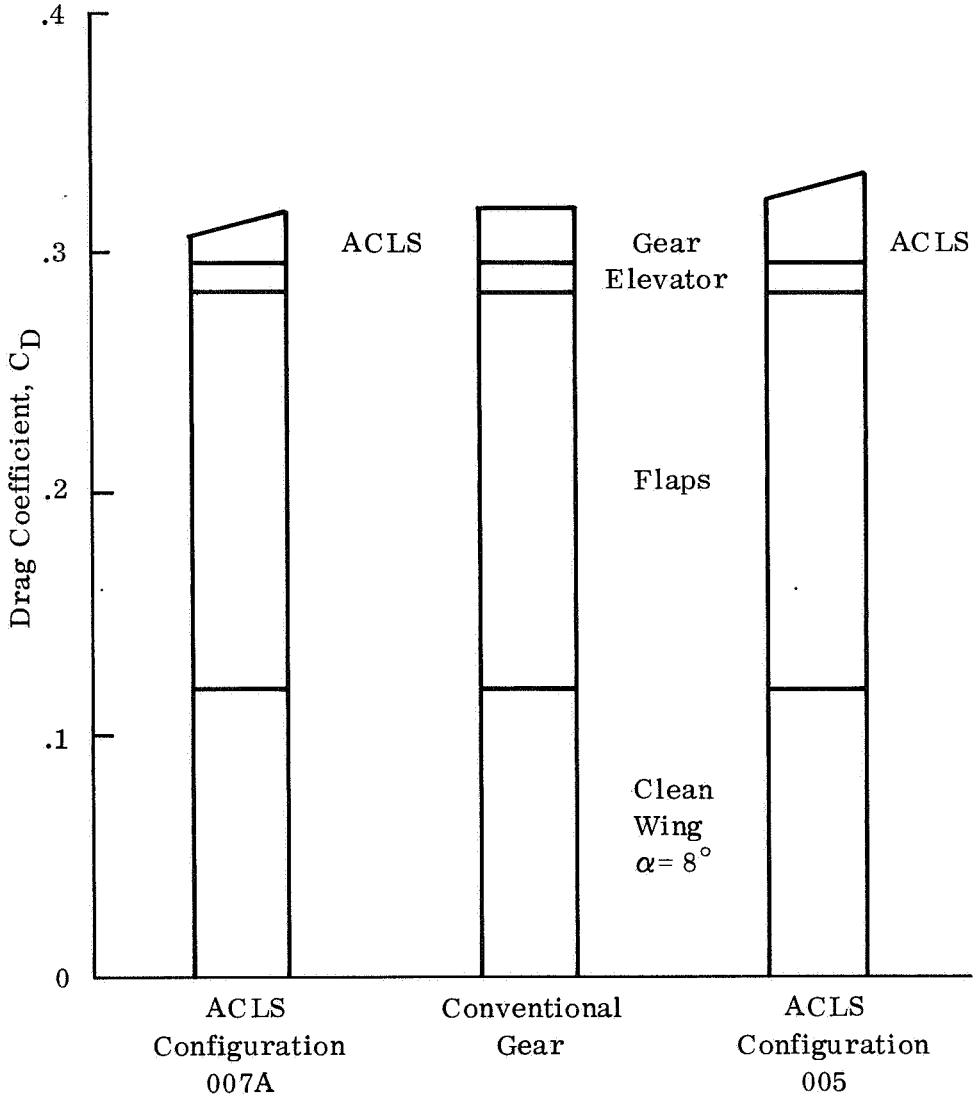

Fig. 73. Booster Drag with ACLS and Conventional Gear

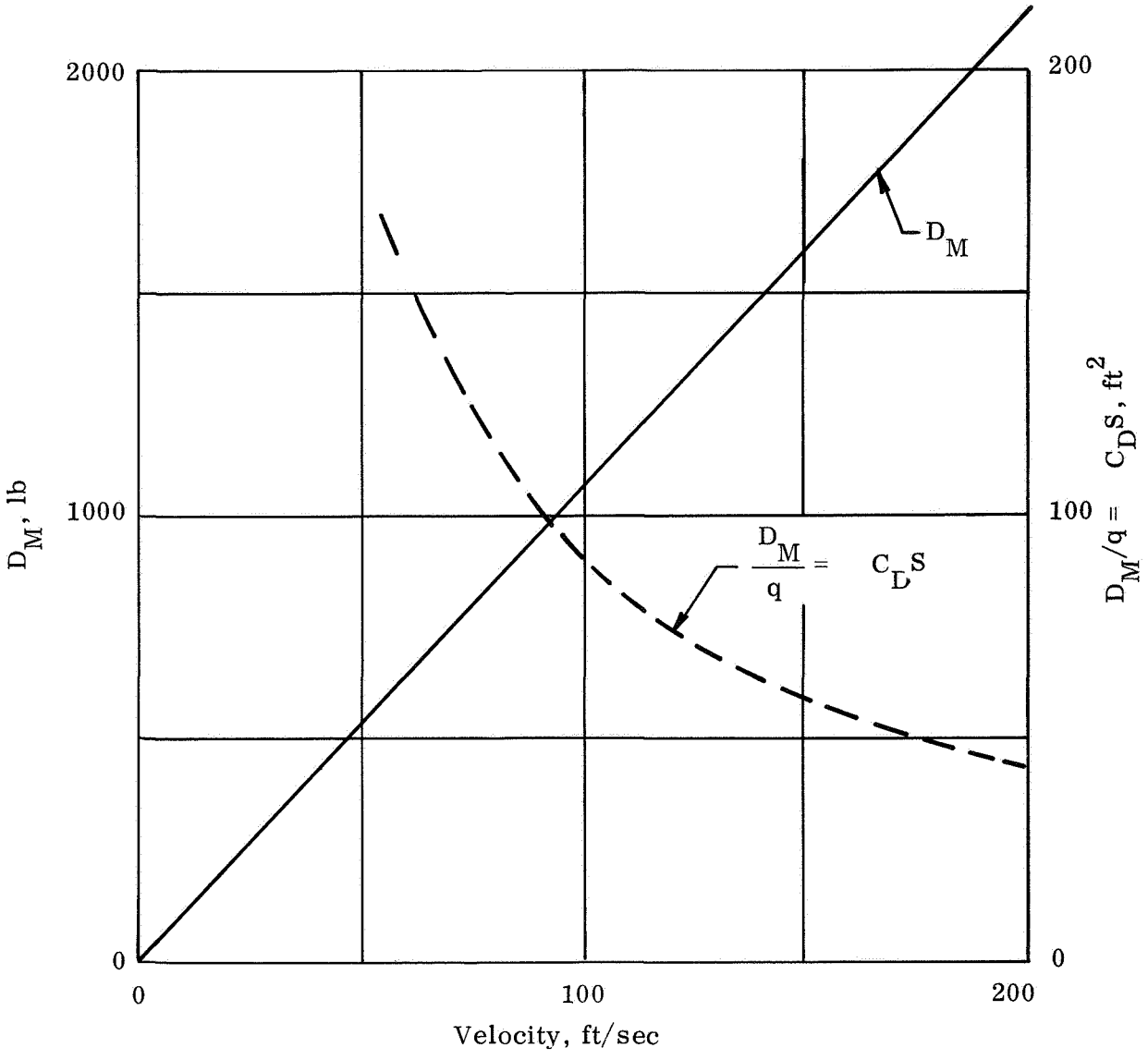

Fig. 74. Booster ACLS Momentum Drag

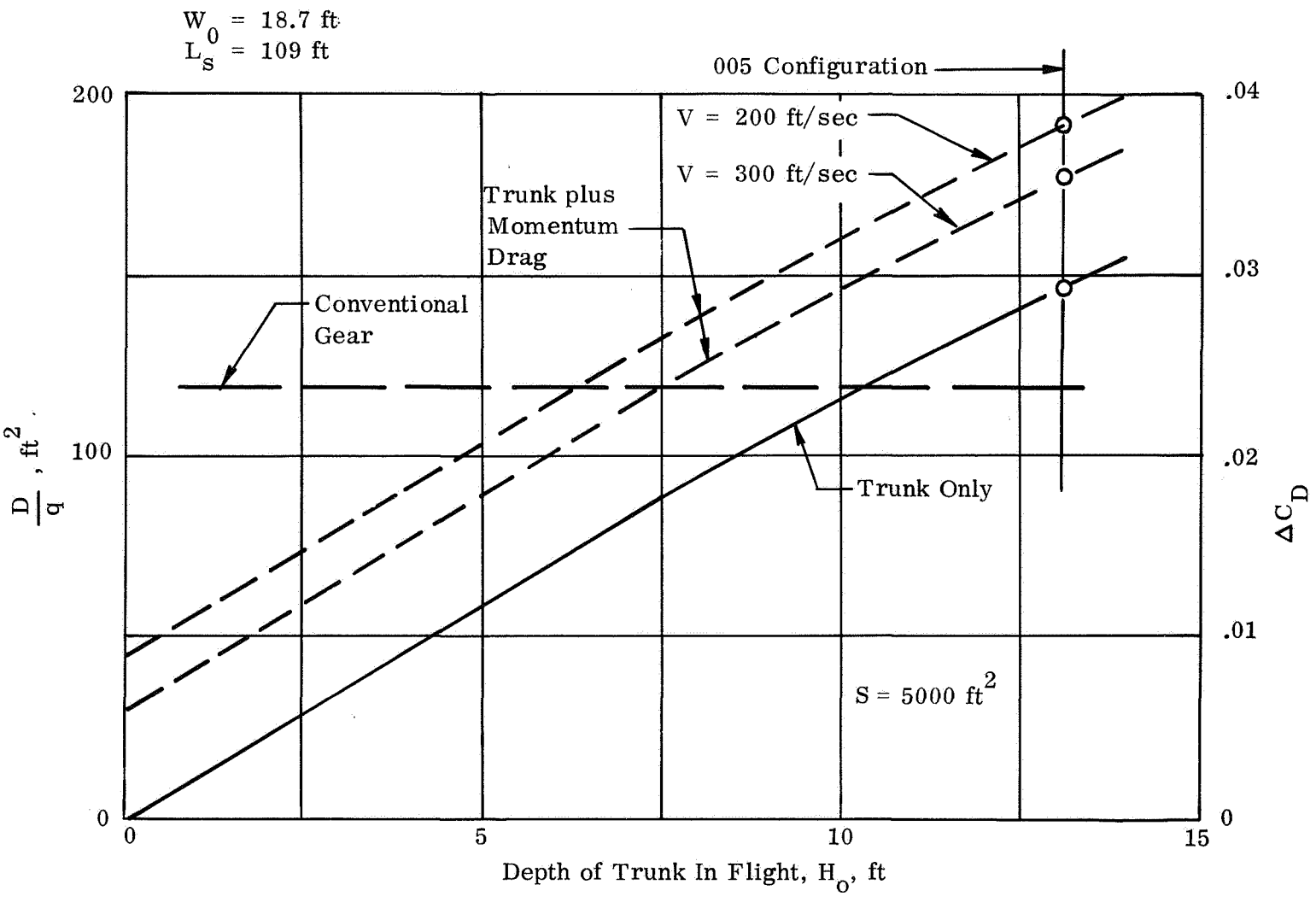

Fig. 75. Effect of Trunk Depth on Booster ACLG Drag

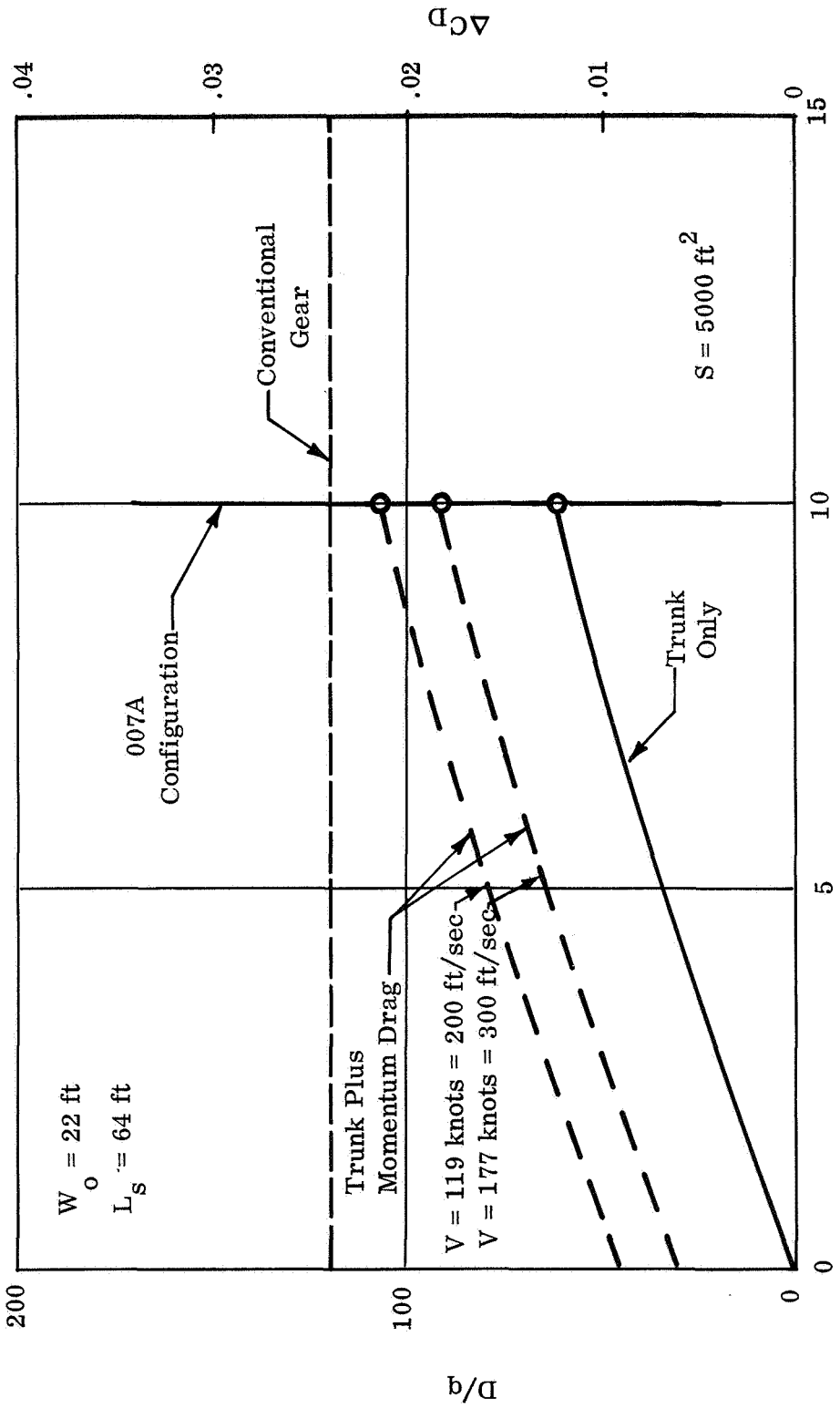

Fig. 76. Effect of Trunk Depth on Booster ACLS Drag

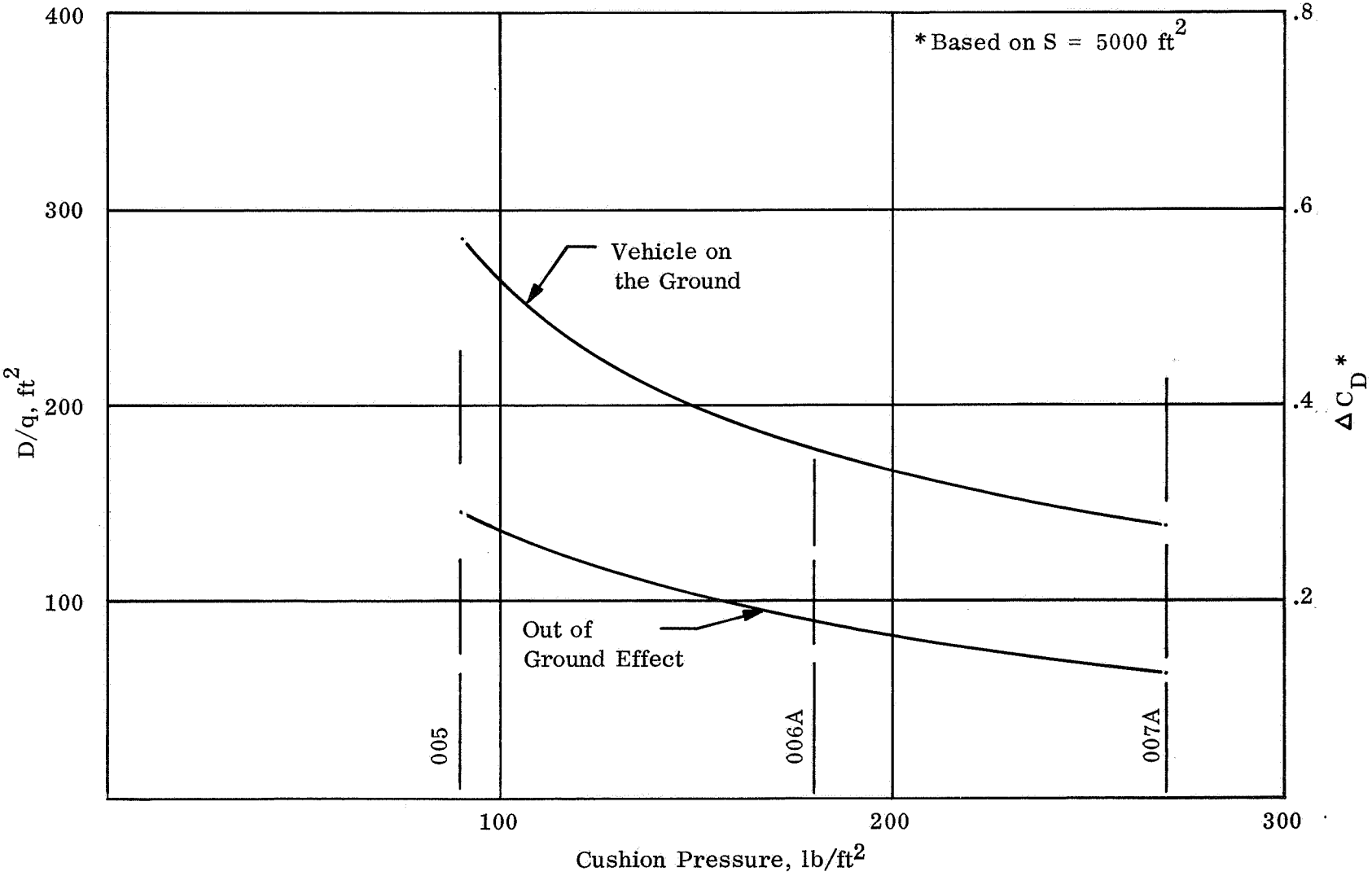

Fig. 77. Estimated Booster Trunk Drag In and Out of Ground Effect

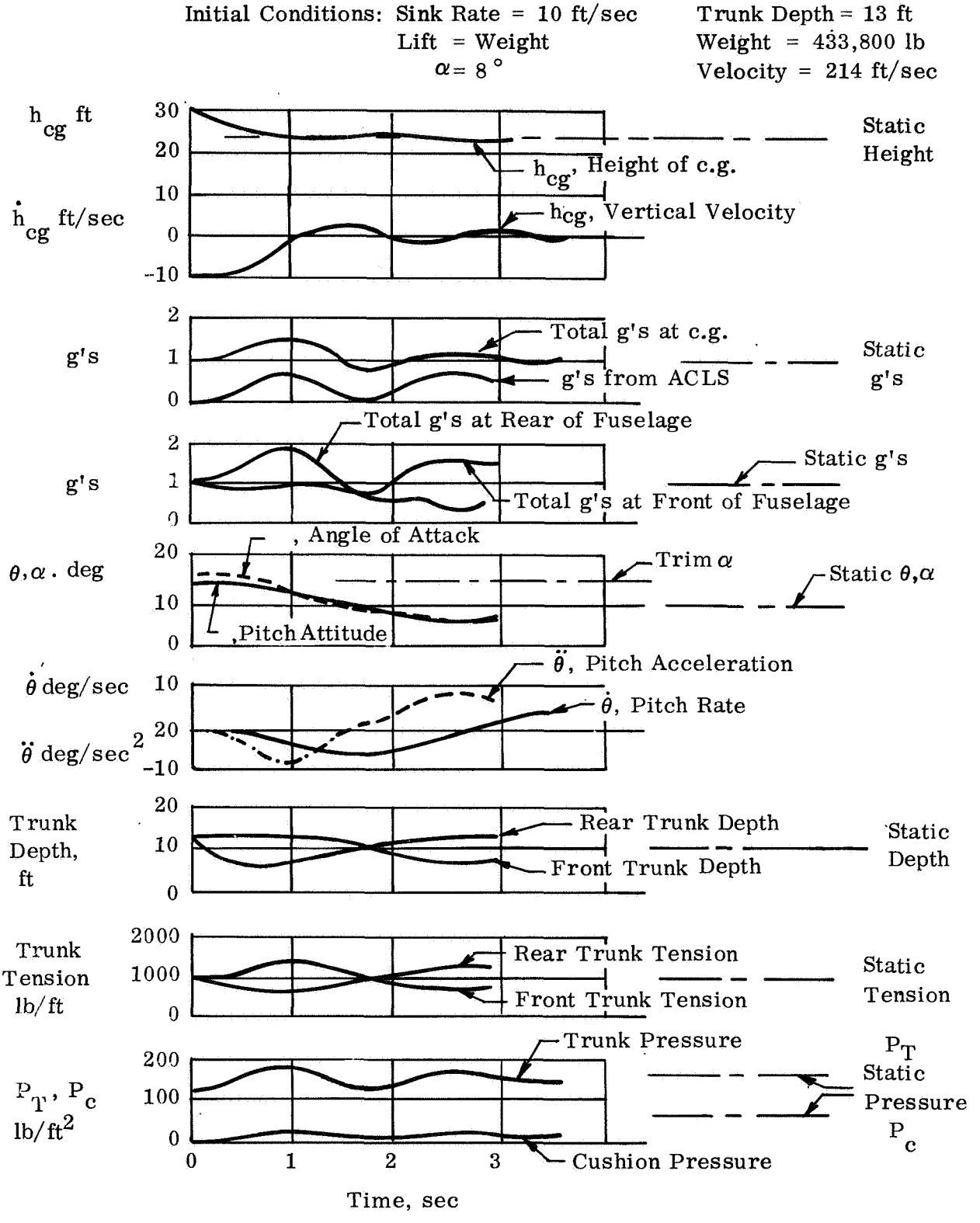

Fig. 78. Simulated Landing of Booster with Low Pressure ACLS

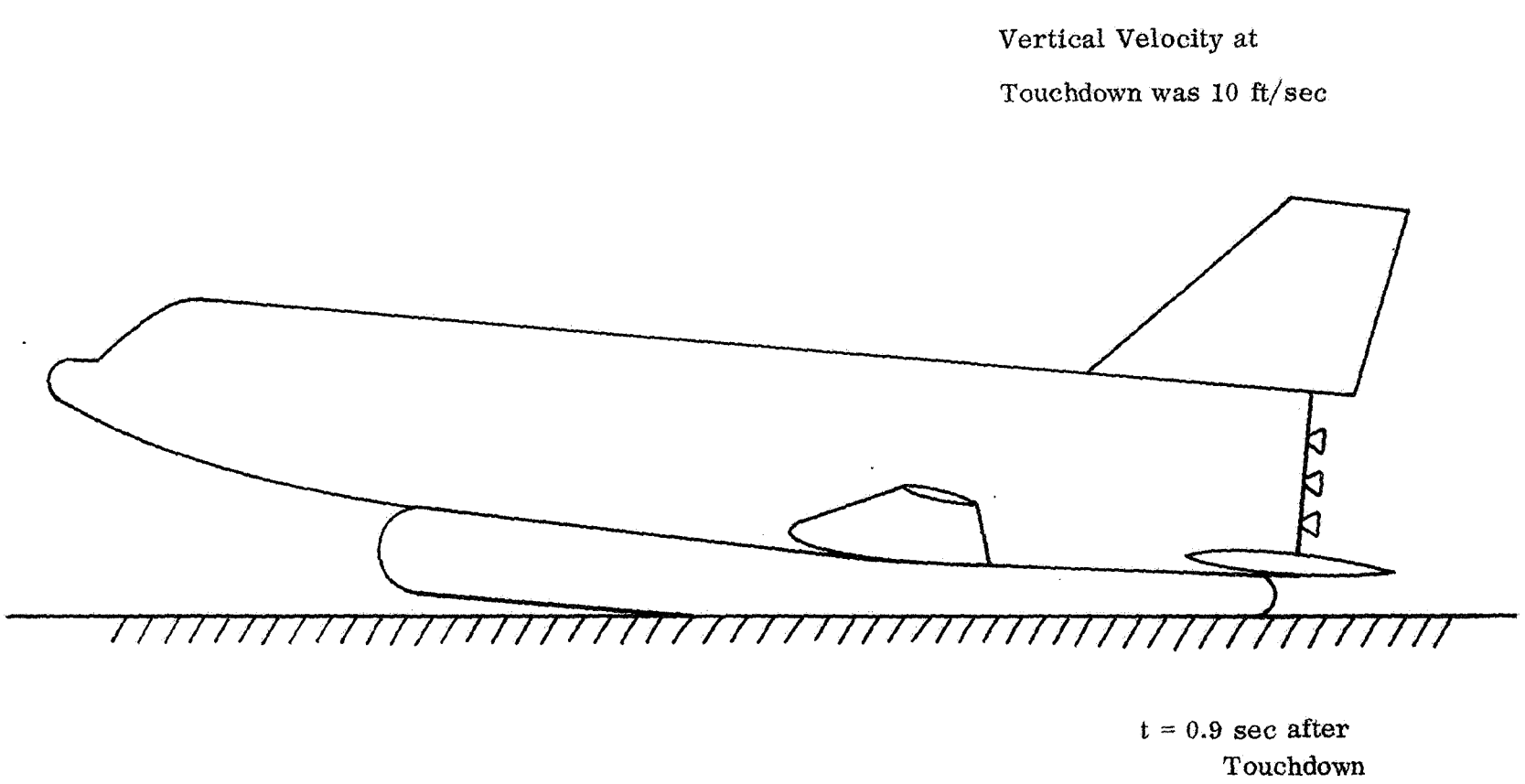

Fig. 79. Booster with Low Pressure ACLS at Time* of Maximum Compression of Trunk

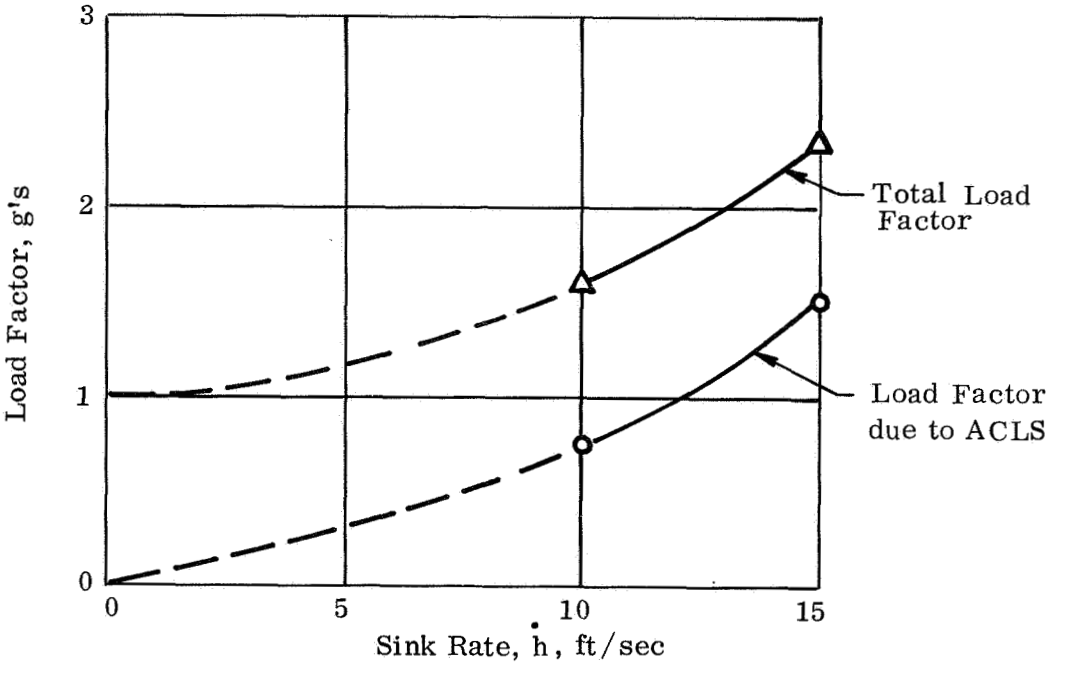

Fig. 80. Booster Vertical Load Factor vs Sink Rate

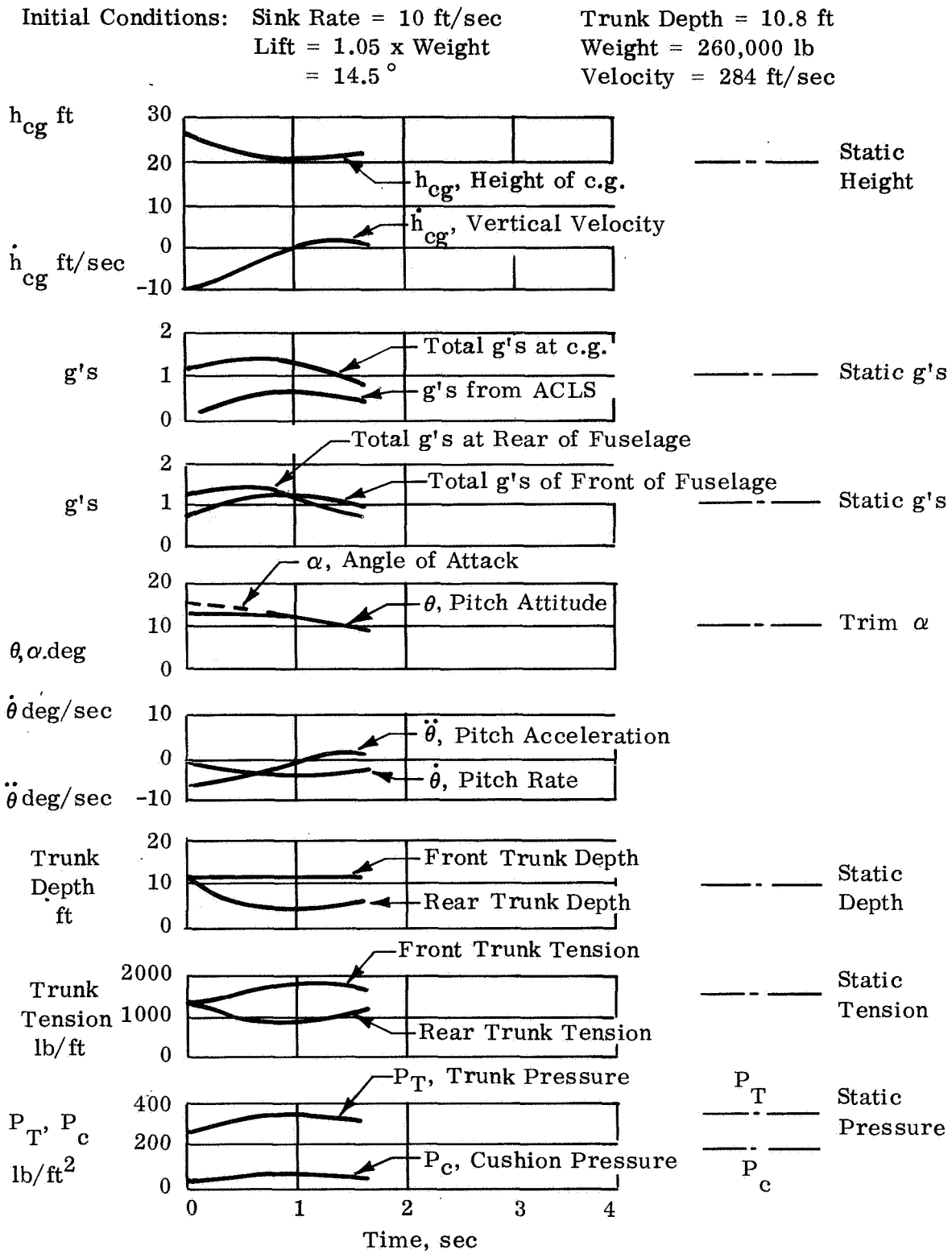

Fig. 81. Simulated Landing of Orbiter with Medium Pressure ACLS

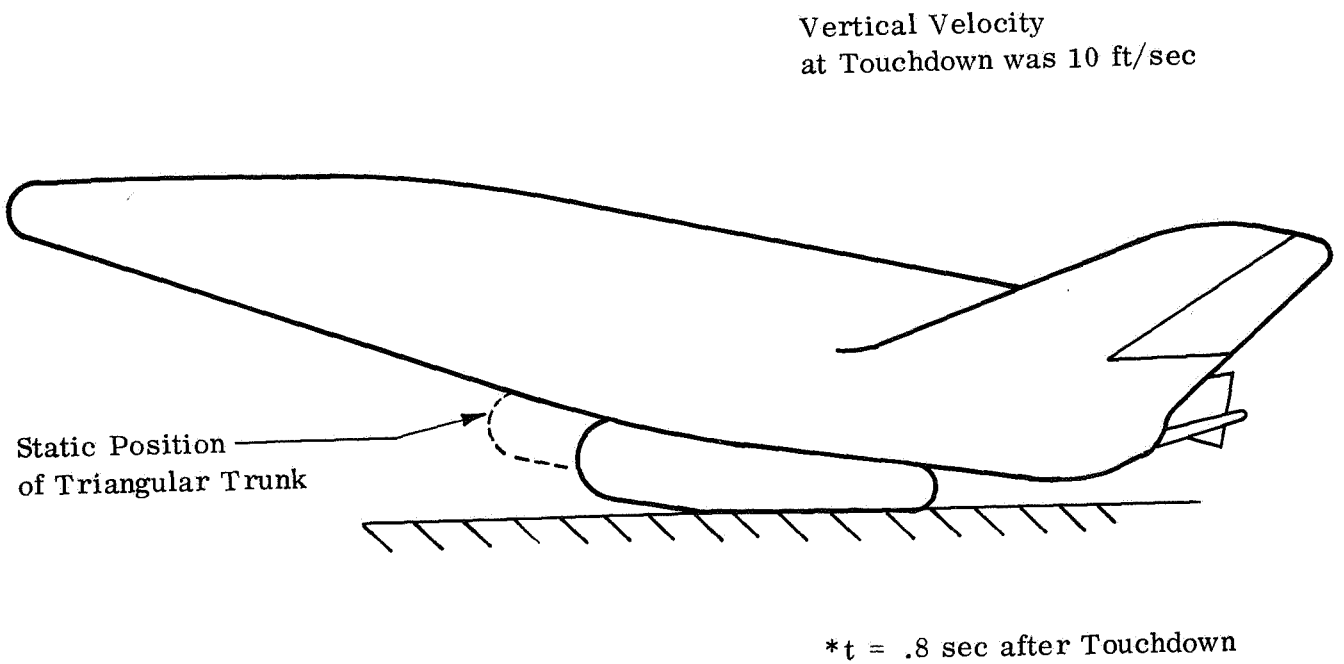

Fig. 82. Orbiter at Time* of Maximum Compression of Trunk

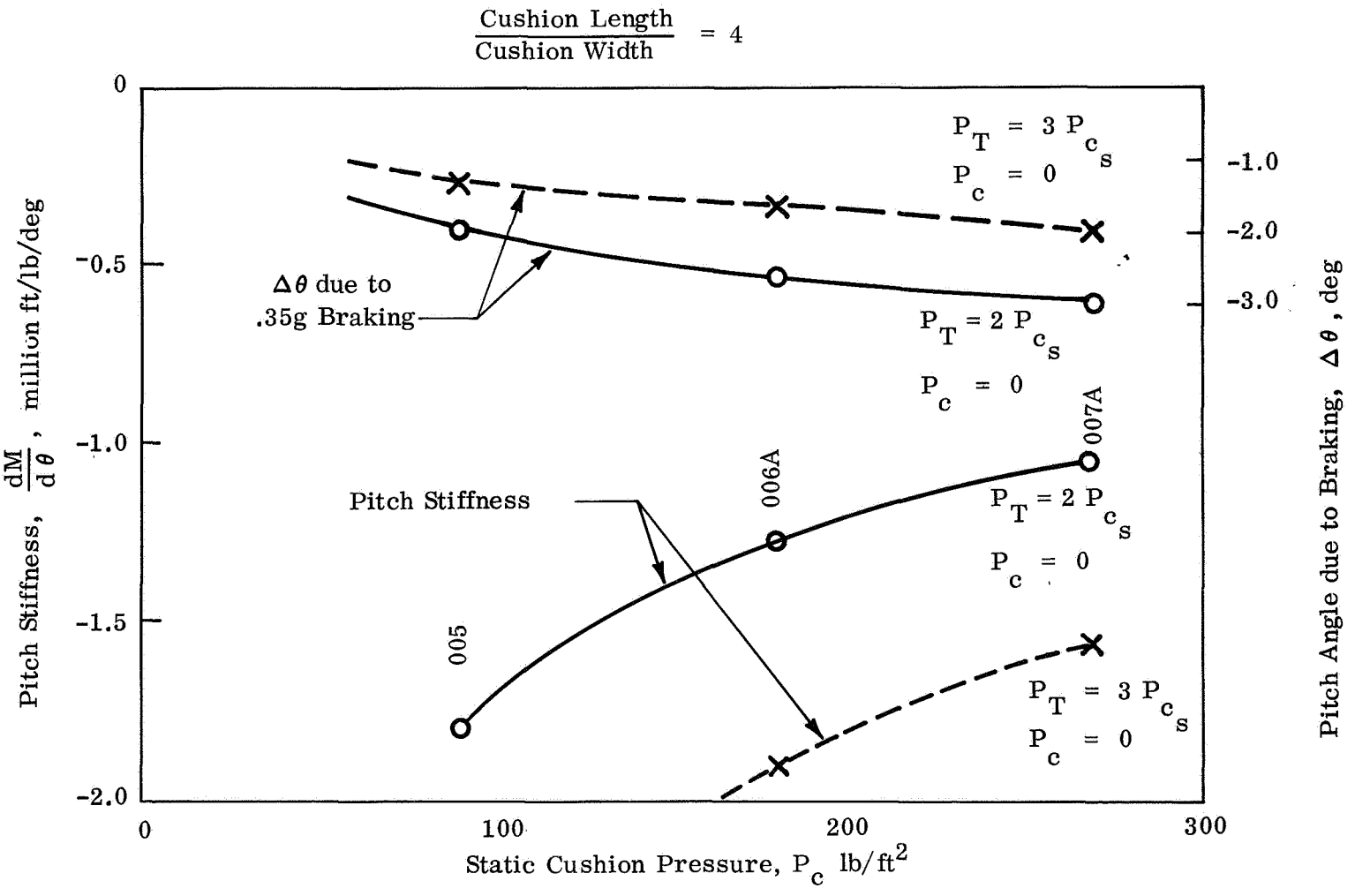

Fig. 83 . Booster ACLS Pitch Stiffness

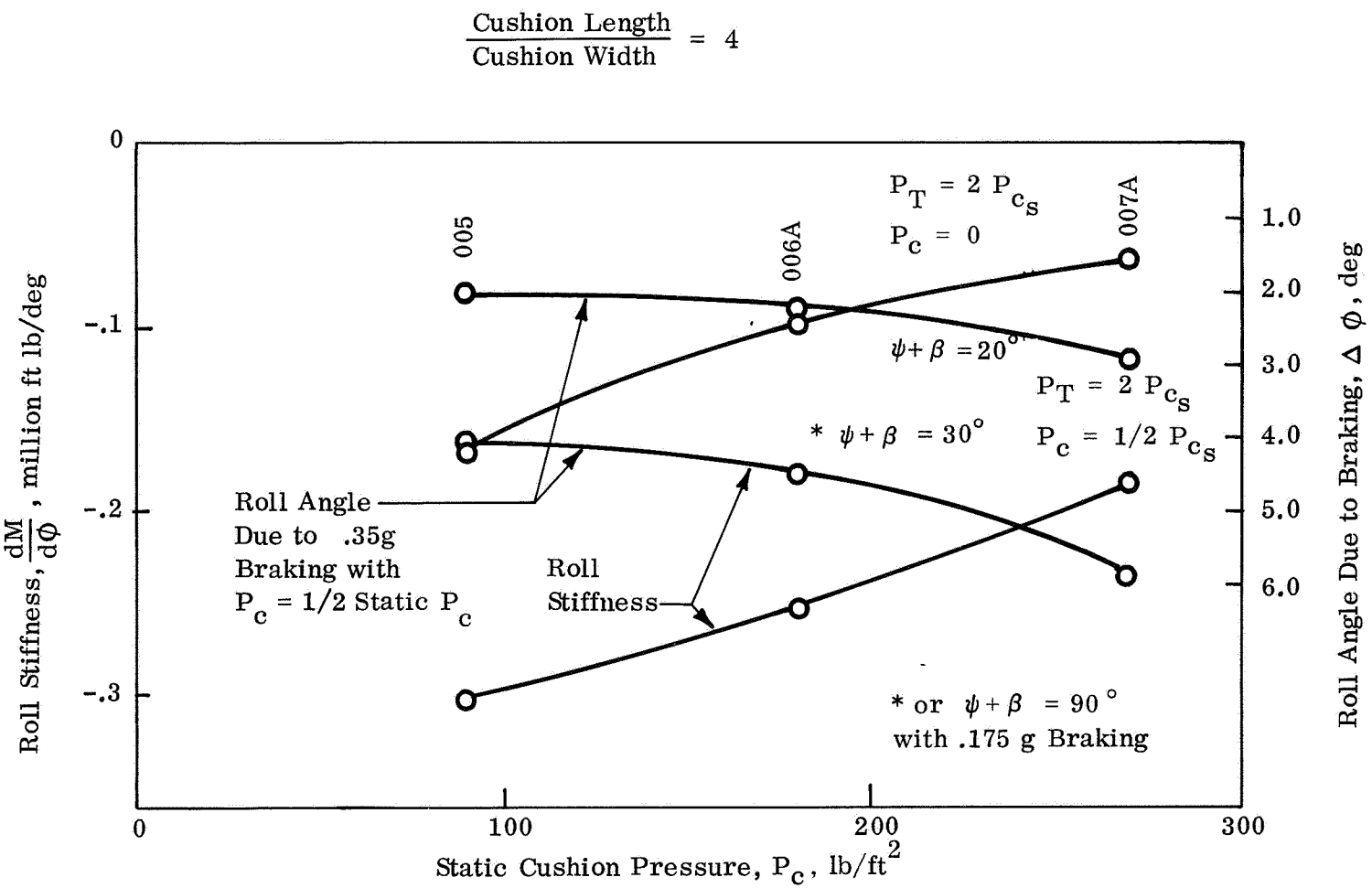

Fig. 84. Booster ACLS Roll Stiffness

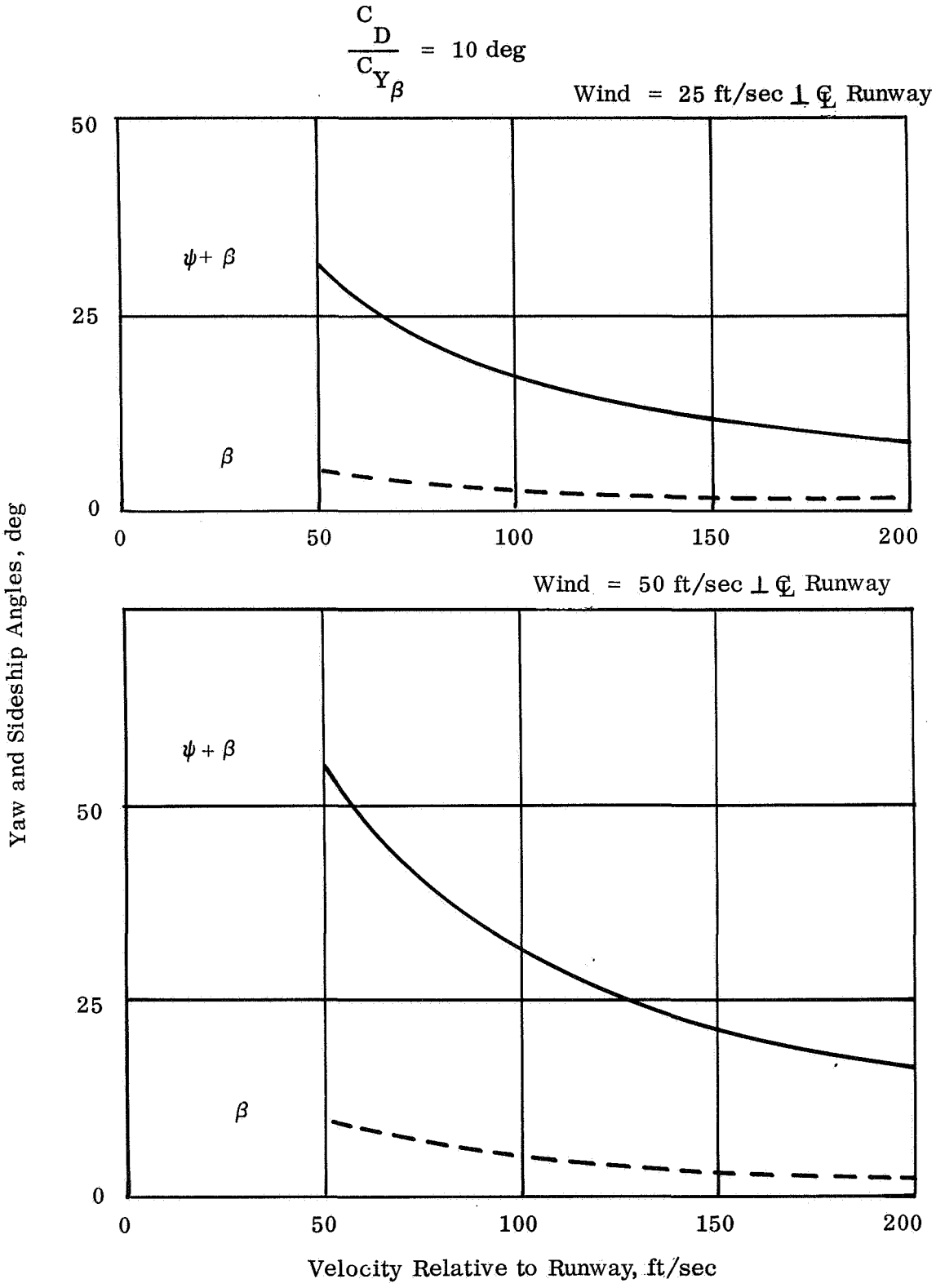

Fig. 85. Yaw Required to Prevent Drift During Rollout in Crosswind